

TREATMENT OF THE INDUSTRIAL WATER USING ION EXCHANGE

A Thesis

**Submitted to the College of Engineering
of Alnahrain University in Partial Fulfillment
of the Requirements for the Degree of
Doctor of Philosophy
in
Chemical Engineering**

by

SANDRA SOLAQA POULUS

(M.Sc. in Chemical Engineering 2001)

Muharram

1434

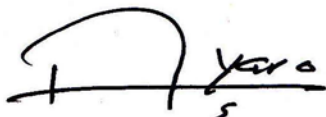
December

2012

Certification

I certify that this thesis entitled "**Treatment of the industrial water using ion exchange**" was prepared by **Sandra Solaqa Poulus** under my supervision at Al-nahrain University / College of Engineering in partial fulfillment of the requirements for the degree Doctor of Philosophy in Chemical Engineering.

Signature:



Name: **Prof. Dr. Aprael S. Yaro**
(Supervisor)

Date: 9 / 12 / 2012

Signature:



Name: **Asst. Prof. Dr. Basim O. Hasan**
(Head of Department)

Date: 9 / 12 / 2012

Certificate

We certify, as an examining committee, that we have read this thesis entitled **"Treatment of the industrial water using ion exchange "**, examined the student **Sandra Solaqa Poulus** in its content and found it meets the standard of thesis for the degree of Doctor of **Philosophy** in Chemical Engineering.

Signature:



Name: Prof. Dr. Aprael S. Yaro
(Supervisor)

Date: 9 / 12 / 2012

Signature:



Name: Asst. Prof. Dr. Basim O. Hasan
(Member)

Date: 9 / 12 / 2012

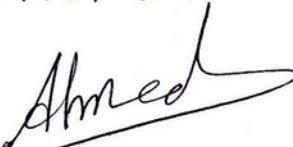
Signature:



Name: Asst. Prof. Dr. Naseer A. Al Habobi
(Member)

Date: 18 / 12 / 2012

Signature:



Name: Asst. Prof. Dr. Ahmed A. Mohammed
(Member)

Date: 9 / 12 / 2012

Signature:



Name: : Asst. Prof. Dr. Basma A. Abdul-Majeed
(Member)

Date: 9 / 12 / 2012

Signature:

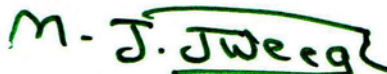


Name: Prof. Dr. Safa A. Al Naimi
(Chairman)

Date: 18 / 12 / 2012

Approval of the college of Engineering

Signature:



Name: Prof. Dr. Muhsin J. Jweeg
(Dean)

Date: 18 / 12 / 2012

Abstract

In this work Eshidiya Plant industrial wastewater, which is one of the phosphate mining industries that located in Jordan, where approximately 450000 m³ wastewater monthly resulted from the flotation cells needs a proper treatment for recycle purposes. The studied wastewater mainly contains phosphate waste and chloride ions. It considers enhanced sedimentation process by dual polyelectrolytes conditioning to remove and dewatering of phosphate waste, followed by a continuous mixed bed ion exchange column to remove the remaining soluble salt in the supernatant water.

The effect of different dose of the binary mixtures of cationic and anionic polyelectrolytes on the flocculation has been studied by measuring the turbidity and zeta potential. The optimum dose of the dual polyelectrolyte was obtained that is related to the target zeta potential of -5.6 mV. Flocculation helps to increase both the settling and dewatering rate of phosphatic waste in order to increase the recycling of the process water. The former criteria increased 20 times by cationic (Zetag 7557) and anionic (Magnafloc 633) polyelectrolyts as compared to the natural settling rate of the same waste, as well as 70% decreasing in the waste volume.

Batch and continuous fixed-bed column ion exchange study was carried out by using Purolite® A400 and Purolite® MB400 ion exchange resins as an adsorbent for the removal of Cl⁻, SO₄⁻² and Na⁺ from the water. Batch studies were performed to investigate the effects of various experimental parameters, such as adsorbent dose and initial concentration on the removal of ions. The maximum efficiency obtained was 98.95% by using 5g adsorbent and 200 mg/l initial chloride concentration. Adsorption equilibrium data were correlated with Langmuir and Freundlich isotherm models.

The column experiments were conducted to study the effect of important parameters such as bed depth, flow rate, feed concentration and the present of the co-ions on breakthrough curve, removal efficiency and the performance of mixed-bed ion exchange. The breakthrough curves of the three ions, plotted as the ratio of effluent to the influent concentration versus run time in minutes, give proper detailed results about the effects of the conditions. A mathematical model that proposed a mixed diffusion mechanism was developed to simulate the performance of the mixed bed ion exchange. The model was solved by a Matlab program and the theoretical results were compared with the experimental.

List of Contents

Content	Page
Abstract	I
Notations	V
List of Tables	VIII
List of Figures	IX
Chapter One: Introduction	1
Chapter Two: Literature Review	6
2.1. Coagulation and Flocculation	8
2.1.1. Stability of Colloids in Suspension	9
2.1.2. Electrical Double Layer (EDL)	10
2.1.3. Zeta Potential	12
2.1.4. Balancing Opposing Forces	13
2.1.5. The Energy Barrier	15
2.2. Flocculation Mechanism	17
2.2.1. Charge Neutralization Mechanism	17
2.2.2. Bridging Mechanism	18
2.3. Polymeric Flocculants	19
2.4. Turbidity	20
2.5. Ion Exchange	20
2.6. Ion Exchange Materials	22
2.6.1. Classification of Ion Exchangers	23
2.6.1.1. Ion Exchangers Classification Based On Matrix.	23
2.6.1.2. Ion Exchangers Classification Based On the Functional Groups	24
2.7. Properties of Ion Exchange Resins	27
2.7.1. Swelling	27
2.7.2. Capacity	28
2.7.3. Particle Size	29
2.7.4. Stability	29
2.7.5. Selectivity	29
2.8. Ion Exchange Techniques	31

2.8.1.	Batch Operations	31
2.8.2.	Column Techniques	32
2.9.	Mixed Bed Ion Exchange	35
2.10.	Breakthrough Curve and Performance of Column	37
2.11.	Ion Exchange Isotherm	40
2.11.1.	Langmuir Isotherm	41
2.11.2.	Freundlich Isotherm	41
2.12.	Hydrodynamic Effects in Columns	43
2.13.	Mechanism of Ion Exchange Processes	45
2.14.	Rate-Determining Step	48
Chapter Three: Experimental Work		50
3.1.	Sedimentation	51
3.2.	Enhanced Sedimentation (Coagulation-Flocculation)	52
3.3.	Ion Exchange Processing	56
3.3.1.	Batch Process	57
3.3.2.	Fixed-bed (column) process	59
Chapter Four: Modeling Fixed-Bed Ion Exchange		62
4.1.	Basic Model Consideration	63
4.1.1.	Material balance equation	63
4.1.2	Rate equations	67
4.1.2.	Equilibrium	68
4.2.	Predictive model	71
Chapter Five: Results and Discussion		74
5.1.	Sedimentation Experiment	74
5.2.	Enhanced Sedimentation (Coagulation-Flocculation)	75
5.2.1.	Determination of Magnafloc 919 and Zetag 7557 Optimum Dosage	76
5.2.2.	Determination of Magnafloc 336 and Zetag 7557 Optimum Dosage	79
5.2.3.	Settling Rate and Volume of the Sediment	82
5.2.4.	Chemical Analysis of the Supernatant Water	83
5.3.	Ion Exchange Experiments	84
5.3.1.	Batch Studies	84

5.3.1.1. Effect of Adsorbent Quantity and Initial Monocomponent Concentration	85
5.3.1.2. Adsorption Isotherm	86
5.3.1.3. Equilibrium Studies	88
5.3.2. Column Studies	90
5.3.2.1. Effect of the Flow Rate on Breakthrough Curve	91
5.3.2.2 Effect of Bed Height on Breakthrough Curve	95
5.3.2.3 Effect of Initial Ion Concentration on Breakthrough Curve	97
5.3.2.4 Effect of Co-Ion on Breakthrough Curve for Cl ⁻	100
5.3.2.5 The Effect of Mixed Bed Ion Exchange on Breakthrough Curve	102
5.3.2.6 Comparison between Model Predictions and Experimental Results	104
Chapter Six: Conclusions and Recommendation for Future Work	109
6.1. Conclusions	109
6.2. Recommendations for future work	111
References:	112
Appendix A: Experimental Result	A1
Appendix B: Cationic and Anionic Polyelectrolytes Specification	B1
Appendix C: Ion Exchange Resin Specification	C1
Appendix D: Determination of Chloride Ion Concentration by Titration	D1

Notations

Symbols		Unit
A	Cross-sectional area of the bed	$[\text{cm}^2]$
a_u	Specific surface area in the bed	$[\text{cm}^2/\text{cm}^3]$
C	The solution concentration or the effluent concentration	$[\text{mg}/l]$
C_e	Equilibrium concentration	$[\text{mg}/l]$
C_E	Exit concentration	$[\text{mole}/\text{vol. of fluid}]$
C_i	The concentration in the solid-fluid interface	$[\text{mg}/l]$
C_{lim}	Allowed effluent concentration	$[\text{mg}/l]$
C_o	Initial concentration	$[\text{mg}/l]$
C_W	Entering concentration	$[\text{mole}/\text{vol. of fluid}]$
D_f	The diffusion coefficient of the molecules in the fluid phase	$[\text{cm}^2/\text{s}]$
D_L	The axial dispersion coefficient	
D_R	The radial dispersion coefficient	
D_s	Molecular diffusion in large pores	$[\text{cm}^2/\text{s}]$
ε_p	Internal porosity of the solid	$[\]$
I_A	Constant defined by Eq.(3.46)	$[\]$
I_B	Constant defined by Eq.(3.47)	$[\]$
K_F	Coefficient of Freundlich isotherm	$[\text{mg}/\text{g}]$
K_f	Film mass transfer coefficient	$[\text{m}/\text{s}]$
k_f	Fluid film mass transfer coefficient	$[\text{cm}/\text{s}]$

K_L	Coefficient of Langmuir isotherm	[ml/mg] , [l/mg]
K_p	Particle mass transfer coefficient	[m/s]
k_s	Coefficient concerning the intraparticle mass transfer rate	[g/cm ² .s]
M	Amount of the ion exchanger used	
n_i	Freundlich constants obtained for i in a single-component system	[]
Q	Adsorption energy (adsorption isotherm)	[mg/g]
q	Total capacity of the ion exchanger	[mg/g]
q_{br}	Breakthrough capacity	[mg/g]
Q_{col}	Total ion exchange capacity of the column	[mg/g]
q_e	Amount adsorbed per unit mass of adsorbent at equilibrium	[mg/g]
Q_f	Water flow rate	[l/min]
q_m	Langmuir monolayer saturation capacity	[mg/g]
q_{max}	Maximum adsorption energy	[mg/g]
q_o	Amount adsorbed in equilibrium with C_o	[mg/g]
R	Reaction term	[]
r	Radial position within particle	[cm]
r_m	Rate of accumulation in the solid face	[mole/mass solid]
r_o	Particle radius	[cm]
t	Time	[s] , [h]
T	Temperature	[K]
t_{br}	Time spent to reach breakthrough point	[s] , [h]
t_{eq}	Time spent to reach the equilibrium point	[s] , [h]
t_{lim}	Time spent to effluent concentration reached its limiting (or allowed) value	[s] , [h]
u_s	The superficial fluid velocity	[cm/s]

V	Total pumped water volume	[Liter]
V_{bed}	Resin volume in the fixed bed column	[cm ³]
V_{br}	Water volume passed until the breakthrough moment	[Liter]
V_{eq}	Total water volume passed until equilibrium point	[Liter]
V_{lim}	Total water volume passed until effluent concentration reached its limiting (or allowed) value	[Liter]
X_τ	Dimensionless column length defined by Eq.(3.49)	[]
Z	Height of the fixed-bed	[cm]
α & n	Constants defined by eq. (10)	[]
γ	Adsorption coefficient (= q_o/C_o)	[cm ³ /g]
ξ	$K_f a_u / k_s a_u \gamma$	[]
ρ_b	The bulk density (= $\rho_p(1 - \varepsilon)$)	[g/cm ³]
ρ_p	Particle density	[g/cm ³]
ε	Void fraction of the bed	[]
Θ_τ	Dimensionless time defined by Eq.(3.48)	[]

Abbreviations

<i>EBCT</i>	Empty bed contact time	[min]
-------------	------------------------	-------

List of Tables

Table 2.1: qualitative comparison of organic and inorganic ion exchangers.....	222
Table 2.2: Functional groups of standard ion-exchange resins.....	24
Table 3.1: Chemical analysis of Eshidiya wastewater (main components).....	51
Table 3.2: Stability criteria based on zeta potential	54
Table 5.1: Chemical analysis of supernatant water.....	83
Table 5.2: Langmuir and Freundlich models parameters for best fit and corresponding correlation coefficients with the experimental isotherm of chloride ion.....	89
Table 5.3 Langmuir and Freundlich models parameters for best fit and corresponding correlation coefficients with the experimental isotherm of Sodium ion.	89
Table 5.4: Langmuir and Freundlich models parameters for best fit and corresponding correlation coefficients with the experimental isotherm of sodium ion.	89

List of Figures

Figure 2.1: The electrical double layer (EDL).	11
Figure 2.2: Repulsion Force.	14
Figure 2.3: Van der Waals attraction.	15
Figure 2.4: The net interaction curve.	16
Figure 2.5: Schematic representations of polymeric ion exchangers.	23
Figure 2.6: Ion exchanger: dry (left panel) and swollen (right panel) states.	27
Figure 2.7: Division of an ion exchange column in three zones.	34
Figure 2.8: Operation steps of a regenerable mixed.	36
Figure 2.9: Breakthrough curve.	38
Figure 2.10: Eddy dispersion caused by different overall cross-section of the pass-ways (a) and by different length of different pass-ways (b).	44
Figure 2.11: Flow maldistribution, caused by non-uniform packing (a), channelling (b), and wall effects (c).	44
Figure 2.12: General mechanism of the ion exchange process.	47
Figure 3.1: Zeta meter 3.0 +unit apparatus.	53
Figure 3.2: Ion exchange resins.	57
Figure 3.3: Schematic diagram of the experimental system.	59
Figure 3.4: Mixed bed ion exchange	61
Figure 4.1: Control volume in a fixed bed.	64
Figure 5.1: Turbidity of the wastewater sample with time.	756
Figure 5.2: Zeta potential and turbidity of the supernatant water as a function of Magnafloc 919 dose and at 5 mg/l of Zetag 7557.	78
Figure 5.3: Zeta potential and turbidity of the supernatant water as a function of Magnafloc 919 dose and at 7 mg/l of Zetag 7557.	79
Figure 5.4: Zeta potential and turbidity of the supernatant water as a function of Magnafloc 336 dose and at 5 mg/l of Zetag 7557.	79
Figure 5.5: Zeta potential and turbidity of the supernatant water as a function of Magnafloc 336 dose and at 7 mg/l of Zetag 7557.	80
Figure 5.6: Effects of adsorbent amount and initial concentration on chloride removal efficiency	867
Figure 5.7: Cl ⁻ adsorption isotherm (Co: 200-800 mg/l; m: 1-5 g).	88
Figure 5.8: Effect of flow rate on the ion exchange breakthrough curve for Cl ⁻ on anion resin at 20 cm bed depth and an initial chloride concentration of 200 mg/l.	912
Figure 5.9: Effect of flow rate on the ion exchange breakthrough curve for Cl ⁻ on anion resin at 10 cm bed depth and an initial chloride concentration of 400 mg/l.	92
Figure 5.10: Effect of flow rate on the ion exchange breakthrough curve for SO ₄ ²⁻ on anion resin at 10 cm bed depth and an initial sulphate concentration of 200 mg/l.	92
Figure 5.11: Effect of flow rate on the ion exchange breakthrough curve for Na ⁺ on mixed resin at 20 cm bed depth and an initial sodium concentration of 355 mg/l.	934

Figure 5.12: Effect of bed height on the ion exchange breakthrough curve for Cl ⁻ on anion resin at 0.05 l/min flow rate and an initial chloride concentration of 600 mg/l.	95
Figure 5.13: Effect of bed height on the ion exchange breakthrough curve for Cl ⁻ on anion resin at 0.1 l/min flow rate and an initial chloride concentration of 600 mg/l.	96
Figure 5.14: Effect of bed height on the ion exchange breakthrough curve for SO ₄ ⁻² on anion resin at 0.1 l/min flow rate and an initial sulphate concentration of 200 mg/l. .	96
Figure 5.15: Effect of bed height on the ion exchange breakthrough curve for Na ⁺ on mixed resin at 0.1 /min flow rate and an initial sodium concentration of 485 mg/l....	98
Figure 5.16: Effect of initial concentration on the ion exchange breakthrough curve for Cl ⁻ on anion resin at 0.05 l/min flow rate and 20 cm bed height.	99
Figure 5.1^v: Effect of initial concentration on the ion exchange breakthrough curve for SO ₄ ⁻² on anion resin at 0.1 l/min flow rate and 10 cm bed height.	100
Figure 5.18: Effect of initial concentration on the ion exchange breakthrough curve for Na ⁺ on mixed resin at 0.05 l/min flow rate and 40 cm bed height.	99
Figure 5.19: Effect of SO ₄ ⁻² initial concentration on the ion exchange breakthrough curve for Cl ⁻ on anion resin at 0.1 l/min flow rate and 10 cm bed height.....	1001
Figure 5.20: Effect of SO ₄ ⁻² initial concentration on the ion exchange breakthrough curve for Cl ⁻ on anion resin at 0.1 l/min flow rate and 10 cm bed height.....	101
Figure 5.21: Effect of flow rate on the ion exchange breakthrough curve for Cl ⁻ on mixed resin at 20 cm bed depth and an initial chloride concentration of 400 mg/l.....	102
Figure 5.22: Effect of bed height on the ion exchange breakthrough curve for Cl ⁻ on mixed resin at 0.1 l/min flow rate and an initial chloride concentration of 600 mg/l.	103
Figure 5.23: Effect of initial concentration on the ion exchange breakthrough curve for Cl ⁻ on mixed resin at 0.05 l/min flow rate and 40 cm bed height.	103
Figure 5.24: Comparison between experimental and theoretical breakthrough curve for Cl ⁻ (flow rate 0.05 l/min and 40 cm bed height).	105
Figure 5.25: Comparison between experimental and theoretical breakthrough curve for Cl ⁻ (20 cm bed height and 400 mg/l Cl ⁻).....	105
Figure 5.26: Comparison between experimental and theoretical breakthrough curve for Cl ⁻ (flow rate 0.1 l/min and 600 mg/l Cl ⁻).	1067
Figure 5.27: Comparison between experimental and theoretical breakthrough curve for Na ⁺ (flow rate 0.1 l/min and 485 mg/l Na ⁺).....	106
Figure 5.28: Comparison between experimental and theoretical breakthrough curve for Na ⁺ (flow rate 0.05 l/min and bed height 40 cm).	107

Chapter One

Introduction

In many developing nations, the control of pollution due to both industrial and domestic wastewater is a continuing major problem. The installation of wastewater treatment facilities lags significantly behind the development of industrial infrastructure. The net result of this lag is major pollution. In the other hand, water scarcity will become an even greater problem over the next two decades due to; population likely to double and climate change potentially causing reduction in precipitation more uncertain and variable, particularly in the Middle East region. Conservation of the quality and utilization of water resources is therefore a key issue facing national water authorities.

The wastewater in Eshidiya Plant, which is one of the phosphate mining industries that is located in Jordan, was studied in the present work. In phosphate mining industries a large amount of water in many stages mainly flotation cells is used to wash up clays and the undesired impurities. The phosphate ore is slurred hydraulically and pumped to a dressing plant, where the fine (slimes) with water are disposed to large impoundment. The immediate problem with phosphate slimes relate to their disposal which is associated with very large volumes, slow settling rate and poor dewatering characteristics. This poses possible environmental problems and delays the reclamation of the affected land for many years plus wasting a substantial amount of water. The district in which that phosphate mine (Eshidiya) lies, is suffering from water resources. The water source is mainly under groundwater which is limited and requires to be pumped to the surface. Hence, conserving and recycling used water is essential.

Effective solid-liquid separation persists to be a major problem in various operation units in wastewater treatment. In the phosphate mining industry the problems associated with disposing have generated research efforts to find economical and practical methods for enhancing the sedimentation and dewatering of the phosphate slimes (Mc Farlin *et al.*, 1993). Some used inorganic salts and organic flocculants to coagulate and flocculate the clays, such as lime, calcium chloride, magnesium chloride, and alum (Bratby, 2006; Gregory, 1993), which have been used for a long time as commercial coagulants in the clarification of water. However, these salts do not work well when the fraction of colloidal in the suspension is low (Hogg, 1980). In recent years, polyelectrolytes have become a primary choice as a conditioner for enhanced sedimentation and dewatering of the phosphate slimes operation. Conventionally, a single polyelectrolyte is used in sludge conditioning in which two main mechanisms are involved: charge neutralization and interparticle bridging (Bohm and Kulicke, 1997). Good control of polyelectrolyte dose is critical in sludge conditioning, since overdosing will increase cost and reduce sludge dewaterability. The optimal polyelectrolyte dosage is usually associated with the colloidal surface of minimum surface charge (minimum zeta potential) and a tendency to aggregate to form large floc (Christensen *et al.*, 1993).

Recently, there have been several studies on dual polyelectrolyte systems to improve flocculation of particles in water and wastewater treatment (Lee and Liu, 2000; Petzold, 2003), which is due mainly to the synergetic effects often observed in such system. While in the single polyelectrolyte system the flocculation is mainly due to charge neutralization, it is the polymer-polymer interaction which results in excellent interparticle bridging so that enhanced flocculation is obtained with double flocculants. Flocculation helps to increase the settling rate of phosphatic slimes waste, sediment dewatering and recycling the process water. Flocculation water treatment is characterized by low capital and operational expenses as compared to the other methods of water treatment (Hughes, 2000).

The supernatant water from the enhanced sedimentation process contains soluble ions which are mainly chloride and sulphate ions. These ions are associated with other cations (such as sodium, magnesium and calcium, etc.) caused blockage by deposits on the

flotation cells. To recycle the supernatant water as a step toward progressive system closure, the dissolved ions should be removed. Common commercial system for chloride and sulphate removal is reverse osmosis, although this system is expensive and difficult to maintain and operate. Occurrence of problems like membrane fouling may require frequent cleaning and production of brine in the form of reject creates a problem of effluent disposal. Mixed bed ion exchange column was chosen to study its performance and efficiency of removal the main dissolved ions in the supernatant water produced from the enhanced sedimentation process.

Mixed bed ion exchange column is a type of the ion exchange process; the cation-exchange and anion-exchange resins are intimately mixed and contained in a column. The thorough mixture of cation-exchangers and anion-exchangers in a single column makes a mixed-bed deionizer equivalent to a lengthy series of two-bed plants. As a result, the water quality obtained from a mixed-bed deionizer is appreciably higher than that produced by a two-bed plant.

An ion-exchange reaction is defined as the reversible stoichiometric interchange of ions between a solid phase (the ion-exchanger or resin) and a solution phase. The ion exchanger resins are solids and suitably insolubilized high molecular weight crosslinked polyelectrolyte hydrocarbon matrix carrying a positive or a negative electric surplus charge which is exchanged by mobile counter ions of opposite sign in the solution (Helfferrich, 1962). The matrix holds these counter ions and is elastic. Therefore, a liquid diffuses into the matrix and ions in the liquid are exchanged with counterions which are attached in the matrix. Exchangeable ions in cation and anion exchange resins are cations and anions respectively. It is the functional group that determines the chemical behavior of resins. Ion exchange beds consist of cation exchange resin or anion exchange resin or a mixture, resulting in removal of ions from the solution. The effluent concentration determines the service cycle operating time of a bed. Further resins are broadly classified as strong or weak acid cation exchange resins or strong or weak base anion exchange resins. This classification depends on the functional group attached to the insoluble polymeric structure. Since ion exchange is a reversible process, the resins can be regenerated so that

they are converted to their original forms and are capable of carrying out further ion-exchange.

As the ion exchange is a process that redistributes counter ions between solution and solid phases by diffusion so the modeling of ion exchange column can be considered as a combination of two mechanisms. Firstly the ions inside the resin particle diffuse to the boundary of resin bead and secondly the ions on the surface of resin bead crossing the film and coming into the bulk phase.

Numerous applications of ion exchange can be found in industrial operations particularly in removal or recovery of specific ions from the solution. Ion exchange is also used in environmental pollution control, particularly in removal of contagious metals, & waste water treatment. Streat (1999) discussed various applications of ion exchange in detail. Although development in different water treatment procedures have resulted in significant reduction of contaminant but ion exchange has not been replaced by any other process because of the high purity achieved by mixed bed exchange. Due to significant rise in high purity water requirement in semiconductor and as a step toward progressive system closure.

The present work considers enhanced sedimentation process by dual electrolytes conditioning followed by a continuous mixed bed ion exchange column to remove the remaining soluble salt, which are mainly chloride ions. Therefore, the main objective of this work is to explore this treatment process and find out the best parameters and a model that simulate the mixed bed ion exchange column.

The aim of the present work includes:

- Comparing the flocculation of different types of flocculants in order to find the most suitable for the studied water sample. The best flocculent is that gives minimum turbidity and zeta potential.
- Investigating the effect of the dual flocculent dosage on the flocculation and determine the optimum dosage of the dual polyelectrolyte added for the

enhancement of sedimentation, from zeta potential values and turbidity measurements and indicating the target zeta potential related to the best dosage of polyelectrolyte.

- Conducting the ion exchange batch experiments to determine the effects of several parameters such as initial solution concentration and amount of adsorbent on chloride, sulphate and sodium removal from the supernatant water.
- Using the Langmuir and Freundlich isotherm models for the evaluation of findings.
- Carrying out experiments using continuous anionic and mixed bed ion exchange to test its performance and find out the best parameters and a model that simulate the mixed bed ion exchange column.

Chapter Two

Literature Review

Waste clay disposal represents one of the most challenging problems for the phosphate industry (Zhang, 1993). Because of their colloidal nature and ultrafine size, the phosphatic clays are very stable in water suspensions and settle extremely slowly. It takes several years for waste clay slurry to thicken from about 3% to 20% solids by gravity settling. On the other hand, the phosphate mining industries required a large amount of water in many stages. More than 4 million m³ clean water annually is used to wash up clays, and the undesired impurities. So the reuse of the waste water is one of the important tasks for these industries (Raden, 1978).

In the phosphate mining industries, the disposing of the phosphatic waste store in ponds. This impounding approach is not preferred by the industry since a tremendous volume of water is tied up after self-weight consolidations, large amounts of phosphate are discarded, large areas of land are occupied, potential dam failures may cause environmental disaster and public outrage, etc.

To overcome the problems associated with the waste water disposal of the phosphate mining industries, many mechanical, biological, and chemical processes have been used, as it is explained in the coming paragraph.

History of the phosphate removal technologies

Since the 1950's, the problems associated with the disposing of phosphate clays and wastewater have generated many researchs to find economical and practical methods for the dewatering of clays and removing of phosphate from the wastewater (Farlin et al., 1993). Actually, the phosphate removal techniques fall into three main categories: physical, chemical and biological (Wang, et al., 2006).

In biological treatment plant, Living microorganisms (i.e. bacteria, microalgae, yeast, macrophytes) was used to enhance the flocculation of the phosphate wastes or to

absorption the dissolved phosphate (Smith et al., 1992, Van Loosdrecht et al., 1997). Even that this method is the less costly alternative to the other methods, but its efficiency is unfortunately much lower than the others in most wastewater treatment plants, so it needs to combine with another method to fulfil the purpose (Seung-Hyun et al., 1997). On the other hand, the biological method can be highly variable due to operational difficulties and the ambient temperature. For example it is observed that the phosphate bacteria are died in a temperature above 42.5°C (Jones and Stephenson, 1996).

The chemical technique is the most common methods for removing suspended solids in waste and drinking water (Stanley, 2001), by addition coagulant and flocculation aids. Some used inorganic salts and organic flocculants to coagulate the suspended solids. The former were inorganic electrolytes, such as lime, alum and ferric sulphate (Packham 1965). These salts are using however, they do not work well when the fraction of colloidal particles in the suspension is low (Hogg, 1980). The latter used were either polyacrylamides, such as those sold under the trade names Superfloc, Polyfloc, Separan, Nalco, or natural organic flocculation, such as starches, guar, gum, and tannins, have been used for the treatment of the phosphate slimes (Bronwell and oxford, 1977 and Gregory, 1978). The main disadvantage of the natural flocculants is that these are more susceptible to the biological attack.

The addition of the inorganic salts are to neutralizing the electric charge on suspended particles or zeta potential* to form microfloc. And to inform flocculation process the addition of salts should be followed by the addition of the flocculation solids (polyelectrolytes), which bringing together the microfloc particles to form large agglomerations (Ebeling, et al., 2004). Recently, the use of high molecular weight long-chain polymers has been used as replacement to the inorganic salts in the wastewater and drinking water industry for removal of suspended solids (David H. Bache, 2007). Advantages of the polymers are:

- lower dosages requirements,
- reduced sludge production,
- easier storage and mixing,
- no pH adjustment required,
- polymers bridge many smaller particles,

- improved floc resistance to shear forces (Tambo and Hozumi, 1979),
- reduced level of aluminium in treated water,
- Cost savings of up to 25-30% (Rout et al., 1999; Nozaic et al., 2001)

Because the chemistry of wastewater has a significant effect on the performance of a polymer, the selection of a type of polymer for use as a coagulant/flocculation aid generally requires testing with the targeted waste stream and the final selection is often more of an “art” than a science. Hundreds of polymers are available from numerous manufactures with a wide variety of physical and chemical properties. And, although the manufactures can often help in a general way, the end user must often determine from all the various product lines which is best for their particular application and waste stream, i.e. most cost effective.

2.1. Coagulation and Flocculation

Colloidal particles in nature normally carry charges on their surface, which lead to the stabilisation of the suspension. By addition of some chemicals, the surface property of such colloidal particles can be changed or dissolved material can be precipitated so as to facilitate the separation of solids by gravity or filtration.

Conversion of stable state dispersion to the unstable state is termed destabilisation and the processes of destabilisation are coagulation and flocculation (Gregory, 1993, Hughes, 2000). Often the terms coagulation and flocculation are used synonymously inspite of existing a subtle difference between the two (Hughes, 2000, Halverson, 1980). The Dispersion is strongly influenced by electro kinetic charge which, the colloidal particle in the wastewater carries it. This charge is usually negative in nature and causes adjacent particles to repel each other and prevents effective agglomeration and flocculation. As a result, charged colloids tend to remain discrete, dispersed, and in suspension. On the other hand, if the charge is significantly reduced or eliminated, then the colloids will gather together (i.e. destabilisation state). First forming small agglomerated groups, then larger

agglomerates of particles in suspension and finally into visible floc particles which settle rapidly and filter easily (Bratby, 2006).

The key to effective coagulation and flocculation is an understanding of how individual colloids interact with each other.

2.1.1. Stability of Colloids in Suspension

The attractive force between particles, known as Van der Waal force exists in case of colloidal particles in suspension. But the electrostatic repulsion of surface charges opposes the particles to come closer and form agglomerates. This surface charge of colloids can be positive or negative. However, most colloidal particles in wastewater have a negative charge.

Particles may acquire surface charges due to unequal distribution of constituent ions on the particle surface, preferential adsorption of specific ions, ionisation of surface groups, crystal imperfection, or any combination of these.

The colloidal particles are commonly classified as hydrophilic (e.g., proteins) and hydrophobic (e.g., clays, metal oxides). The principal mechanism controlling the stability of both hydrophobic and hydrophilic particles is the electrostatic repulsion (Montgomery, 1985).

- Hydrophobic colloids are made of small colloidal particles having little or no affinity for water (the solvent). Their stability is due to the presence of a charge which attracts other ionic species present in water and results in the formation of an electrically charged layer around the colloidal particles. So the colloidal dispersions of the hydrophobic type are thermodynamically unstable. If the charge layer is removed these particles tend to agglomerate spontaneously and can be removed from the wastewater.
- Hydrophilic colloids are typically formed by large organic molecules that become hydrated (solvated) when they are in the presence of water, so these molecules are thermodynamically stable in their solvated form. The charge in such molecules

originates from the presence of ionizable groups on the molecule that transform the molecule in a "macro-ion" when placed in solution. As a result of these charges hydrophilic colloidal particles are significantly hydrated when placed in solution and the agglomeration of these colloids typically involves the addition of significant amounts of ions which compete with the colloids for water molecules thus resulting in the dehydration of the colloidal particles ("salting out" of the colloid).

Besides electrical repulsion, a suspension may be stable due to the presence of adsorbed water molecules that provide a physical liquid barrier preventing particulates from making collisions and destabilisation.

2.1.2. Electrical Double Layer (EDL)

Oppositely charged ions in an electrolytic solution are attracted to the surface of a charged particle and can either be closely associated with the surface or distributed some way into the solution. Thus the two opposite forces, electrostatic attraction and ionic diffusion, produce a diffuse cloud of ions surrounding the particulate, which can extend up to 300 nm. This co-existence of original charged surface and the neutralizing excess of counter-ions over co-ions distributed in a diffused manner are known as the electrical double layer (Kruyt, 1952). Figure 2.1 gives a schematic diagram showing the nature of electrical forces around a colloidal particle in bulk solution and the various electrical potentials thus developed in the double layer.

An electric double layer consists of three parts:

- **Surface charge:** Charged ions (commonly negative) adsorbed on the particle surface.
- **Stern layer:** An inner layer of counterions (charged opposite to the surface charge) attracted to the particle surface and closely attached to it by the electrostatic force.
- **Diffuse layer (Gouy-Chapman layer):** A film of the dispersion medium (solvent) adjacent to the particle. Diffuse layer contains free ions with a higher concentration

of the counterions. The ions of the diffuse layer are affected by the electrostatic force of the charged particle.

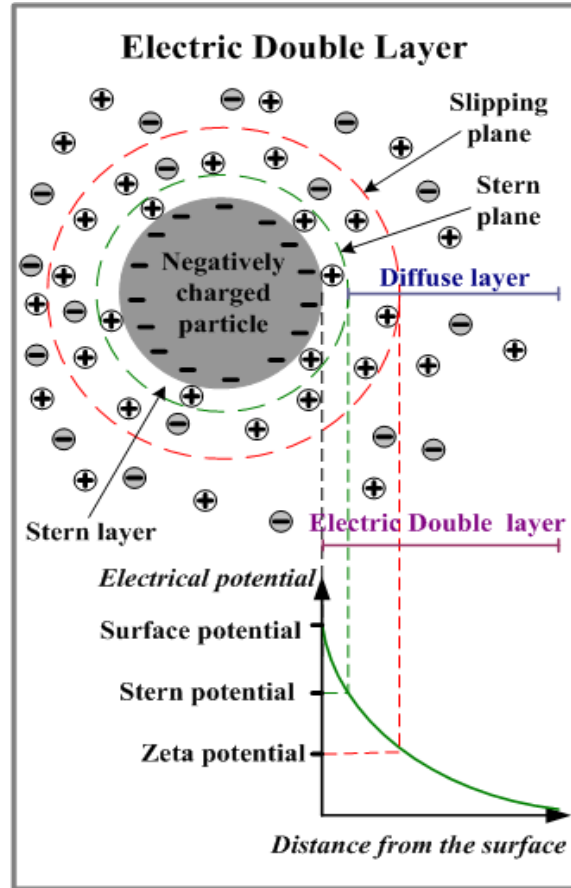


Figure 2.1: The Electrical Double Layer (EDL), (Hunter, 2001).

The thickness of the double layer depends upon the concentration of the ions in solution. A higher level of ions means more positive ions are available to neutralize the negative charge of the colloidal particle, and in turn a thinner double layer leading to an increased probability of intimate contact or collision between collide particles and hence coagulation or colloidal particle growth. On the other hand, a decrease in the ionic concentration reduces the number of positive ions resulting in a thicker double layer leading to increased dispersion. The electrical potential is at its maximum at the surface of the colloid and drops toward zero as the distance increases across the Stern layer and the diffuse layer, i.e., with increasing distance from the surface of the particle.

The potential curve indicates the strength of the repulsive force and the distance at which these forces come into play. The potential at the junction of the Stern layer and the diffuse layer is known as the Zeta potential (Hunter, 2001).

The stability of colloidal suspension is greatly influenced by the potential of the Stern layer. Though this potential cannot be measured directly, it is approximated to the zeta potential representing the electrical potential between the shear plane and the bulk solution (Russel et al, 1995).

2.1.3. Zeta Potential

A charged particle dispersed in an ionic medium tends to have a concentration of opposite ions attracted towards it. For example, a negatively charged particle collects a number of positive counter-ions. As one move further away from the particle, concentration of counterions decreases due to diffusion until ionic equilibrium is reached. A plot of the charge contributed by these ions versus distance from the particle surface (i.e. as it is plotted in Fig. 2.1) reveals the familiar exponential decay. Now, if the particles were imagined to be moving, it would tend to drag its counterions along with it while leaving behind the ions that are further away from its surface. This would set up a plane of shear and the value of the electric potential at the shear plan is called Zeta potential (ζ). In other words, zeta potential is the potential difference between the dispersion medium and the stationary layer of fluid attached to the dispersed particle and it is a scientific term for electrokinetic potential.

The significance of zeta potential is that its value can be related to the stability of colloidal dispersions. The zeta potential indicates the degree of repulsion between adjacent, similarly charged particles in dispersion. For molecules and particles that are small enough, a high zeta potential will confer stability (i.e. the solution or dispersion will resist aggregation). When the potential is low, attraction exceeds repulsion and the dispersion will break and flocculate. So, colloids with high zeta potential (negative or positive) are electrically stabilized while colloids with low zeta potentials tend to coagulate or flocculate.

Zeta potential is widely used for quantification of the magnitude of the electrical charge at the double layer. However, zeta potential is not equal to the Stern potential or electric surface potential in the double layer (Kirby, 2010). Such assumptions of equality should be applied with caution. Nevertheless, zeta potential is often the only available path for characterization of double-layer properties. Zeta potential should not be confused with electrode potential or electrochemical potential because electrochemical reactions are generally not involved in the development of zeta potential.

Zeta potential is measuring related to an experimentally-determined of the electrophoretic mobility. In practice, the Zeta potential of dispersion is measured by applying an electric field across an electrolyte, charged particles suspended in the electrolyte are attracted towards the electrode of opposite charge. Viscous forces acting on the particles tend to oppose this movement. When equilibrium is reached between these two opposing forces, the particles move with constant velocity. The velocity of a particle in a unit electric field is referred to as its electrophoretic mobility, which is proportional to the magnitude of the zeta potential. So the Zeta potential can be read off directly.

Drinking and wastewater in the developed nations of the world is treated to remove contamination. Zeta potential measurements can both evaluate the effectiveness of the chemicals used to clarify the water supply and optimize the amount of coagulant needed in the clarification process (Hendricks, 2011). Zeta potential can be used to monitor the water manufacturing process allowing for the adjustment of coagulant dosage levels periodically in order to minimize cost of chemicals in a water purification facility.

2.1.4. Balancing Opposing Forces

The DLVO Theory (named after Derjaguin, Landau, Verwery and Overbeek) is the classic explanation of how particles interact. It looks at the balance between two opposing forces (the electrostatic repulsion and Van der Waals attraction) to explain why some colloids agglomerate and flocculate while others will not.

- **Repulsion:** Electrostatic repulsion becomes significant when two particles approach each other and their electrical double layers begin to overlap. Energy is required to overcome this repulsion and force the particles together. The level of energy required increases dramatically as the particles are driven closer and closer together. An electrostatic repulsion curve is used to indicate the energy that must be overcome if the particles are to be forced together. The maximum height of the curve is related to the surface potential (Gregory, 1993).

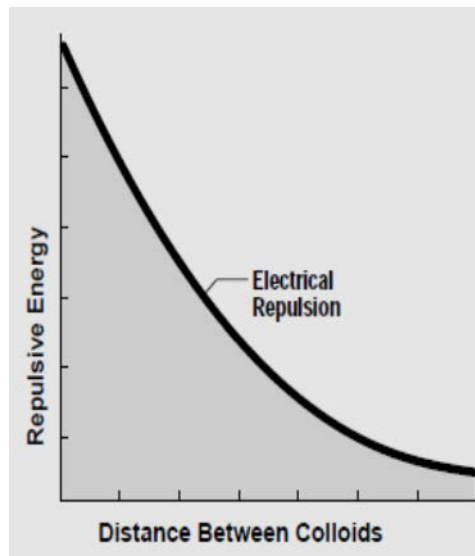


Figure 2.12: Repulsion Force, (Hunter, 2001).

- **Attraction:** Van der Waals attraction between two colloids is actually the result of forces between individual molecules in each colloid. The effect is additive; that is; one molecule of the first colloid has a Van der Waals attraction to each molecule in the second colloid. This is repeated for each molecule in the first colloid and the total force is the sum of all of these. An attractive energy curve is used to indicate the variation in attractive force with distance between particles (Gregory, 1993).

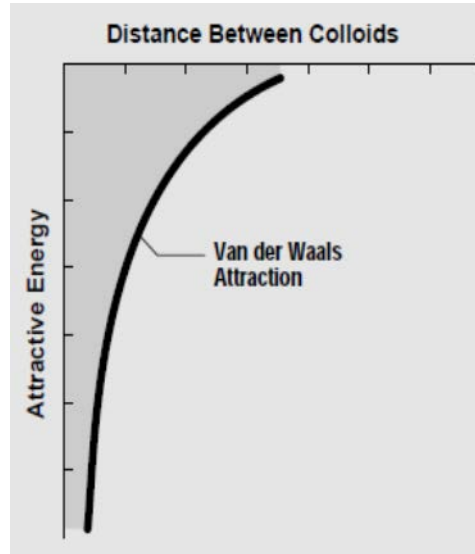


Figure 2.3: Van der Waals attraction, (Hunter, 2001).

2.1.5. The Energy Barrier

The DLVO theory combines the Van der Waals attraction curve and the electrostatic repulsion curve to explain the tendency of colloids to either remain discrete or to flocculate. The combined curve is called the net interaction energy (Gregory, 1993). At each distance, the smaller energy is subtracted from the larger to get the net interaction energy. The net value is then plotted (above if repulsive, below if attractive) and the curve is formed.

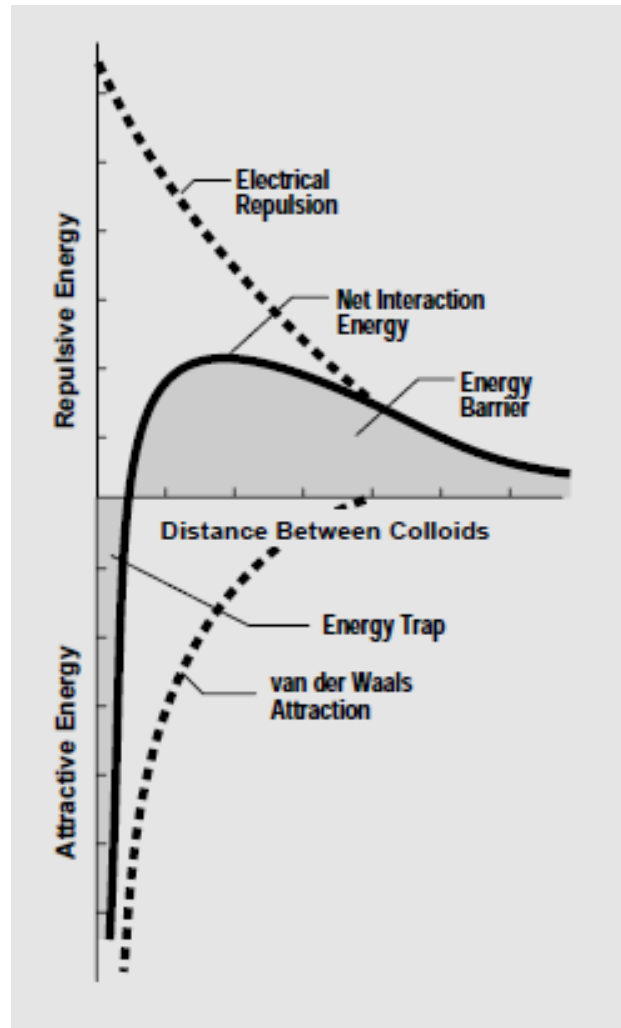


Figure 2.4: The net interaction curve, (Hunter, 2001).

The net interaction curve can shift from attraction to repulsion and back to attraction with increasing distance between particles. If there is a repulsive section, then this region is called the energy barrier, and its maximum height indicates how resistant the system is to effective coagulation.

In order to agglomerate, two particles on a collision course must have sufficient kinetic energy (due to their speed and mass) to “jump over” this barrier. Once the energy barrier is cleared, the net interaction energy is all attractive. No further repulsive areas are encountered and as a result the particles agglomerate. This attractive region is often referred to as an “energy trap” since the colloids can be considered to be trapped together by the Van der Waals forces (Hunter, 2001).

2.2. Flocculation Mechanism

As discussed earlier, the charge structure surrounding the particles is called the electrical double layer, which, for convenience is divided into Stern, and Diffuse (or Gouy-Chapman) layers. The former is the initial layer of adsorbed ions and molecules located at the particle surface. The charge presented to the solution at the Stern layer naturally attracts a diffuse layer of free ions with a net different opposite charge. For particles to make contact and aggregate, the potential at the Stern layer must be overcome (Hughes, 2000).

In order to cause the particles of a stable dispersion to flocculate, it is necessary to provide enough kinetic energy to particles to overcome the potential energy barrier (i.e. DLVO energy barrier). Alternatively, the barrier can be eliminated by surface-charge neutralization. This may be accomplished either by double layer compression (charge neutralization mechanism) or adsorption of flocculent onto the particle surface (bridging mechanism).

2.2.1. Charge Neutralization Mechanism

Polyelectrolytes of opposite charge to colloid surface, often work through charge neutralization. It is a practical way to lower the DLVO energy barrier and form stable flocs. The charge is neutralized by adsorption of these species onto the particle surface. An important case of this is the flocculation of negative colloidal particles with cationic polymers. In fact, in many cases, the action of cationic polymers can be explained in terms of their strong adsorption on negatively charged particles and consequent reduction of double layer repulsion, allowing aggregation to occur (Hunter, 2001).

Charge neutralization in fact occurs is reported by comparison of zeta-potential measurements with flocculation results, when it is found that optimum flocculation occurs at the point of total charge neutralization. For flocculation to proceed with pure charge-neutralization mechanism, it is neutral to expect that zeta-potential will be zero at the point of optimum flocculation. But in practice, the zeta potential tends to become negative at optimum flocculation with an increase in molecular weight of the polyelectrolyte

(Hendricks, 2011). This is because increasing molecular weight of flocculent favours bridging relative to charge neutralization mechanism. Thus in any system where flocculation is affected by the addition of electrolyte or oppositely charged polyelectrolyte, it is likely that some degree of charge neutralisation occurs, the extent depending upon the system characteristics.

It may be noted that the overdosing of the polyelectrolyte, can reverse the charge on the colloid, and redisperse it as a positive colloid. This process known as Steric stabilization and as a result the system will be poorly flocculated, this can be avoided by controlling the charge neutralization in the system by using the zeta potential. The detrimental effect of overdoing is especially noticeable with very low molecular weight cationic polymers that are ineffective at bridging (Hunter, 2001).

2.2.2. Bridging Mechanism

Long chain polymers, when added in small dosage to a suspension of colloidal particles, adsorb onto them in such a manner that an individual chain can become attached to two or more particles thus “bridging” them together. But interestingly this phenomenon is observed up to a particular optimum polymer dosage beyond which flocculation diminishes, a process being known as Steric stabilization (Hunter, 2001). The essential requirements for polymer bridging are that there should be sufficient unoccupied particle surface for attachment of polymer segments from chains attached to other particles and that the polymer bridges should be of such an extent that they span the distance over which interparticle repulsion prevails. Thus, at lower dosages, there is insufficient polymer to form adequate bridging links between particles (Hunter, 2001). With excess polymer, there is no longer enough bare particle surface available for attachment of segments and the particles become destabilized, which may involve some Steric repulsion. On average, bridging flocculation gives aggregates (flocs), which are much stronger than those produced by addition of salts (i.e., by reduction in electrical repulsion). However, such stronger flocs produced by the bridging mechanism may not reform once broken at high shear rates (David, 2007).

2.3. Polymeric Flocculants

Polymers or polyelectrolytes consist of simple monomers that are polymerized into high-molecular-weight substances (Metcalf and Eddy, 1991) with molecular weights varying from 10^4 to 10^6 Daltons are mostly water-soluble. Polymers can vary in molecular weight, structure (linear versus branched), amount of charge, charge type and composition. The intensity of the charge depends upon the degree of ionization of the functional groups, the degree of copolymerization and/or the amount of substituted groups in the polymer structure. With respect to charge, organic polymers can be cationic (positively charged), anionic (negatively charged) or nonionic (no charge) (David, 2007). Polymers in solution generally exhibit low diffusion rates and raised viscosities, thus it is necessary to mechanically disperse the polymer into the water. This is accomplished with short, vigorous mixing (velocity gradients, values of 1500 s^{-1} , although smaller values have been reported in the literature, 300 to 600 s^{-1}) to maximize dispersion, but not so vigorous as to degrade the polymer or the flocs as they form.

Polyelectrolytes act in two distinct ways: charge neutralization and bridging between particles as discussed earlier. The main applications of polyelectrolytes in potable water production are in coagulation and flocculation, and in the dewatering of treatment plant sludges. The sludges obtained from the various separation processes have very high water contents and must be further concentrated to minimize transportation costs; polymers have a role in this sludge conditioning.

Polymers are especially beneficial in coping with the problems of slow-settling flocs in low-temperature coagulation or in treating soft coloured waters, where they improve settle ability and increase the toughness of flocs (Faust and Aly, 1983). The capacity of a treatment facility may be more than doubled with the formation of larger and stronger flocs the rate of solid and water phase separation can be significantly increased, and the dosage of other chemicals lowered. Also, the range of waters that can be treated is wider.

2.4. Turbidity

Water containing particles is not clear and it is more or less cloudy. This cloudiness of water is called turbidity. Turbidity is a direct consequence of light scattering and it can be measured in two different ways. One way is to measure a reduction in intensity of the transmitted light and the other way, which has been used in the present work, is to measure an increase in scattered light intensity at a chosen angle (often 90 degrees) to the beam.

Light scattering depends on the size of the particles, their shape and their refractive index (Gregory, 2006).

Turbidity particles range in size from about 0.01 to 100 microns. The larger size particles tend to settle out or can be filtered out easily. The smaller sizes, (colloidal particles in the .01 to 5 microns), presents the real challenge. Their settling times are intolerably slow and they easily escape filtration, so as the phosphate colloidal nature (David, 2007).

2.5. Ion Exchange

Ion exchangers are solid materials that are able to take up charged ions from a solution and release an equivalent amount of other ions and of the same charge into the solution. The ability to exchange ions is due to the properties of the structure of the materials (Slater, 1991). The exchanger consists of also called matrix, with positive or negative excess charge. This excess charge is localized in specific locations in the solid structure or in functional groups. The charge of the matrix is compensated by the so-called counterions, which can move within the free space of the matrix and can be replaced by other ions of equal charge sign (Helfferich, 1962).

The pores sometimes contain not only counterions but also solvent. When the exchanger is in contact with the liquid phase, the solvent can travel through the exchanger and cause “swelling” to an extent that depends on the kind of counterions. Some electrolytes can also penetrate into the exchanger along with the solvent. As a result, there

are additional counterions, the so-called co-ions, which have the same charge sign as the fixed ions.

Although ion exchange is similar to sorption since a substance is captured by a solid in both processes, there is a characteristic difference between them: ion exchange is a stoichiometric process in contrast to sorption (Helfferich, 1995). It means that in the ion-exchange process, for every ion that is removed, another ion of the same sign is released into the solution. In contrast, in sorption, no replacement of the solute takes place.

Ion exchange is similar to adsorption, since mass transfer from a fluid to a solid phase is common in both processes, i.e. they are basically diffusion processes. So, it is generally accepted that adsorption and ion exchange can be grouped together as sorption for a unified treatment in practical applications.

Most of the mathematical theories and approaches have been developed originally for sorption rather than ion exchange. According to Helfferich (1995), the applicability of a simplified theory depends more on the mode of operation than on the particular mechanism of solute uptake.

A significant feature of physical adsorption is that the rate of the phenomenon is generally too high and consequently, the overall rate is controlled by mass (or heat transfer) resistance, rather than by the intrinsic sorption kinetics (Ruthven, 1984). Thus, ion exchange is viewed and in the present work as a “diffusion-controlled” process.

Ion exchange can be seen as a reversible reaction involving chemically equivalent quantities (Perry and Green, 1999). However, the characterization of an ion exchange as a “chemical process” is rather misleading. Ion exchange is in principle a redistribution of ions between two phases by diffusion, and chemical factors are less significant or even absent. The absence of any actual chemical reaction explains why the heat evolved in the course of an ion exchange is usually very small to negligible, often less than 2kcal/mol (Helfferich, 1995). Only when anion exchange is accompanied or followed by a reaction such as neutralization can the whole phenomenon be characterized as “chemical” A characteristic example is in chelating resins where the ion exchange is followed by a chemical reaction and bond formation between the incoming ion and the solid matrix.

2.6. Ion Exchange Materials

Ion exchangers are insoluble solids materials, which carry exchangeable cations or anions. When the ion exchanger is in contact with an electrolyte solution, these ions are exchanged with an equivalent amount of other ions of the same sign. Cation and anion exchangers are the materials that carry cations and anions, respectively. There are a number of different natural and synthetic materials that show ion-exchange properties. The predominant type used today is the synthetic organic resins because their characteristics can be tailored to specific applications. In table 2.1, a comparison of organic and inorganic ion exchangers is presented.

Table 2.1: Qualitative comparison of organic and inorganic ion exchangers.

Property	Organic Exchangers	Inorganic Exchangers
Chemical Stability	Good	Fair to poor
Thermal Stability	Fair to poor	Good
Mechanical Strength	Good	Variable
Exchange capacity	High	Variable
Regeneration	Good	Limited regeneration performance
Immobilization	Good	Good
	Immobilized in a variety of matrixes or can be incinerated	Converted into equivalent mineral structures
Cost	Medium to high	Low to high

One cannot say which resin structure is "better" without knowing the site-specific operating conditions. The "better" resin will be the one that has operating properties that match up best with the site's operating parameters, thus maximizing operating efficiency and cost effectiveness.

The resin matrix is a flexible network of hydrocarbon chains, where fixed ionic charges at various fixed positions are contained. They made insoluble by cross-linking the various hydrocarbon chains which forms a three-dimensional polymeric

structure. Cross-linked functional hydrocarbons are not soluble but can swell to a very high degree of the water content. Water molecules and ions (counterions) can migrate within the swollen polymeric network (i.e. network of hydrocarbon chains), but the counterions movement have to be compensated by corresponding counter-movements of other ions of the same charge to fulfill the electro neutrality principle (Inglezakis, 2006). The network structure of the ion exchanger is illustrated in Fig. (2.5).

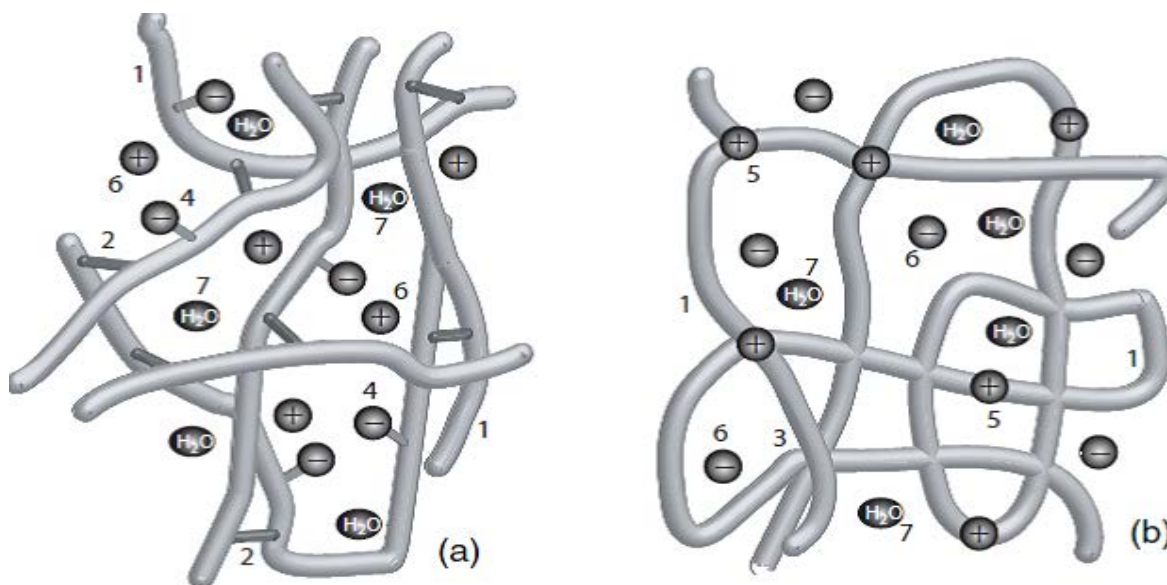


Figure 2.5: Schematic representations of polymeric ion exchangers, (Zagorodni, 2007).

2.6.1. Classification of Ion Exchangers

2.6.1.1 Ion Exchangers Classification Based On Matrix.

Polystyrene divinylbenzene: Ion-exchange resins are commonly manufactured from aco-polymer of styrene and divinylbenzene, this type of resin is the most conventional because of its chemical and mechanical stability (Zagorodni, 2007). The divinylbenzene content in the matrix determines the degree of cross-linking. So, 5% moldivinylbenzene in the matrix corresponds to 5% cross-linking. The degree of cross linking (i.e. the density of cross-links between polymeric chains) is connected to the properties of the resin. Low divinylbenzene

content means low cross-linking and the result is a soft resin prone to swelling in solvents. Then, the ion exchange potential is created by introducing fixed ionic groups (i.e. functional groups) into the resin matrix. Styrene-divinylbenzene matrixes can bear a wide diversity of functional groups. There are different cation exchange, anion exchange, amphoteric, and chelating materials of this type (Inglezakis, 2006).

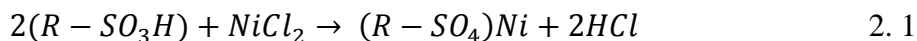
2.6.1.2 Ion Exchangers Classification Based On the Functional Groups

On the basis of the charge of the exchangeable ions, there are cation (positive mobile ions) and anion (negative mobile ions) resins. Both types are manufactured from the very same basic organic polymers. However, the ionic groups that are introduced into the matrix define the chemical behavior and the specific applications of the resin (Streat, 1999). Generally, resins can be typified into strong or weak acid cation exchangers and strong or weak base anion exchangers as it is present in Table 2.2.

Table 2.2: Functional groups of standard ion-exchange resins, (Inglezakis, 2006).

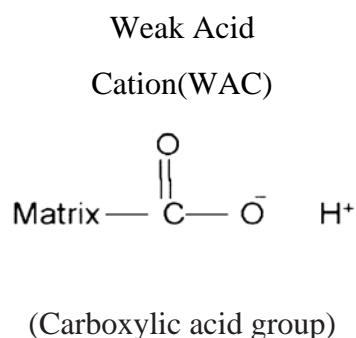
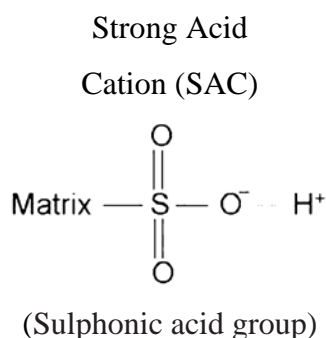
Type	Functional group
Cation exchange materials; negatively charged groups	
Strongly acidic	$-\text{SO}_3^-$
Weakly acidic	$-\text{COOH}^-$
Other acidic	$-\text{PO}_3^{2-}$
	$-\text{HPO}_2^-$
	$-\text{AsO}_3^-$
	$-\text{SeO}_3^-$
Anion exchange materials; positively charged groups	
Strongly basic	$-\text{[N(CH}_3)_3]^+$
	$-\text{[N(CH}_3)_2\text{C}_2\text{H}_4\text{OH}]^+$
Weakly basic	$-\text{NH}_3^+$
	$-\text{R1-NH}_2^+-\text{R2}$

Strong Acid Cation Resins (SAC): Strong acid resins are so named because their chemical behavior is similar to that of a strong acid. The resins are highly ionized in both the acid ($R-SO_3H$) and salt ($R-SO_3Na$) form. They can convert a metal salt to the corresponding acid by the reaction (Inglezakis, 2006):



R indicates the organic portion of the resin and SO_3 is the immobile portion of the ion active group. The hydrogen and sodium forms of SAC resin are highly dissociated and the exchangeable Na^+ and H^+ are readily available for exchange over the entire pH range. Consequently, the exchange capacity of SAC resin is independent of solution pH. These resins would be used in the hydrogen form for complete deionization; they are used in the sodium form for water softening (calcium and magnesium removal). After exhaustion, the resin is converted back to the hydrogen form (regenerated) by contact with a strong acid solution, or the resin can be converted to the sodium form with a sodium chloride solution.

Weak Acid Cation Resin (WAC): In WAC resin, the ionizable group (i.e. functional group) is a carboxylic acid ($COOH$) as opposed to the sulfonic acid group (SO_3H) used in SAC resin. The functional group of SAC and WAC resins are as below (Moses Road, 2004):



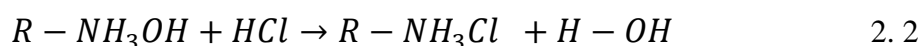
In the case of SAC resin, the sulphur atom is highly electro-negative and therefore attracts the electrons from the oxygen atom, which in turn attracts electrons from the hydrogen

atom making it more electro-positive. This property enables the resin to behave like a strong acid. It is therefore capable of splitting both types of salts (i.e. alkaline as well as neutral).

In the case of a WAC resin, however, the carbon atom is relatively less electro-negative and hence there is relatively less flow of electrons from the hydrogen atom, making it behave like a weak acid. While it is capable of splitting alkaline salts, it has no action on neutral salts.

In the other site, WAC resins exhibit a much higher affinity for hydrogen ions than do SAC resins. This characteristic allows for regeneration to the hydrogen form with significantly less acid than is required for SAC resins. The degree of dissociation of a WAC resin is strongly influenced by the solution pH. Consequently, resin capacity depends in part on solution pH, i.e. being able to exchange ions only if pH allows ionization of their functional groups (Cheremisinoff, 2002).

Strong Base Anion Resins (SBA): Like strong acid resins, SBA resins are highly ionized and can be used over the entire pH range. These resins are used in the hydroxide (OH) form for water deionization. They will react with anions in solution and can convert an acid solution to pure water (Inglezakis, 2006):



Regeneration with concentrated sodium hydroxide (NaOH) converts the exhausted resin to the hydroxide form.

Weak Base Anion Resins (WBA): These resins are like WAC resins, in that the degree of ionization is strongly influenced by pH. Consequently, WBA resins exhibit their maximum exchange capacity in the pH range up to 7.0. They hardly adsorb any strong acids but they cannot split salts.

2.7. Properties of Ion Exchange Resins

2.7.1. Swelling

Ion exchange resins are hygroscopic. Frequent swelling and contraction reduce the resin life.

Organic ion exchangers are hydrophilic, despite the hydrophobic nature of polymeric chains. And this is mainly because of the hydrophilic nature of functional groups and counterions and that is why, the amount of moisture hydrated by a resin is determined by the cross-linking and the type of functional group. Functional groups in both ionized and non-ionized states are solvated with polar molecules of the solvent (water in most cases). When an exchanger (ion exchange resin) is dry, its groups are non-ionized but polar, and thus hydrophobic. Sorption of the initial amount of water results in the ionization of the groups increasing their hydrophilicity even more (Gantman, 1992). Taking up the solvent usually increases the overall volume of organic ion exchangers, i.e. the materials expand, as shown in Fig. (2.6). This phenomenon is common for functionalized polymers. Inorganic ion exchangers are permeable to water; however, their expansion is restricted due to the rigidity of the crystalline structure.

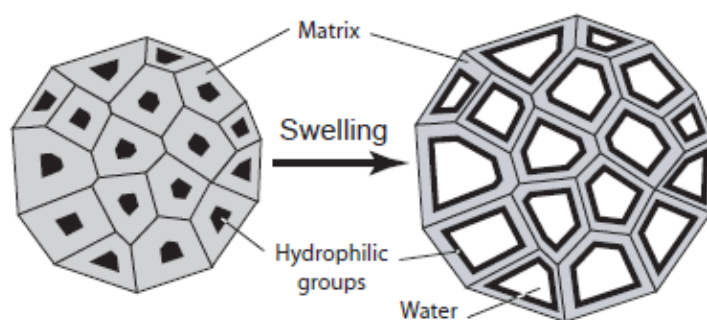


Figure 2.6: Ion exchanger, (Freger, 2002): dry (left panel) and swollen (right panel) states.

The main factors affecting the swelling of ion exchange resins are (Helfferich, 1962):

- Nature of the matrix.
- Degree of cross-linking.

- Nature of the functional groups.
- Capacity of the resin.
- Macrostructure of the exchanger.
- Nature of the counterion.
- Degree of association between functional groups and counterions (if there is any association).
- Nature of the solvent.
- Composition of the external solution.

Only the first five items reflect the intrinsic properties of the ion exchange material. Items 6 and 7 reflect the dependence of the swelling on the ionic form. The last two factors can be attributed to the external medium.

2.7.2. Capacity

Ion exchange capacity is a major characteristic of ion exchange materials. From a practical point of view, an ion exchanger can be considered as a “reservoir” containing exchangeable counterions. The counterion content in a given amount of material is defined essentially by the amount of fixed charges which must be compensated by the counterions, and thus is essentially constant. According to this fact, ion exchangers are quantitatively characterized by their capacity which is defined as the number of counterion equivalents in a specified amount of the material (dry weight/wet weight/wet volume, of the material) (Zagorodni, 2007).

Cross-linking decreases the capacity measured on the dry basis (fewer functional groups may be attached to highly cross-linked polymer molecules). However cross-linking also decreases hydration of the resin therefore the capacity measured on the wet basis increases with an increase of the cross-linking level.

Capacity data supplied by manufacturers occasionally refer to “air-dry” material (i.e. to the material containing an indistinct amount of water). A question may arise of how the

presence of counterions (the amount of the material) is taken into account in the capacity of the ion exchange resin. In most of the cases, the H^+ form of cation exchangers and Cl^- form of anion exchangers are selected as standard (i.e. the capacity is calculated per weight of the material including the weight of sorbed H^+ and/or Cl^- ions.).

The Cl^- form has been selected despite the logical use of OH^- form because of certain difficulties in handling the hydroxide forms.

2.7.3. Particle Size

Ion exchange resins are available in different particle (bed) size. Common ion exchange resins are manufactured in form of polydispersed spherical beds with the size distributed within the range 0.25-1.25mm or in form of uniform particle size (UPS). Smaller particles improve the kinetics of the ion exchanging reaction but cause increase of the water pressure drop and decrease of the flow rate (Streat, 1999).

2.7.4 Stability

Mechanical (physical) stability of ion exchange resins is determined mainly by the toughness of the polymer structure (cross-linking) and by the frequency of swelling-contraction cycles. Chemical degradation of ion exchange resins may be caused by fouling the resin pores by precipitates (e.g., iron hydroxide), breaking polymer structure, and loss of ion exchange capacity due to a modification of the functional groups (Streat, 1999).

2.7.5. Selectivity

Ion exchange works, in part, by selectivity. That is, ions with higher charge potential (valence) will usually replace those with lower strength charges. The selectivity of trivalent ions is higher than the divalent ions and divalent ions are higher than the monovalent ions.

For example we see aluminum (Al^{+3}), the trivalent charge of aluminum makes it very tightly held by a softener resin, and it may actually foul the resin because it becomes very difficult to remove unless regenerated with very high doses of salt at higher concentration (i.e., 15 percent).

The following will help put a value on selectivity (Slater, 1991):

Strong-acid cation (SAC 8-percent crosslinked) resin selectivity

- **Trivalent**

Lanthanum > cerium > chromium

- **Divalent**

Barium > lead > strontium > calcium > manganese > beryllium > nickel > cadmium
> copper > cobalt > zinc > magnesium

- **Monovalent**

Silver > cesium > rubidium > potassium > ammonium > sodium > hydrogen > lithium

As with any rule of thumb, there are exceptions. Barium is more selective than lanthanum. Lead is more selective than chromium (Cr^{+3} - Cr^{+6} is an anion specie). Silver is more selective than chromium and strontium. In fact, increasing the crosslinking (the divinylbenzene content) to 10 percent for SAC resin, it becomes more selective for silver than any other ion listed here (Slater, 1991).

Strong-base anion (SBA Type I) selectivity

Perchlorate > uranyl carbonate > citrate > iodide > bisulfate > nitrate > bromide > nitrite > cyanide > bisulfite > bromate > chloride > hydroxide > bicarbonate > acid phosphate > fluoride

The above is for a Type I SBA. Type IIs and weak-base anion have a slightly different order, which makes resin choice of prime importance when addressing different streams. Sulfate, for instance is preferred about 1.3:1 over nitrate with a Type I, whereas it is about 2:1 with a Type II. This makes a Type I less likely to dump nitrate towards exhaustion.

Anion exchangers can have multiple chemical functionalities, which can shift the selectivity from one ion to another for a specific task. So that selectivity is a comparative value, i.e. it indicates the preference of the material to one ion in comparison with another ion (Streat, 1999).

Property of the ion exchange material is the first option that is considered when a selective ion exchange system is designed. The most obvious starting point is the search for a possibility to exploit specific interactions between the ion exchanger and the targeted ion.

Direct electrostatic interactions between counterions and fixed groups can influence the selectivity even without formation of coordination or other chemical bonds. It can be considered as a formation of incompletely dissociated ion pairs. The strength of the electrostatic attraction depends on the ionic charge and the distance of closest approach between the counterion and the functional group. As a result, strong cation exchangers often prefer counterions with higher valence and smaller size. Higher polarisability of counterions also favor such interactions that is most pronounced for phosphonic acid groups which are excellent proton acceptors (Helffferich, 1962).

2.8. Ion Exchange Techniques

The two most common ion exchange techniques are the batch operation and the fixed-bed column operation (Lehto, 1995). First let us briefly discuss the advantages of these two techniques.

2.8.1. Batch Operations

These operations are rarely used in industrial processes, but they are well-suited for laboratory purposes due to the simplicity of the experimental setup. The treated solution and exchanger are simply mixed together in an agitated reactor. When the exchange is accomplished the phases are separated. Thus, a large number of experiments can be

carried out simultaneously. Batch technique is the only choice in a few cases. For example, many inorganic ion exchange materials (e.g. clays and some synthetic materials) are fine powders that often tend to agglomerate. When they are settled, a dense cake is formed blocking access of the solution to the particles and thus preventing any reasonable rate of Exchange (Lehto, 1995). The main drawback of batch process is that it cannot separate the ions completely if the material has a moderate affinity and hence, equilibrium distribution is established. The same can be said about non-separation applications where completeness of the process is also highly desirable. Other disadvantages of batch processes are their discontinuity and the requirements of the complicated phase-separation operations.

2.8.2. Column Techniques

The column techniques are used instead to achieve completeness of ion exchange reactions. This is possible even with the use of ion exchangers which do not possess a specific preference towards the target ion. In this, the most frequently used ion exchange technique, the material is packed in a column and all necessary operations are carried out in the bed (Dorfiner, 1991). Columns allow exploiting fine differences between properties of ions and fine preferences of ion exchange systems (which is usually impossible under batch conditions). The ions-containing solution moves through the column subsequently coming in contact with fresh portions of the material; this forces the reaction to shift increasingly in the desired direction (Irving, 2000). In effect, column exchange resembles carrying out a large number of successive batch operations in series (Lehto, 1995).

The column technique has many advantages in comparison to the batch operations and thus ion exchange in columns is widely used in practical applications.

A simplest column is a cylinder loaded with beads of an ion exchange material. The whole bulk of the exchanger inside the column including inter-bead voids is called the bed of ion exchanger or simply the bed. One or two sides of the cylinder are supplied with sieve- or grid-like manifolds that allow a free pass for solutions but keep the material from washing out. The beads do not move in course of the exploitation, while the flow of solution could

be both laminar and turbulent. Such reactors are called packed bed or fixed bed columns. The most conventional direction to pump solutions is up–down (Zagorodni, 2007).

Composition of the solution passing through the bed is changed due to the ion exchange reaction. The changes are not the same during the column process and depend on (Zagorodni, 2007):

- Properties of the ion exchanger (ionic form, capacity, degree of crosslinking, etc.).
- Composition of the feed solution.
- Operating conditions (flow rate, temperature, etc.).
- Shape and dimensions of the column.

The column technique is a logical replacement for the batch sequence. Passing through the bed, the solution contacts with fresh portions (layers, which are still completely in A form) of the exchanger again and again (see Fig. 2.7). One might say that, in the column, the solution goes routinely through a series of batch operations (Helfferich, 1962). If the column has sufficient length, the number of “batches” can be considered as infinite and complete exchange of ion can be achieved. Thus, all B ions are eventually replaced by A before the solution appears in the effluent.

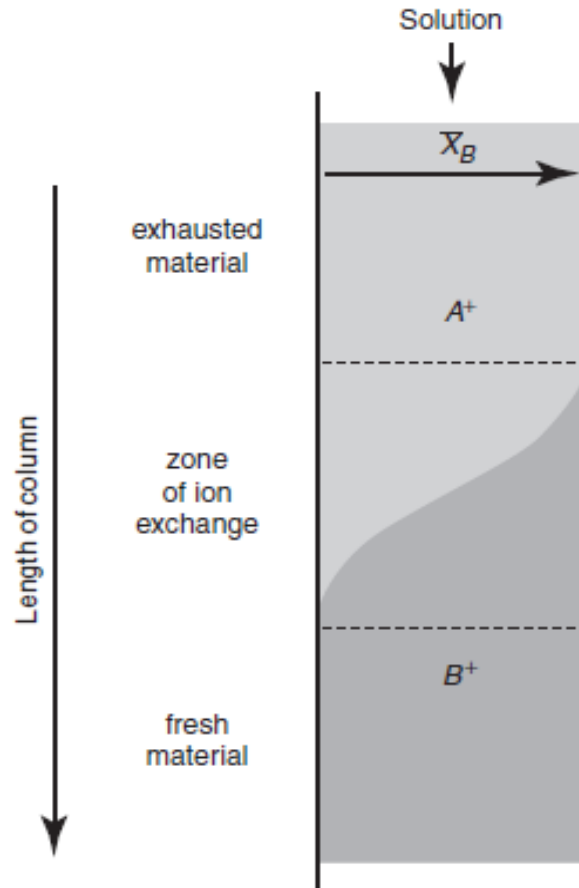
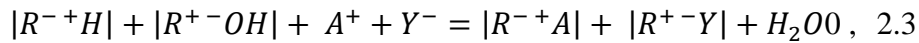


Figure 2.7: Division of an ion exchange column in three zones, (Zagorodni, 2007).

At any moment of the process, the bed can be divided in three regions as shown in Fig. (2.7). When the solution is first fed to the column, all B ions are exchanged for A in a zone at the top of the bed. The solution (now containing only AY) passes through the lower part of the column without further change in the composition. As the feed is continued, the top layers of the bed are constantly exposed to the fresh solution BY. Eventually, the top layer is completely converted to B form and loss their efficiency; they become “exhausted”. The zone of the column where the ion exchange takes place is thus transferred downstream. In due course, this zone reaches the bottom of the column and ions B first appear in the effluent. This moment is called the “breakthrough” of B. If the process targets purification of the solution, the operation is interrupted at or just before the breakthrough. Continuation beyond breakthrough results in a more complete conversion of the exchanger from ionic form A to B. When the conversion is completed, the whole material is in equilibrium with the feed solution. If pumping of the solution is continued, no further changes in the phase composition take place (Helfferich, 1962).

2.9. Mixed Bed Ion Exchange

In mixed-bed ion exchange the cation-exchange and anion-exchange resins are intimately mixed and contained in a single vessel. The thorough mixture of cation-exchangers and anion-exchangers in a single column makes a mixed-bed deionizer equivalent to a lengthy series of two-bed plants. And the water quality obtained from a mixed-bed deionizer is appreciable higher than that produced by two-bed plant (Helfferrich, 1962; Bennett, 2004). As a result of the close distances between beads belonging to two types of ion exchangers, the cation and anion exchange reactions take place in close proximity to each other. The overall reaction can be written as



where R^{-} and R^{+} represent two different ion exchange materials. The disappearance of H^{+} and OH^{-} ions due to the water formation shifts the equilibrium to the right-hand side. All interactions described by reaction (2.3) take place locally; the solution remains neutral. This secures a highly favourable equilibria of both processes involved and thus almost a perfect utilisation of the capacity and the highest degree of deionisation. Mixed bed provides ultra-pure water which is used in many industries with the major users being in nuclear power and electronics (Lehto *et al.*, 1999).

Significant drawback in the practical use of mixed bed systems is the difficulty of regeneration. No perfect solution has been found yet. In most of the cases two ion exchangers are separated, individually regenerated, and remixed again. The separation of two materials can be performed by pumping water upward through the column (Helfferrich, 1962; Bennett, 2004). After cutting off the water flow, the heavier cation exchanger settles below the lighter anion exchanger (density of conventionally used cation exchangers is ≈ 1.26 ; density of the anion exchangers is ≈ 1.07). A typical operation for the regenerable mixed bed column is presented in Fig. (2.8) (Helfferrich, 1962). After the sorption step the bed is fluidised with water. When the water flow is cut off the anion exchange resin settles on top of the cation exchange resin. The two layers are regenerated in sequence. First, alkaline solution is fed downward and removed through an outlet positioned at the

interface of the two materials. After a rinse removing the alkaline solution, the acidic regeneration is performed by pumping the acid at the interface and collecting the effluent at the bottom of the column. The residual acid is rinsed out and finally the bed is remixed (e.g. with air agitation). Feeding the regenerating solutions is accompanied by water pumping through “idle” layers. This is done to prevent the regenerants from entering the “wrong” ion exchangers.

Unfortunately, the complete separation is difficult to achieve. Remains of the foreign exchangers, undesirably involved in the separate regeneration procedures affect quality of the water produced in the following cycle. Thus, the main problem of the mixed bed reuse is mechanical in origin and arises from the need to separate the exchangers for regeneration. Cross-contamination of the individual materials with the wrong regenerant is a common outcome of incomplete separation of the cation and anion exchangers prior to the regeneration stage. As a result, non-regenerable mixed bed units are used in cases of high demand for the product quality. The mixture of exchangers is disposed after exhausting.

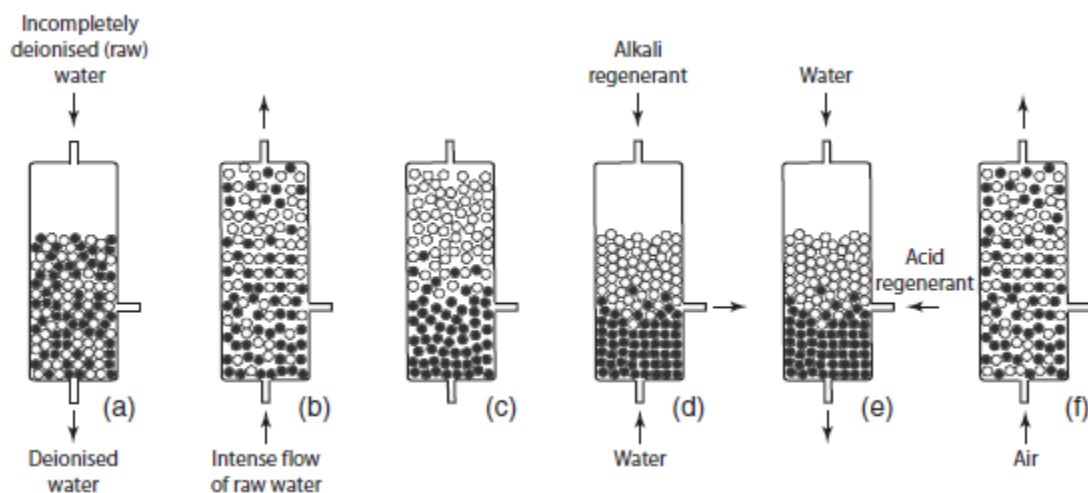


Figure 2.8: Operation steps of a regenerable mixed, (Helfferich, 1962).

2.10. Breakthrough Curve and Performance of Column

Any treatment of a solution with ion exchanger results in altering the solution composition. So far as the overall column process is dynamic, concentration variations at the column outlet are of primary concern. Plots

$$C_i = f(t) \quad \text{or} \quad C_i = f(V), \quad 2.3$$

represent concentration of species i at the outlet of the column. They are called breakthrough curves. In (2.4), t represents time from beginning of the process and V is the total pumped volume.

Let us continue to consider Fig. (2.7) suggesting a practical task to remove all B ions from the solution. Continuous pumping of the solution through the column gradually shifts the zone of ion exchange downwards. As was described in Section (2.8.2), at a certain moment of time the zone of fresh exchanger disappears and ion B breaks through the column. At breakthrough, the bottom layers of the bed are not yet completely converted to B form but the task of complete ion removal cannot be accomplished any longer. Figure (2.9) (Zagorodni, 2007) shows dependency (2.4) for the case when the pumping is continued after the breakthrough. Such plots are widely used to reflect the performance of ion exchange columns.

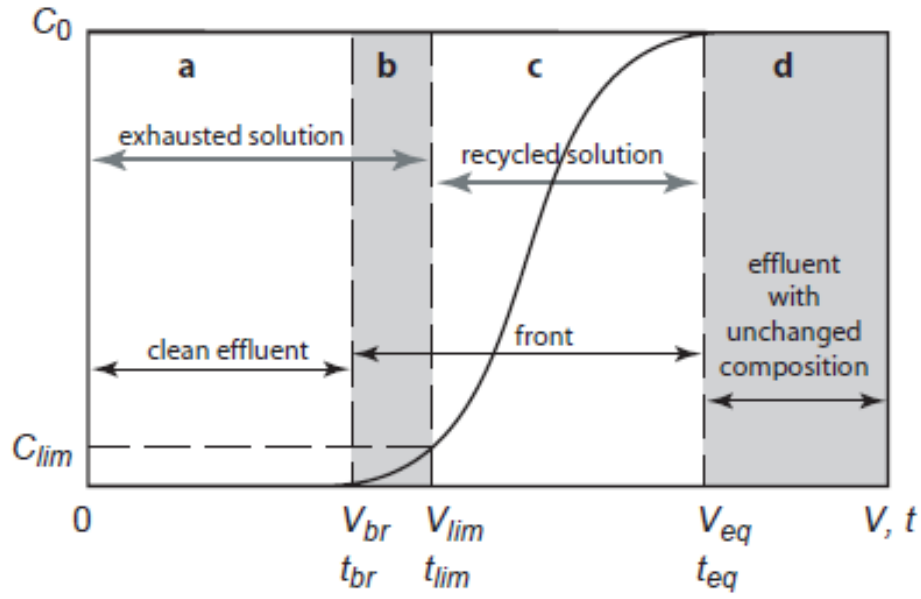


Figure 2.9: Breakthrough curve, (Zagorodni, 2007).

Breakthrough capacity is another important concept. The breakthrough capacity of the ion exchange column is the amount of ions (B in considered example) that can be removed from the solution by the column prior to the breakthrough. It is represented by region (a) in Fig. (2.9) and can be expressed as

$$Q_{br} = \int_0^{V_{br}} (C_o - C) dV, \quad 2.4$$

where C_o is the initial concentration of the targeted ion, C is the targeted ion concentration in the effluent, V is the volume passed, V_{br} is the volume passed until the breakthrough moment. For the simplest case the breakthrough capacity can be calculated as

$$Q_{br} = C_o \cdot V_b. \quad 2.5$$

More complicated expressions could be written if, for example, one specific ion is removed from a mixture. It should be noted that, contrary to different definitions of ion exchange capacity considered in section (2.7.2), breakthrough capacity is not a property of

the ion exchange material but a characteristic of the column performance under particular conditions. The breakthrough capacity is always less than the total ion exchange capacity of the column.

The total ion exchange capacity of the column can be determined from Fig. (2.9) summarizing square of regions (a), (b), and (c) laying above the breakthrough curve. The general expression for the column total capacity is

$$Q_{col} = \int_0^{\infty} (C_o - C) dV_0. \quad 2.6$$

That is directly related to the total capacity of the ion exchanger

$$Q_{col} = q \cdot m, \quad 2.7$$

where q and m are the total capacity of the exchanger and amount of the exchanger in the column, respectively. Of course, an infinite volume is not pumped through the column in practical operations. The pumping is completed when $C = C_o$ i.e. when the effluent composition does not differ from the composition of initial solution any more.

The approach based on Eqs (2.7) and (2.8) is commonly used for determination of the total ion exchange capacity (Zagorodni, 2007).

Practical operations do not require performing the process exactly until breakthrough or equilibrium points. The solution is pumped through the bed in one ionic form so far as the satisfactory conversion to another form is achieved (e.g. from economical or other practical point of view). Some limit for the effluent concentration (C_{lim}) is usually established. If removal of an ion is the purpose, C_{lim} reflects the maximum content of this ion allowed in the effluent ($C_{allowed}$). If the process is continuous, i.e. if the effluent is continuously sent for the following use, $C_{lim} = C_{allowed}$. If the effluent is averaged after the ion exchange treatment, for example, if the produced solution is collected in one reservoir, the following expression is valid.

$$C_{allowed} \cdot V_{lim} = \int_0^{V_{lim}} dV_0, \quad 2.8$$

Where V_{lim} is the volume pumped through the column until the moment when C_{lim} is achieved. Estimation of C_{lim} with Eq. (2.9) usually requires an extensive mathematical modeling of the column process to express the dependence $C = f(V)$. Direct monitoring of the effluent concentration followed, for example, by simple computer integration is a more convenient option for practical operations (Zagorodni, 2007).

Hereby, only a part of the exchanger bed capacity can be utilized for the practical purpose.

2.11. Ion Exchange Isotherm

Similar to other chemical processes, the ion exchange equilibrium can be characterized by the corresponding equilibrium isotherm, which are often described by isotherm equation that have been developed for processes other than the stoichiometric exchange i.e. adsorption or sorption. Generally, the isotherm is a graphical representation of the relationship between the equilibrium and all possible experimental conditions at constant temperature (Slater, 1991).

The physical process (reaction) of ion exchange or adsorption is considered to be so fast relative to diffusion steps that in and near the solid particles, a local equilibrium exists. Then, the so-called adsorption isotherm of the form $q = f(C_e)$ relates the stationary and mobile-phase concentrations at equilibrium.

The basic difference between adsorption and ion exchange is that while there is only one isotherm at a specified temperature for adsorption, more than one isotherm can exist at a specified temperature for different normalities of the solution in the exchange of ions of different valences due to the concentration–valence effect (Helfferrich, 1962). Thus, a specific ion-exchange system presents one equilibrium curve (isotherm) only under constant temperature and normality. This is why, while the term “isotherms” is used for the equilibrium curves in the case of adsorption, the term “isotherm–isonormal” should be used for ion exchange.

The surface equilibrium relationship between the solute in solution and on the solid surface can be described by simple analytical equations and the most important isotherm types are:

2.11.1. Langmuir Isotherm

Adsorbents that exhibit the Langmuir isotherm behavior are supposed to contain fixed individual sites, each of which equally adsorbs only one molecule, forming thus a monolayer, namely, a layer with the thickness of a molecule (Perry and Green, 1999):

$$\frac{q_e}{q_m} = \frac{K_L C_e}{1 + K_L C_e}, \quad 2.9$$

where q_e is the amount adsorbed per unit mass of adsorbent at equilibrium concentration C_e , q_m is the final adsorption capacity corresponding to complete monolayer coverage (mg/g), and K_L is an equilibrium Langmuir constant. The units of K_L are l/mol provided that C_e is expressed in (mol/l). Linearization of Langmuir model equation to fit experimental data requires rewriting it as:

$$\frac{1}{q_e} = \left(\frac{1}{q_m} \right) + \left(\frac{1}{q_m K_L} \right) \frac{1}{C_e} \quad 2.10$$

A plot of $(1/q_e)$ versus $(1/C_e)$ would result in a straight line with intercept $(1/q_m)$ and a slope of $(1/q_m K_L)$.

2.11.2. Freundlich Isotherm

The Freundlich monocomponent isotherm is obtained when an exponential distribution of adsorption energies is assumed,

$$N(Q) = \alpha \exp(-nQ/RT), \quad 2.11$$

where $N(Q)$ is the number of sites having adsorption energy Q and α, n are constants. It is assumed further that for each energy level, the coverage Θ follows the Langmuir isotherm

$$\Theta = \frac{bC}{1+bC}, \quad 2.12$$

where C is the sorbate concentration and the adsorption coefficient b depends on the adsorption energy in the form

$$b = b_0 \exp(Q/RT). \quad 2.13$$

The fraction of adsorption sites having energy of adsorption between Q and $Q+dQ$ occupied by sorbate is

$$d\Theta T(Q) = \Theta(Q)N(Q)dQ. \quad 2.14$$

The total coverage by the sorbate is obtained by integration of Eq. (2.15) over the whole range of adsorption energies, i.e. between the limits $-\infty$ and $+\infty$. The integral after substitution of $\Theta(Q)$ and $N(Q)$ from Eqs. (2.12)-(2.14) is

$$\theta_T = \int_{-\infty}^{\infty} \frac{b_0 \exp(Q/RT).C}{1+b_0 \exp(Q/RT).C} \times \alpha \exp(-nQ/RT) dQ, \quad 2.15$$

which yields

$$\theta_T = \frac{\alpha R T b_0^n}{n} C^n = A C^n, \quad 2.16$$

where A is constant under isothermal conditions. If the adsorption is expressed in terms of weight of adsorbate per unit weight of adsorbent q , then the Freundlich isotherm is written in the form

$$q_e = K_F C^{n,0} \quad 2.17$$

where $K_F = q_m A$ and q_m is a characteristic adsorption capacity. A and n are equilibrium constants characteristic to the system. To get the Freundlich equilibrium constants, Freundlich equation is written in an algorithmic form i.e. linearised form as (Fourest, 1994):

$$\log q_e = \log K_F + \frac{1}{n} \log C_e \quad . \quad 02.18$$

A plot of $\log q_e$ versus $\log C_e$ gives a straight line with a slope equal $(\frac{1}{n})$ and an intercept equal to $\log K_F$.

Thus, Freundlich adsorbents that follow the Freundlich isotherm equation are assumed to have a heterogeneous surface consisting of sites with different adsorption potentials, and each type of site is assumed to adsorb molecules, as in the Langmuir equation (Perry and Green, 1999).

2.12. Hydrodynamic Effects in Columns

Elements of a liquid flowing through a bed of exchanger beads do not have equal residence time (Slater, 1991) (i.e. velocity of the solution pumped through the bed is not the same in different points of the column). The non-uniform velocity of the solution is a result of the randomly packing with beads of the ion exchanger inside the columns which cause non-uniform cross section of voids between the beads. The phenomenon is illustrated by panel (a) of Fig. (2.10). The voids inside the column can be considered as a system of channels available for the liquid. The length of neighbouring channels is not necessarily the same. This contributes to the dispersion because different portions of the solution could pass different distances before joining together at some point of the bed (panel (b) of Fig. 2.10). The phenomenon is more pronounced for beds containing beads of non-uniform size and shape (Fig. 2.11a), but can however happen with any kind of packing. The resulting scattering of the front obeys, like diffusion, the laws of statistics with elements of fluid moving forwards, sideways, and backwards varying with position and time. The process

can be visualized as a random three-dimensional diffusion superimposed on the constant velocity flow. Such motion is also associated with a scatter in the residence time. While the phenomenon is well-pronounced, there is no unanimous point of view on its quantitative effect (Slater, 1991).

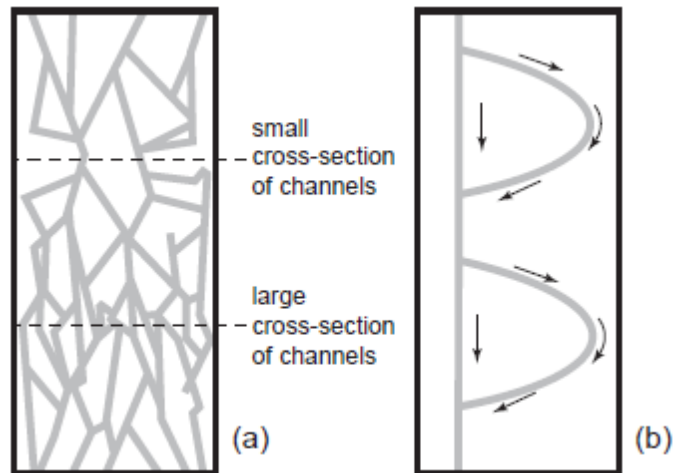


Figure 2.10: Eddy dispersion caused by different overall cross-section of the pass-ways (a) and by different length of different pass-ways (b), (Zagorodni, 2007).

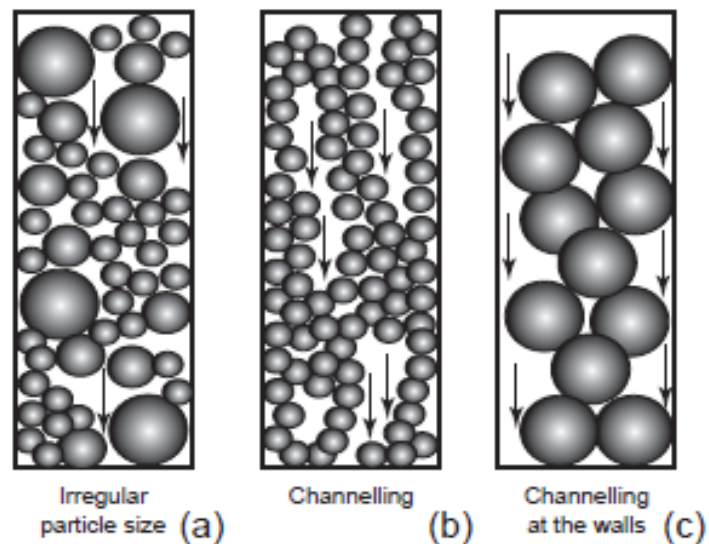


Figure 2.11: Flow maldistribution, caused by non-uniform packing (a), channelling (b), and wall effects (c), (Zagorodni, 2007).

Non-uniformity of the inter-bead voids is not the only cause for the hydrodynamic inhomogeneity. In an extreme case, relatively long open channels may form in the bed as shown in panel (b) of Fig. (2.11). The probability of such channeling is high if the bed significantly shrinks and swells during the operation. The channels cause a partial bypassing of the liquid to the exit without proper contact with the exchanger (Slater, 1991). The channeling phenomena caused by swelling can appear during the operation and, in some cases, only at repeated use of the same poorly packed column. This results in early breakthroughs of target ions through the column (Ernest, 1997), and in pure repeatability of operational cycles.

An uneven distribution of the solution velocity across the bed often occurs in columns of small diameter where most of the exchanger is located close to the walls (that is the most common case in laboratory experiments). The packing density is necessarily lower near continuous surfaces which restrict arrangement of the particles. The phenomenon is illustrated by panel (c) of Fig. (2.11). The flow rate at a distance of about one particle diameter from the wall can be more than twice as high as in center of the column (Schwartz 1953). The wall effect becomes significant when the bed diameter is less than thirty times the particle diameter (Helfferich 1962, Schwartz 1953).

The previously described hydrodynamic phenomena can be minimized by regular packing of the column and selecting the material with uniform particle size and shape.

2.13. Mechanism of Ion Exchange Processes

Ion exchange, like any heterogeneous process, is accomplished by transfer of ions to and from the inter-phase boundary, i.e. the chemical reaction itself, diffusion inside the material, and diffusion in the surrounding solution should be taken into account. Besides the two major phases, the thin film of solution at surface of the exchanger should be accounted separately. The film properties differ from properties of the surrounding bulk solution. Formation of this film is unavoidable.

The thickness of the inter-phase film be reduced by a rigorous agitation (an intensive stirring in batch processes or turbulent hydrodynamic flow in column systems), but can never take it completely.

To complete the overall picture of the interaction mechanism, the stoichiometric character of ion exchange must be emphasised. Any counterions which leave the ion exchanger are replaced by an equivalent amount of other counterions (Helfferrich, 1962).

This is a consequence of the electroneutrality requirement. When a counterion crosses the inter-phase boundary, an electric potential is created between two phases. This potential must be compensated by the movement of another counterion in opposite direction (ion exchange) or by the movement of a co-ion in the same direction (salt transfer).

As long as an ion exchanger can be considered as a “quasi-liquid”, the interface between the material and surrounding solution is no more than a limit beyond which the matrix (or crystalline structure in case of inorganic materials) does not extend (Helfferrich, 1991). No significant resistance to mass transfer can be expected from such an interface unless some species are deposited on the surface of the material. Thus, the mechanism of ion exchange can be presented by Fig. (2.12). The following steps can be listed:

- The first step is diffusion of the first ion from bulk of the solution towards the interphase film (process 2 in Fig. 2.12). This step can be easily manipulated because the diffusion transport in the bulk solution can be assisted with agitation. If a column process is considered, turbulence of the local flows between the exchanger beads can assist the mass transfer towards and from the inter-phase boundary.

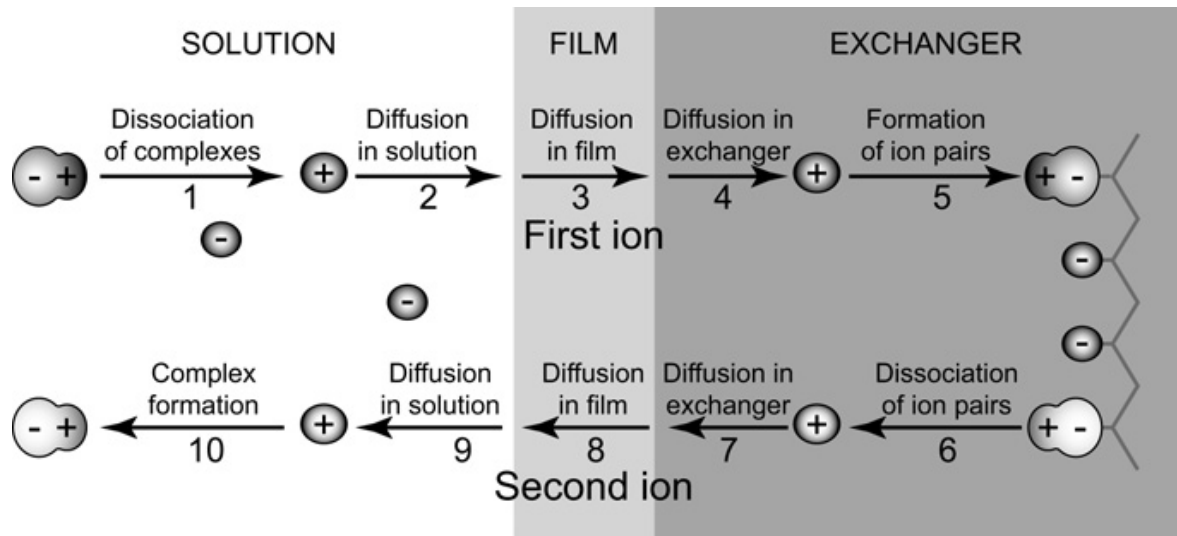


Figure 2.12: General mechanism of the ion exchange process, (Zagorodni, 2007).

- The next step is diffusion of the ion through the Nernst film (process 3). No convection can be established here. The mass transfer is defined solely by mobility of the ion. Agitation of the external solution can somehow reduce the thickness of the film but cannot remove it completely.
- After the transfer of the ion through the boundary between the film and the solid, the ion diffuses inside the phase of material (process 4). This process is defined solely by properties of the material and of the ion. The only driving force is the concentration gradient.

In order to fulfill the electro-neutrality principle, the above mentioned steps are compensated by the following:

- Second counterion diffuses from bulk of the ion exchange material towards the surface (process 7).
- After transfer of the second ion, through the boundary, it diffuses through the film towards the bulk solution (process 8).
- Finally, the second ion diffuses from the film into bulk of the solution (process 9).

There are also few steps which could accomplish the process:

- Dissociation of dissolved complexes which incorporate first ion (process 1).
- Association between first ion and functional group (process 5).
- Dissociation of associates between second ion and functional group (process 6).
- Association of second ion in the solution phase (process 10).

These processes could take place only if the system contains species which are able to form corresponding associates.

2.14. Rate-Determining Step

The mechanism of ion exchange consists of several steps, which take place in the heterogeneous system solution–Nernst film–ion exchanger. Simultaneous accounting of all these steps is a difficult, if possible, task. A conventional kinetic approach used to simplify calculations consists of selecting a limiting step for each process (Selemenev, 2004). According to this approach, rate of a multi-step process is defined by rate of the slowest step, i.e. the slowest step is the bottleneck for the overall rate (Helfferich, 1983).

This allows kinetic description of complicated heterogeneous processes with well-known equations developed for homogeneous systems. The heterogeneity is taken into account by use of corresponding limiting conditions (Selemenev, 2004).

The mechanism of ion exchange processes defines possible rate-determining steps. Let us continue to consider Fig. (2.12) and identify the crucial stages.

- Mass transfer (diffusion) in the solution or in other external medium (processes 2 and 9 in Fig. 2.12) is an unavoidable step in any ion exchange interaction. The process is well-known and described by conventional equations of diffusion. It can be easily assisted by hydrodynamic turbulences (for example, by stirring) and thus, is not considered as a possible limiting step for ion exchange.

- Mass transfer (diffusion) through the film surrounding the ion exchanger is represented by processes 3 and 8 in Fig. (2.12). The film is a solution zone of certain thickness with no convection. The mass transfer in the film is defined solely by the diffusion coefficients. The film thickness can be reduced by an agitation of the solution but the zero-thickness is not achievable.
- Mass transfer (diffusion) in the exchanger phase (processes 4 and 7) depends on the physico-chemical properties of the system and cannot be enhanced without altering the chemical system itself, i.e. without affecting selectivity and other important characteristics.
- Reactions between counterions and fixed groups (ion-pair association/dissociation), presented by processes 5 and 6, are the only chemical interactions that can affect the overall rate of the ion exchange.
- Complexes dissociation and formation in solution (processes 1 and 10 in Fig. 2.12) is not considered as a part of the ion exchange. Nevertheless, the complex formation can be the bottleneck for the overall process. In this case, the description uses well known mathematical approaches developed for solution chemistry and thus can be left out of this discussion.

As follows from these considerations, most of the ion exchange processes are purely diffusion phenomena, i.e. they are controlled by diffusion of the counterions rather than by actual chemical reactions. The main two rate determining steps which are diffusion-controlled and considered in most of the cases: diffusion of ions inside the material is referred to as particle diffusion and diffusion through the Nernst film is referred to as film diffusion. In simple cases, the rate of ion exchange is determined by the slower of these two processes (Helfferich, 1962).

The distinguishing between particle and film diffusion control is not an easy task because a simple increase of the solution concentration could alter the mechanism from film diffusion to particle diffusion control (Zagorodni, 2007). Cases intermediate between two described mechanisms are much more common i.e. the inter diffusion is almost equally fast in the bead and in the film. Thus, both mechanisms affect the rate of ion exchange and have to be accounted. This case is called mixed diffusion mechanism (Zagorodni, 2007).

Chapter Three

Experimental Work

The samples taken from the wastewater of Eshidiya phosphate plant located in Jordan to the laboratories of Al-Balqa Applied University for testing against enhanced sedimentation and for ion exchange investigations.

All the enhanced sedimentation experimental work was carried out in Zai water treatment station laboratories, while the ion exchange experimental work was carried out in Al-Balqa Applied University laboratories.

The water sample from all the experiments were collected and shipped in time to the Environmental Engineering Laboratory at the University of Jordan. The analysis was performed by using Titroprocessor and Ion Chromatography (IC).

- Titroprocessor manufactured by Metrohm Ltd., Titrimetric standard (Potassium hydrogen phthalate $\text{C}_8\text{H}_5\text{KO}_4$), Electrode (Combined pH electrode, e.g.6.0259.100).
- DX-120 Ion Chromatography (IC), Manufactured by Dionex,

The water obtained from Eshidiya mines was chemically analyzed; the results are shown in table 3.1.

Table 3.1: Chemical analysis of Eshidiya wastewater (main components).

Compositions	Concentrations (ppm)
Calcium ion, Ca^{2+}	234.4
Magnesium ion, Mg^{2+}	58.7
Sodium ion, Na^{+}	311.7
Potassium ion, K^{+}	7.2
Chloride ion, Cl^{-}	886
Sulfate ion, SO_4^{-2}	185
Phosphate ion, PO_4^{-3}	800
Nitrate ion, NO_3^{-}	58
Bicarbonate ion, HCO_3^{-}	95
pH=7.3	

3.1. Sedimentation

The sedimentation behavior of Eshidiya industrial wastewater was investigated using batch test analysis.

Equipment:

1000 ml graduated cylinder and a stop watch to measure the time need for sedimentation.

Procedure:

1. Wastewater sample obtained from Eshidiya mine complex was gently mixed to obtain homogeneity before pouring it into a graduated cylinder.
2. A volume of 1000 ml of the mixed sample was poured into a graduated cylinder.
3. The solids in the graduated cylinder started settling and a sample of water was taken for the turbidity test, with time recording for each sample.
4. After wastewater sample settling, the relative volume of the settled solid's layer in the graduated cylinder is recorded.

3.2. Enhanced Sedimentation (Coagulation-Flocculation)

Dual polymer systems (i.e. cationic and anionic polymers) were used in this study for enhanced sedimentation and water recovery. It was presumed that addition of cationic polymer neutralizes resistance of suspended solids to being agglomerated and forming distinguishable pinflocs. While the addition of anionic polymer achieve flocculation and clarity by attracts the pinfloc into a large snowflake-like formation which are heavy enough to settle faster under gravity force.

Chemicals used:

1. Cationic polyelectrolyte, Zetag 7557
2. Anionic polyelectrolyte, Magnafloc 919 and Magnafloc 336

Equipments used:

1. Zeta meter, the Zeta Meter 3.0 + Unit shown in Fig. (3.1) was used in the present study.
2. Turbidity meter, Micro 100 Turbid-meter was used in the present study.
3. Magnetic stirrer
4. Mixer with a flat paddle driven by a variable speed motor from 0 to 320 rpm.
5. Balance, (accuracy $\pm 0.001\text{g}$).
6. Graduated Beakers of 500 and 1000 ml, clear glass.
7. Graduated 250 ml cylinder, clear glass.
8. Syringe Injection.

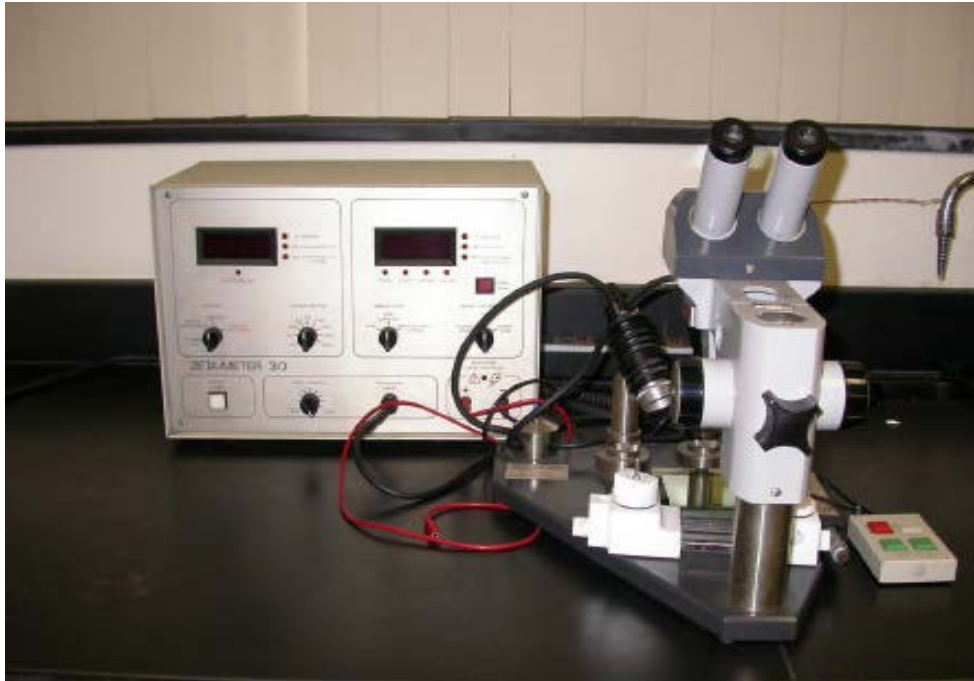


Figure 3.1: Zeta meter 3.0 +unit apparatus.

There are empirical "rule of thumb" that can be used to give a first estimate of the colloidal stability that the system is likely to have if the zeta potential of the particles is known.

An expanded set of guidelines, developed for particle suspensions, is given in table 3.2 (Schramm, 2005). Such criteria are frequently used to determine optimal dosages of polyelectrolytes used to effect coagulations in treatment plants.

The data obtained from turbidity meter and zeta meter were used to determine the most effective synthetic polymeric flocculants and optimum dosage for a successful operation.

Table 3.22 : Stability criteria based on zeta potential, (Schramm, 2005).

Stability Characteristics	Zeta potential (mV)
Maximum agglomeration and precipitation	+3 to 0
Excellent agglomeration and precipitation	-1 to -4
Fair agglomeration and precipitation	-5 to -10
Threshold of agglomeration (agglomerates of 2 to 10 colloids)	-11 to -20
Plateau of slight stability (few agglomerates)	-21 to -30
Moderate stability (no agglomerates)	-31 to -40
Good stability	-41 to -50
Very good stability	-51 to -60
Excellent stability	-61 to -80
Maximum stability- for solids	-81 to -100
Maximum stability - for emulsions	-81 to -125

The Experimental Procedure

1. A concentrated polymer solution of 0.5% (i.e. stock solution) was prepared by dissolving 0.5 g of dry polymer in 5 ml acetone and 95 ml de-ionized water. Then, the stock solution was mixed using a magnetic stirrer until all the granules have disappeared into homogeneous solution without lumps or fish eyes. After as much as 60 minutes of stirring, a viscous and homogeneous solution was formed, which was used within two days of preparation. A fresh working polymer solution of 0.05% was prepared by dilution of concentrated stock solution.
2. To determine the optimum dosage of the co-mixed cationic and anionic polyelectrolytes, a sample of untreated wastewater was poured first in a beaker and mixed at 100 rpm to be homogeneity. The cationic polymer was initially added to

the beaker using the syringe and mixed at 100 rpm for 30 s. The anionic polyelectrolyte was then added and mixed for 30 s at 100 rpm, and subsequently with slow mixing (50 rpm) for another 90 s. Then, the stirrer was removed from the sample to allow the flocculation under gravity for 10 minutes.

3. All the water samples were taken using syringe at a 3 cm below the surface of treated wastewater to measure its zeta potential and turbidity. It should be mentioned that the water sample is taken for zeta potential measurement direct after removing the mixer, while the sample for turbidity measurement is taken after 10 minutes of sedimentation.
4. Zeta potential was measured for the water sample. It should be noted that when measuring zeta potential each sample was measured 10 times, i.e. there was the same sample portion in the cell under 10 measurements. These results are reported as repeatability in this work. Repeatability was expressed as standard deviation.
5. The turbidity was measured for the supernatant water.
6. The experimental procedure from step 2 was repeated by varying the anionic dosage (5, 7, 10, 15, 20, 25 and 30 mg/l) with the several doses of the cationic polyelectrolyte. The turbidity and zeta potential of the supernatant water samples produced from using different polymers have been compared under different dosage to find the optimal dosage of the co-mixed cationic and anionic polymer.
7. The volume of sludge and settling rate, that obtained by using the optimal dosage of dual polyelectrolyte, was measured. The results were compared with the results that measured for the wastewater sample without any addition of the flocculants.

The measuring procedure was as follows:

- a. A graduated 250 ml cylinder was filled with 250 ml wastewater sample.
- b. The pre-calculated dose of cationic polymer was added to the water sample by using syringe. Then, cylinder was inverted six times followed by the addition of the pre-calculated anionic polymer and again cylinder was inverted six times. The consistent mixing is important.
- c. The time required for the sludge zone to move from the 220 ml mark and the 170 ml mark on the graduated cylinder was recorded.

- d. The settling rate was calculated by dividing the measuring distance between 220 ml and 170 ml, by the recorded time (from step c).
- e. The sample was allowed to settle for 30 minutes and the final sludge volume was measured.
- f. The experimental procedure of measuring settling rate was repeated but without using flocculants and the sample was left for 24 hours before measuring the settling volume.

3.3. Ion Exchange Processing

Ion exchange processing can be accomplished by either a batch method or a fixed-bed (column) method. In the first method, the resin and solution are mixed in a batch tank, the exchange is allowed to come to equilibrium, and then the resin is separated from solution. In the fixed-bed (column) method, solution passing through a column, containing a bed of exchange resin, is analogous to treating the solution in an infinite series of batch tanks.

Chemicals used:

- Purolite® MB400
- Purolite® A400
- Sodium hydroxide (NaOH)
- Sodium chloride (NaCl)
- Sodium sulfate (Na₂SO₄)
- Silver nitrate (AgNO₃)
- Potassium chromate (K₂CrO₄)

Equipment used:

- Magnetic stirrer.
- Filter papers.

- Glass column made of Pyrex glass (3 cm internal diameter and 65 cm long). The inside walls of the column are welded in the bottom section with a glass dish to support the resin.
- Pump.
- Flowmeter.
- Tank for solution.
- Burette and stand.
- Volumetric and conical flasks.
- Beakers.
- Graduated cylinders.

3.3.1. Batch Process

The stock solution was prepared and used with a clear water sample layer (supernatant water sample) in the batch test to find out:

1. The effect of adsorbent (ion exchange resin) quantity and initial contaminations concentration.
2. The isotherm model.



Purolite® MB400 (Mixed Resin)



Purolite® A400 (Anion Resin)

Figure 3.2: Ion exchange resins

Preparation of the ion exchange resin

The ion exchange resin (Purolite® A400) is a strong base, anionic ion exchange resin. Before the ion exchange resin was used in the experiments, it underwent pretreatment according to a procedure recommended by the manufacturer, which is as follows:

- First the resin was loaded into a column and washed several times with deionized water.
- The resin was converted to the OH⁻ form by washing it with 1N NaOH.
- The washing process was completed, when the pH of the influent and effluent solution is equal.
- Next, the resin was washed with deionized water until the pH is near neutral or at an acceptable level.

The experimental procedure of the batch method

1. Sodium chloride solutions (200, 400, 600, 800 mg/l chlorid) were prepared by weighing in analytical balance and dissolving an appropriate quantity of sodium chloride (NaCl) in deionized water, and the same procedure was followed to prepare sodium sulphate solutions (100 and 200 mg/l sulphate) from sodium sulfate (Na₂SO₄). These solutions are used with the anion resin.
2. Other working solutions were prepared containing both the chloride and sulphate ions. The chloride concentrations used are (200, 400, 600, 800 mg/l) that variation with the sulphate concentrations (100 and 200 mg/l). These solutions used with the mixed bed resin.
3. To observe the effect of adsorbent dosage on the contaminations removal, different amounts of anion resin and mixed bed resin were used with 100 ml of prepared water solution at different concentrations to conduct the batch ion exchange experiments.
4. The samples were agitated at constant speed with magnetic stirrer during 1.5 h and then filtered by a filter paper to get the clear solution.
5. The clear solution was analyzed in order to determine the contaminations content.
6. All the experiments have been taken at room temperature.

7. The initial and final concentrations of the contaminations ions were measured to obtain the sorption capacity (q) and the removal efficiency.
8. It is worth to mention that the experimental runs, which were done by using chloride stock solution, were repeated twice to insure reproducibility of the results. The reported experimental data is the average of the two runs.

3.3.2. Fixed-bed (column) process

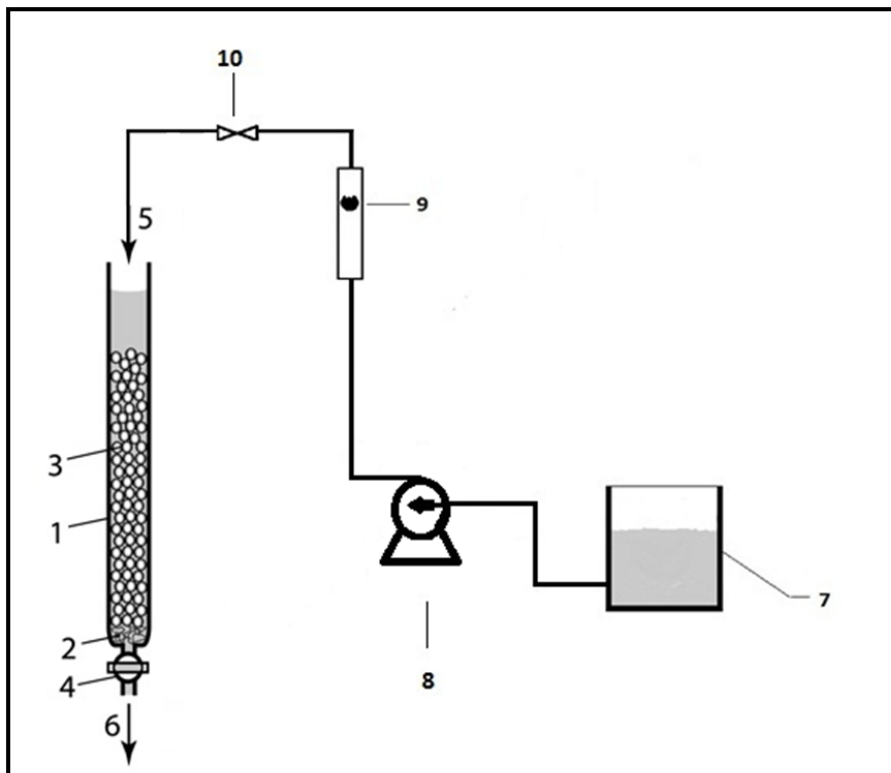


Figure 3.3: Schematic diagram of the experimental system: (1) Vertical cylindrical glass column; (2) a glass dish; (3) granular ion-exchange material (resin); (4) flow adjustment valve; (5) flow of raw solution; (6) effluent; (7) feed solution tank; (8) inlet feed pump; (9) flowmeter; (10) flow adjustment valve.

The experimental procedure

1. The same working solutions that were used in the batch test were prepared to use in the column test.
2. 20 l of the working solution which is prepared in a specific contaminations concentration was poured in the main tank.
3. The anion resin was used after the regeneration process, by pouring a small portion of it in the column then deionized water was added to keep about 1/4 inch of it above the resin.
4. The deionized water and resin was poured to the column alternatively until reaching the desired height of the bed.
5. To remove any trapped air bubbles in the packed bed, the column was tapped during packing with deionized water.
6. The experimental system used is schematized in Fig. (3.3), and before operation, the bed was left overnight to ensure a closely packed arrangement of particles with no void, channels, or cracks.
7. The pump was turned on and the flow rate was adjusted to the desired amount.
8. The discharged water sample was titrated with 0.01N silver nitrate during the experiment, to estimate the chloride concentration in the samples. 2-3 drops of potassium chromate was added to the water sample before titration as indicator.
9. The fixed-bed ion exchange experiment was complete when the concentration of chloride in the main tank is equal to its concentration in the effluent water (i.e. from the packed column) which is both measured by titration with silver nitrate.
10. A sample of effluent water is taken every ten minutes and sent to the laboratory for analyzing.
11. It should be mentioned that the height of water over the resin (i.e. packed bed) is controlled by adjusting the manual valve in the end of the packed column, so it does not became more than 20-30% of the total bed height.
12. The mixed ion exchange resin was used directly as it comes from the container. And when the column was packed, the mixed resin was washed with three bed volume of the deionized water and also was left overnight before starting the experiment.

13. The same experimental procedure was done with the mixed resin, but this type of resin contains an indicator that changes the resin color when it is exhausted. So the chloride concentration does not need to be calculated. The mixed resin color changing can be seen clearly in Fig. (3.4).

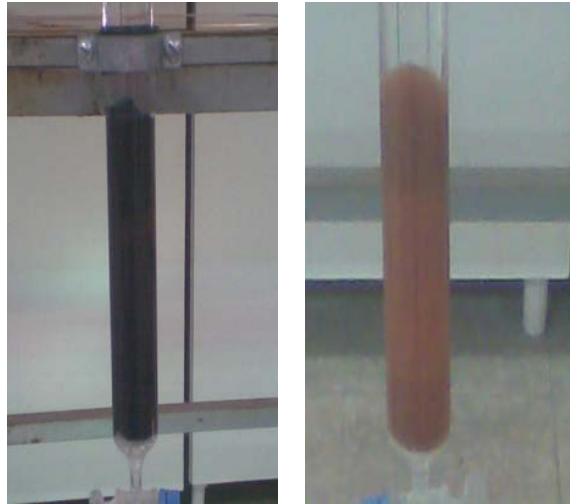


Figure 3.4: Mixed bed ion exchange

Chapter Four

Modeling Fixed-Bed Ion Exchange

In the modeling and design of an ion exchange system, the knowledge of the main principle is important and many practical aspects have to be dealt with adequately. For example time have to be included in our model, since ion exchange operations are held in batch or fixed beds and exhibit a dynamic behavior. It means that steady state operation is not the case in ion exchange systems in contrast to many other chemical operations that are independent of time. Fixed bed is the most frequently used operation for ion exchange and adsorption, as it is the predominant way of conducting such sorption separations. Moreover, ion exchange and adsorption are common operations used for wastewater treatment. The breakpoint concentration is a selected limiting value (according to the needs of the treatment) where the operation should be stopped and the breakpoint volume is the most important information, which is the fluid volume that can be treated by the column until a pre-specified breakpoint.

Predictive modeling of fixed-bed systems requires extensive experimental information (laboratory and pilot-scale experiments) and complex mathematical tools; and in many cases, for complicated multicomponent solutions, the full modeling of the process is extremely difficult (Zagorodni, 2007).

Different models have been developed targeting to solve different problems and discrepancies in the description of ion exchange equilibria. No approach satisfying all the demands has been found yet. Probably, the problem is very far from its solution (Zagorodni, 2007). For example, one of the main obstacles is the dualistic nature of ion exchange materials i.e. describing the ion exchange as a chemical reaction or as an inter-phase distribution process.

4.1. Basic Model Consideration

In the following, the one-dimensional model is adopted. The ideal models assume that concentration and temperature gradients occur in the axial direction (Froment and Bischoff, 1990).

4.1.1. Material balance equation

Consider a solution of concentration of C_W (mol/vol of fluid) entering at W in a control volume of length Δz and effective cross-sectional area A , with a volumetric flow rate Q (figure 4.1). The reaction takes place with rate $(-R)$ in (mol disappearing/time vol of the reactor) and the exit concentration is C_E (mol/vol of fluid).

Under the assumption of complete mixing in the radial direction, the material balance is

$$\left\{ \begin{array}{l} \text{Rate of change} \\ \text{in the direction} \\ \text{of flow due to} \\ \text{flow and axial} \\ \text{dispersion} \end{array} \right\} - \left\{ \begin{array}{l} \text{rate} \\ \text{of} \\ \text{consumption} \end{array} \right\} = \left\{ \begin{array}{l} \text{rate of} \\ \text{accumulation} \\ \text{of moles} \end{array} \right\} . \quad 4.1$$

The terms in this material balance are in moles per unit time.

In the following analysis, ε is the volume occupied by the fluid phase per unit volume of the control element. Then, the corresponding volume fraction for the solid phase is $(1 - \varepsilon)$.

The first term in Eq. (4.1) is:

$$\left\{ \begin{array}{l} \text{Rate of change} \\ \text{in the direction} \\ \text{of flow due to} \\ \text{flow and axial} \\ \text{dispersion} \end{array} \right\} = \left\{ \begin{array}{l} \text{axial} \\ \text{dispersion} \\ \text{term} \end{array} \right\} + \left\{ \begin{array}{l} \text{flow} \\ \text{term} \end{array} \right\} , \quad 4.2$$

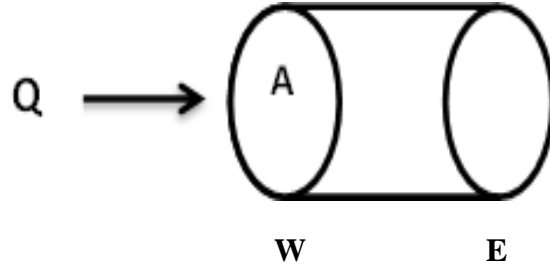


Figure 4.1: Control volume in a fixed bed.

where

$$\left\{ \begin{array}{c} \text{Axia} \\ \text{Dispersion} \\ \text{Term} \end{array} \right\} = [\text{outlet} - \text{inlet}] = \left(-D_L A \frac{\partial c}{\partial z} \Big|_W \right) - \left(-D_L A \frac{\partial c}{\partial z} \Big|_E \right), \quad 4.3$$

$$\left\{ \begin{array}{c} \text{Flow} \\ \text{Term} \end{array} \right\} = [\text{outlet} - \text{inlet}] = (Q C_W) - (Q C_E).$$

The reaction is considered to take place only on or within the solid particles and thus the consumption rate per unit volume of particles is

$$\rho_p (-r_m) \quad . \quad 4.4$$

The volume of particles in the control element is

$$(1 - \varepsilon) A \Delta z \quad . \quad 4.5$$

Thus,

$$\left\{ \begin{array}{c} \text{Rate} \\ \text{of} \\ \text{consumption} \end{array} \right\} = A(1 - \varepsilon) \Delta z [\rho_p (-r_m)] \quad . \quad 4.6$$

The accumulation of moles in the liquid phase is

$$\frac{C_E - C_W}{\Delta t} . \quad 4.7$$

The units of this term are moles per unit time per unit volume of fluid phase. The volume of the fluid phase in the control element is

$$\varepsilon A \Delta Z , \quad 4.8$$

and thus

$$\left\{ \begin{array}{c} \text{Rate} \\ \text{of} \\ \text{consumption} \\ \text{of moles} \end{array} \right\} = \varepsilon A \Delta Z \frac{C_E - C_W}{\Delta t} . \quad 4.9$$

The material balance becomes:

$$\begin{aligned} & \left(-D_L A \frac{\partial C}{\partial z} \Big|_W + Q C_W \right) - \left(-D_L A \frac{\partial C}{\partial z} \Big|_E + Q C_E \right) \\ & - (1 - \varepsilon) A \Delta Z [\rho_p (-r_m)] = \varepsilon A \Delta Z \frac{C_E - C_W}{\Delta t} . \end{aligned} \quad 4.10$$

Dividing by the term $(A \Delta Z)$ we have:

$$\begin{aligned} & \frac{D_L}{\Delta Z} \left(-\frac{\partial C}{\partial z} \Big|_W + \frac{\partial C}{\partial z} \Big|_E \right) + \frac{Q}{A \Delta Z} (C_W - C_E) \\ & - (1 - \varepsilon) [\rho_p (-r_m)] = \varepsilon \frac{(C_W - C_E)}{\Delta t} . \end{aligned} \quad 4.11$$

Setting $\Delta Z \rightarrow 0$, we can derive the differential form of Eq. (4.11). Taking into account that

$$\begin{aligned} \Delta Z & \rightarrow \partial Z \\ \Delta t & \rightarrow \partial t \\ C_W - C_E & \rightarrow \partial C \\ \frac{\partial C}{\partial z} \Big|_E + \frac{\partial C}{\partial z} \Big|_W & \rightarrow \partial \left(\frac{\partial C}{\partial z} \right) \\ \frac{\partial \left(\frac{\partial C}{\partial z} \right)}{\partial Z} & = \frac{\partial}{\partial z} \left(\frac{\partial C}{\partial z} \right) = \frac{\partial^2 C}{\partial z^2} \end{aligned} \quad 4.12$$

Eq. (4.11) becomes

$$D_L \frac{\partial}{\partial z} \left(\frac{\partial C}{\partial z} \right) - \frac{Q}{A} \frac{\partial C}{\partial z} - (1 - \varepsilon) [\rho_p (-r_m)] = \varepsilon \frac{\partial C}{\partial t} , \quad 4.13$$

or

$$D_L \frac{\partial^2 C}{\partial z^2} - u_s \frac{\partial C}{\partial z} - (-R) = \varepsilon \frac{\partial C}{\partial t} . \quad 4.14$$

where:

ε = the bed voidage

ρ_b = the bulk density

u_s = the superficial fluid velocity

D_L = the axial dispersion coefficient

C = the solution concentration.

For an ideal plug-flow operation, the material balance Eq. (4.14) is greatly simplified:

$$-u_s \frac{\partial C}{\partial z} - (-R) = \varepsilon \frac{\partial C}{\partial t} . \quad 4.15$$

This equation holds for ion exchange, adsorption as well as for catalytic systems, which are in transient operating condition, e.g. during severe catalyst deactivation.

It should be noted here that while in catalytic systems the rate is based on the moles disappearing from the fluid phase $-r_m$, in ion exchange and adsorption, the rate is normally based on the moles accumulated in the solid phase r_m , and the rate is expressed per unit mass of the solid phase as

$$r_m = \frac{\partial q}{\partial t} , \quad 4.16$$

where q is the moles per unit mass of the solid phase (solid loading).

Note that the material balances for fixed bed are valid for the case of constant-density (constant volume) system. The important term here is the one including the fluid velocity, i.e. the term $u_s \partial C / \partial z$.

Rearranging the material balance equation for fixed bed Eq. (4.14) and using Eq. (4.16) for the rate expression $-R$ in ion exchange and adsorption system, we obtain

$$\frac{D_L}{u_s Z} \frac{\partial^2 C}{\partial (z/Z)^2} - \frac{\partial C}{\partial (z/Z)} - \rho_b \frac{Z}{u_s} \frac{\partial q}{\partial t} = \varepsilon \frac{Z}{u_s} \frac{\partial C}{\partial t} , \quad 4.17$$

where the term Z/u_s is the fluid residence time (or contact time). Both C and q are dependent on time t and height Z . Hence, the expression is in the form of a partial differential equation.

4.1.2 Rate equations

There are two basic types of kinetic rate expression. The first and simpler is the case of linear diffusion equation or linear driving forces (LDF) and the second and more rigorous is the case of classic Fickian differential equations.

Linear diffusion equation is the simplest case and is used extensively in the related literature (Perry and Green, 1999; Hashimoto et al., 1977; Cooney, 1990, 1993).

The equations are the followings:

Solid diffusion control:

$$\frac{\partial q}{\partial t} = K_s (q_i - q) , \quad 4.18$$

fluid – film diffusion control:

$$\frac{\partial q}{\partial t} = K_f (C - C_i) , \quad 4.19$$

where K_s and K_f are constants related to the local mass transfer coefficient. The subscript "i" corresponds to the concentrations in the solid-fluid interface.

Differential diffusion equations: In this case, we have differential equations, one for each diffusion step (Perry and Green, 1999; Hall et al., 1966):

$$\frac{\partial q}{\partial t} = K_f(C - C_e), \quad 4.20$$

$$\frac{\partial q}{\partial t} = K_s \left(\frac{\partial^2 q}{\partial r^2} + \frac{2}{r} \frac{\partial q}{\partial r} \right), \quad 4.21$$

$$\frac{\partial q}{\partial t} = K_p \frac{1}{r^2} \frac{\partial}{\partial r} \left(R^2 \frac{\partial C}{\partial r} \right), \quad 4.22$$

where K_s , K_p and K_f are constants related to the local mass transfer coefficients. Eq. (4.20) is for the case of fluid-film diffusion control, Eq. (4.21) for solid diffusion control, and Eq. (4.22) for pore diffusion control. Pore diffusion is similar to solid diffusion; it, however, represents the fluid diffusion in pores and is considered to be an intermediate diffusion step, between fluid-film and solid diffusion. For the case of fluid-film diffusion, the equation is the same as the LDF equation. However, here, the equilibrium concentration (C_e) is used in place of the interface concentration (C_i) to illustrate one significant point.

4.1.2. Equilibrium

Equilibrium and capacity relationships for monocomponent systems are well established and quantitatively expressed by various types of adsorption isotherms, as described briefly in section (2.11).

In wastewater purification processes, multicomponent systems are most common. The Sheindorf-Rebuhn-Sheintuch (SRS) equation for multicomponent isotherm of the Freundlich type (Sheindorf et al., 1981) was used to represent experimental data of the present work.

In deriving the multicomponent isotherm it is assumed that each component individually obeys the Freundlich isotherm.

$$N_i(Q) = \alpha_i \exp(-n_i Q/RT) \quad i=1, \dots, k, \quad 4.23$$

where $N(Q)$ is the number of sites having adsorption energy Q for adsorption of component i . If the coverage by each sorbate at each energy level is given by

$$\theta_i = \frac{b_i C_i}{1 + \sum_{j=1}^k b_j C_j}, \quad 4.24$$

where the adsorption coefficients b_i vary with the adsorption energy in the form

$$b_i = b_{io} \exp(Q/RT), \quad 4.25$$

then the fraction of total sites having adsorption energy between Q and $Q+dQ$, which are occupied by sorbate I is given by

$$d\theta_{Ti}(Q) = \theta_i(Q) N_i(Q) dQ. \quad 4.26$$

The total coverage by sorbate I is given by integration of Eq. (4.26) over the whole range of adsorption energies,

$$\begin{aligned} \theta_{Ti} &= \int_{-\infty}^{\infty} \frac{b_{oi} \exp(Q/RT) \cdot C_i}{1 + \sum_{j=1}^k b_{oj} \exp(Q/RT) \cdot C_j} \\ &\times \alpha_i \exp(-n_i Q/RT) dQ, \end{aligned} \quad 4.27$$

which yields

$$\begin{aligned} \theta_{Ti} &= \frac{\alpha_i RT b_{oi}}{n_i} C_i \left(\sum_{j=1}^k b_{oj} C_j \right)^{Fr_i - 1} \\ &= A_i C_i \left(\sum_{j=1}^k a_{ij} C_j \right)^{Fr_i - 1}, \end{aligned} \quad 4.28$$

where

$$\begin{aligned} A_i &= \frac{\alpha_i RT b_{oi}^{Fr_i}}{Fr_i}, \\ a_{ij} &= \frac{b_{oj}}{b_i}. \end{aligned} \quad 4.29$$

a_{ij} is defined as competition coefficient. A_i and n_i are constants under isothermal conditions and can be determined from the monocomponent system (i.e. from Eq. 2.16) and the competition coefficients a_{ij} can be determined from the multicomponent systems, or from thermodynamic information if the b_{oj} coefficients are known.

The adsorption isotherm expressed in term of weight of sorbate is written in the form

$$q_i = K_{Fi} C_i \left(\sum_{j=1}^k a_{ij} C_j \right)^{Fr_i - 1}, \quad 4.30$$

with $K_i = q_{mi} A_i$. K_i and n_i are the Freundlich constants obtained for i in a single-component system; and can be determined from the monocomponent system. The multicomponent isotherm Eq. (4.30) reduces to the monocomponent isotherm Eq. (2.17) when $k=1$. For a biocomponent system the adsorption by each component is given by

$$\begin{aligned} q_1 &= K_{F1} C_1 (C_1 + a_{12} C_2)^{Fr_1 - 1}, \\ q_2 &= K_{F2} C_2 (a_{21} C_1 + C_2)^{Fr_2 - 1}, \end{aligned} \quad 4.31$$

the adsorption of the first component in a three-component system is

$$q_1 = K_{F1} C_1 (C_1 + a_{12} C_2 + a_{13} C_3)^{Fr_1 - 1}, \quad 4.32$$

and the competition coefficients can be determined from the respective biocomponent systems.

The biocomponent isotherm, Eq. (4.31), can be written in the form

$$\begin{aligned} \frac{C_1}{C_2} &= \frac{1}{C_2} \beta_1 - a_{12}, \\ \frac{C_2}{C_1} &= \frac{1}{C_1} \beta_2 - a_{21}, \end{aligned} \quad 4.33$$

with

$$\beta_1 = \left(\frac{K_1 C_1}{q_1} \right)^{\frac{1}{(1-n_2)}},$$

$$\text{and } \beta_2 = \left(\frac{K_2 C_2}{q_2} \right)^{1/(1-n_2)} . \quad 4.34$$

If both concentrations vary during the experiment, then plotting C_1/C_2 vs β_1/C_2 yields a straight line-of-unity slope and the competition coefficient could be determined from the intercept.

4.2. Predictive model

Mass transfer (controlled systems) diffusion models and combined resistances models is adopted in this study, which covers the case where we have combined resistances to diffusion (fluid-film and solid diffusion). In this case, the concentration in the main phase of the fluid (bulk concentration) is different from the one at the interface due to the effect of the fluid film resistance (Hashimoto et al., 1977).

To use simplified models (i.e. to reduce mathematical complexities in the mass balance equation of the bed), the following two approximations have been frequently introduced:

1. Plug flow (ideal mixed): In this case, the effects of axial dispersion have been studied by several investigators (Acrivos, 1960; Colwell, 1971; Garg, 1972), and were found to be negligible in most cases. So the material balance in a fixed bed Eq. (4.14) can be written as follows:

$$u_s \frac{\partial X}{\partial z} + \rho_b \frac{q_{max}}{C_o} \frac{\partial Y}{\partial t} + \varepsilon \frac{\partial X}{\partial t} = 0 , \quad 4.35$$

where:

$$X = C/C_o \text{ and } Y = q/q_{max}$$

2. Constant pattern condition: This means that all points on the breakthrough curve are travelling in the bed under the same velocity, and thus a constant shape of this curve is established (Wevers, 1959). This condition reduces the mass balance

equation (4.14) to the simple relation: $C/C_o = q/q_{max}$. (i.e. $\partial Y/\partial X = \text{const.}$) (Perry and Green, 1984).

It should be mentioned that the diffusivity is assumed to be constant.

For gel-type exchange resins and for macropore resins with a low degree of cross linking, the following equation is proposed for the solid diffusion coefficient (Helfferich, 1962):

$$D_s = D_f \left(\frac{\varepsilon_p}{2 - \varepsilon_p} \right)^2, \quad 4.36$$

where:

D_f is the diffusion coefficient of the molecules in the fluid phase.

ε_p is the internal porosity of the solid.

The solution of the fixed-bed model for the Freundlich isotherm is the following (Hashimoto et al., 1977):

$$\theta_\tau - X_\tau = \frac{1}{1+\xi} \omega_1 + \frac{\xi}{1+\xi} \frac{1}{\eta} \omega_2 + \frac{1}{1+\xi} \frac{\xi}{\xi+\eta} \omega_3 \quad 4.37$$

$$\omega_1 = \frac{F_r}{F_r-1} \ln(X_i^{F_r-1} - 1) + 1 + \frac{\eta}{\xi+\eta} \frac{F_r^2}{F_r-1} I_A \quad 4.38$$

$$\omega_2 = \frac{1}{F_r-1} \ln(1 - X_i^{1-F_r}) + \frac{\xi}{\xi+\eta} \frac{1}{F_r-1} I_B \quad 4.39$$

$$\omega_3 = F_r - 1 + \frac{F_r}{F_r-1} (I_A + I_B) \quad 4.40$$

$$\eta = 0.808 + 0.192 F_r \quad 4.41$$

$$I_A = \sum_{n=1}^{\infty} \frac{1}{n[n(1-F_r)] + F_r} \quad 4.42$$

$$I_B = \sum_{n=1}^{\infty} \frac{1}{n[n(1-F_r)] + 1}, \quad 4.43$$

Where

$$\theta_\tau = \frac{k_s a_u}{\rho_b(1+1/\xi)} \left(t - \frac{\varepsilon Z}{u} \right) \quad 4.44$$

$$X_\tau = \frac{k_s a_u \gamma}{1+1/\xi} \frac{Z}{u} \quad 4.45$$

$$k_s a_u = \frac{15 D_s \rho_b}{r_o^2} \quad 4.46$$

$$\gamma = \frac{q_{max}}{C_o} \quad 4.47$$

$$\xi = \frac{k_f a_u}{k_s a_u \gamma} \quad 4.48$$

$$a_u = \frac{3}{r_o} (1 - \varepsilon) . \quad 4.49$$

Here, q_{max} is in mass of solute per unit mass of solid and C_o is in mass of solute per unit volume of fluid.

The interface relative concentration X_i is related to the respective bulk relative concentration X as follows:

$$X = \frac{\xi X_i + X_i^{Fr}}{\xi + \eta} \quad 4.50$$

In order to predict the breakthrough curves for single-component packed-bed adsorption, the equations above were solved using a Matlab programme.

Chapter Five

Results and Discussion

The phosphate was removed from the wastewater by the addition of different types and amount of flocculants to find the suitable one for this type of water as well as the optimum dosage that gives the best results. Then the ion exchange process was used to remove the last contaminations in the supernatant water. It should be mentioned that all the results from these experiments are shown in appendix A.

5.1. Sedimentation Experiment

The turbidity of Eishidiya wastewater was measured with time up to 30 hrs of sedimentation. The solids in the wastewater were left to settle slowly under their own weight and the turbidity was measured with time. The phosphate concentration in the solution decreased to about 3 ppm giving a turbidity of 4.5 NTU after 24 hrs of undergoing sedimentation without adding coagulant. The volume of the sediment after 30 hrs of sedimentation was 364 ml. The variation of turbidity with time is presented in Fig. (5.1).

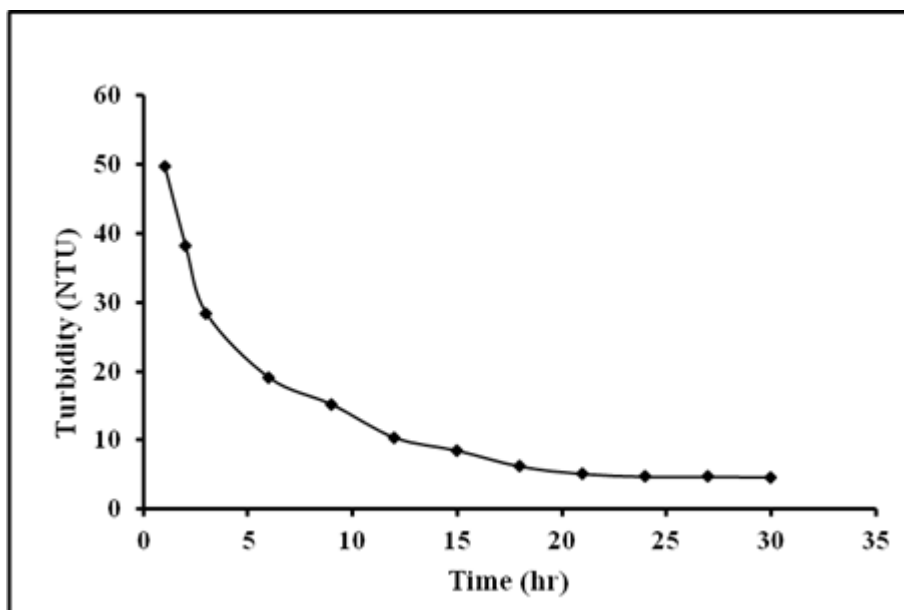


Figure 5.1: Turbidity of the wastewater sample with time.

5.2. Enhanced Sedimentation (Coagulation-Flocculation)

The effect of binary mixtures of cationic and anionic electrolytes on the flocculation process, charge of the suspended particle, clearness of the supernatant's water, settling rate and sludge volume, was studied in this section.

A different type of anionic polyelectrolyte was mixed with a cationic, to find the most suitable mixture for our studied water sample. And the dual polyelectrolyte dosage was changed to find the optimal dose. The optimal polyelectrolyte dosage is usually associated with the colloidal surface of minimum surface charge (i.e. minimum zeta potential value) and a tendency to aggregate to form large floc, resulting in a decrease in the value of the turbidity (Christensen et al., 1993).

The zeta potential that corresponds to optimum coagulation is often called the target zeta potential. Once a target value is set, routine control is relatively simple and merely involves measuring the zeta potential of a sample from the flash mix. If the measured value is more negative than the target value, just increase the primary coagulant dose. If it is

more positive, then lower the dose. Good control of polyelectrolyte dose is critical in sludge conditioning, since overdosing will increase cost and reduce sludge dewaterability.

5.2.1. Determination of Magnafloc 919 and Zetag 7557 Optimum Dosage

The first set of experiments was carried by adding 5 mg/L of Zetag 7557 polymer (cationic polyelectrolyte) with different dosages (5, 7, 10, 15, 20, 25 and 30 mg/l) of Magnafloc 919 polymer (anionic polyelectrolyte) to the wastewater to enhance the sedimentation process.

Figure (5.2) demonstrates the zeta potential of the supernatant water and its turbidity as a function of Magnafloc 919 dose (anionic polyelectrolyte) at a constant dose of the Zetag 7557 (cationic polyelectrolyte). Upon the addition of 10 mg/l of the anionic polyelectrolyte, the zeta potential increased to -10.1 mV with increasing dosage, and after this point it decreased to -13 mV by increasing the anionic polyelectrolyte dosage. It should be mentioned that the decreasing of the zeta potential was not sharp as its increasing (i.e. did not changed much on further increase of polyelectrolyte concentration). On the other hand, turbidity decreased sharply with increasing the anionic polyelectrolyte dosage upon the 10 mg/l dosage, and then it slightly began to increase by increasing of polyelectrolyte dosage.

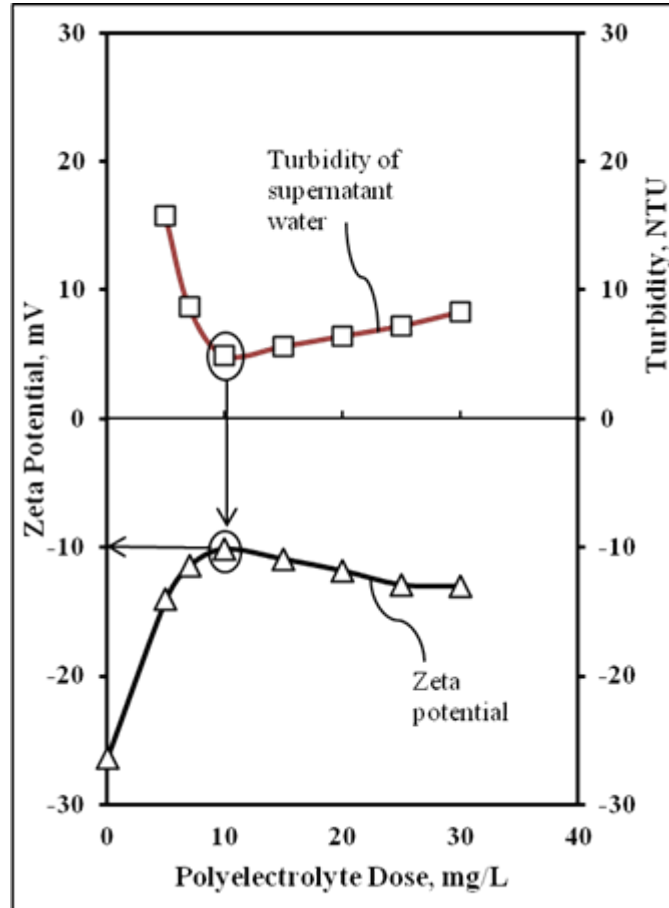


Figure 5.2: Zeta potential and turbidity of the supernatant water as a function of Magnafloc 919 dose and at 5 mg/l of Zetag 7557.

The simultaneous plots of zeta potential and turbidity in Fig. (5.2) are used to determine the target zeta potential and the optimum polyelectrolyte dosage. The target zeta potential was -10.1 mV using turbidity as a criterion and the optimum dose of the anionic polyelectrolyte is 10 mg/l in addition of 5 mg/l of the cationic polyelectrolyte.

The second set of experiments was done by mixing 5 mg/l of Zetag 7557 polymer with a different dosages (5, 7, 10, 15, 20, 25 and 30 mg/l) of Magnafloc 919 polymer. The zeta potential and turbidity of the supernatant water were measured and the results are shown in Fig. (5.3).

In figure (5.3), zeta potential is increased with increasing the amount of the anionic polyelectrolyte till it became 15 mg/l, and after this point the behaviour of zeta potential was reversed (i.e. it increased with increasing the addition of the polymer). Turbidity is

decreased sharply with increasing the amount of the anionic polyelectrolyte upon the addition of 10 mg/l of the anionic polymer.

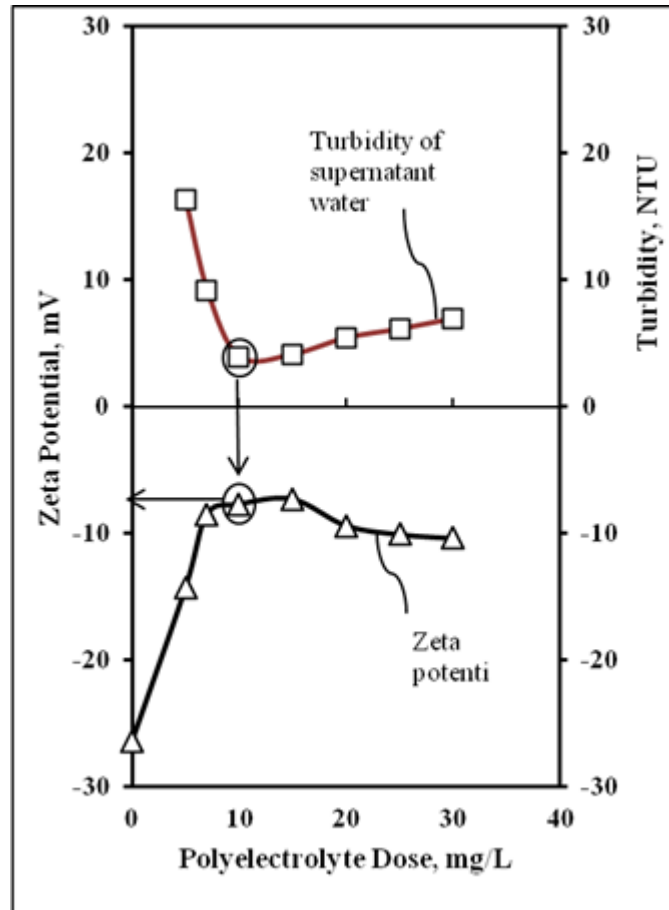


Figure 5.3: Zeta potential and turbidity of the supernatant water as a function of Magnafloc 919 dose and at 7 mg/l of Zetag 7557.

As shown in Fig. (5.3) the optimum dosage is 10 mg/l and it was selected as it gives a minimum turbidity of 3.9 NTU at a zeta potential of -7.7 mV. So the optimum dose for Magnafloc 919 is 10 mg/l and 7 mg/l of Zetag 7557, since this optimum dose gives turbidity much lower than that selected in Fig. (5.2).

5.2.2. Determination of Magnafloc 336 and Zetag 7557 Optimum Dosage

To enhance the sedimentation process, a different amounts of Magnafloc 336 (5, 7, 10, 15, 20, 25 and 30 mg/l) alternatively with 5 and 7 mg/l of Zetag 7557, were added to the waste water samples. Zeta potential and turbidity for all the supernatant water, which produced from the enhanced sedimentation experiments, were measured. The results are shown in Fig (5.4) and Fig (5.5).

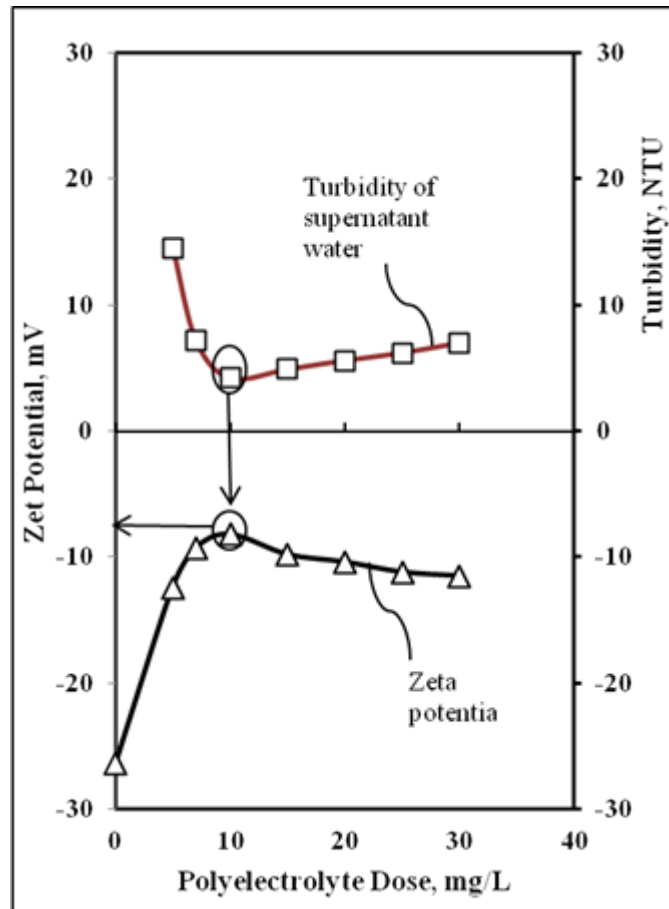


Figure 5.4: Zeta potential and turbidity of the supernatant water as a function of Magnafloc 336 dose and at 5 mg/l of Zetag 7557.

The zeta potential and turbidity curves in Fig. (5.4) showed the same behaviour as in Fig (5.2), even that the selected optimum dose in Fig. (5.4) gives a better turbidity, which is 4.2 NTU at a target zeta potential of - 8.2 mV.

In the other hand, the zeta potential and turbidity curves in Fig. (5.5) showed a similar trend as in Fig. (5.3). And a polymer dose of 10 mg/l was selected, as a more practical optimum because it produced almost the same turbidity, as it produced by the dose of 15 mg/l, at a substantial savings in polymer.

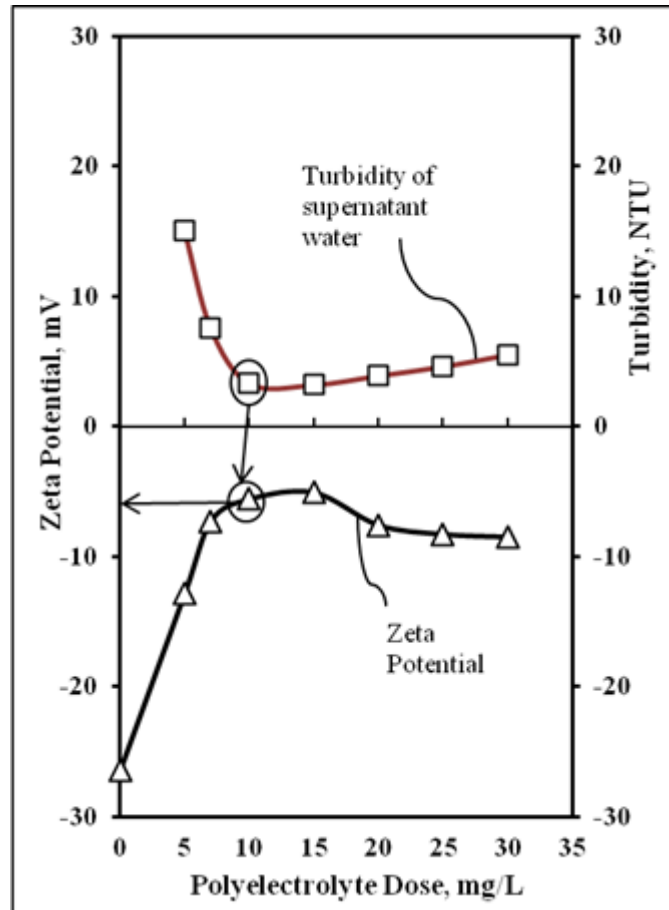


Figure 5.5: Zeta potential and turbidity of the supernatant water as a function of Magnafloc 336 dose and at 7 mg/l of Zetag 7557.

The conclusion from all the enhanced sedimentation experiments, is that the optimum dose of 10 mg/l of the anionic polymer, Magnafloc 336 in addition of 7 mg/l of the cationic polymer, Zetag 7557 gives a superior results as in a comparison with the other selected optimum dose and a target zeta potential is - 5.6 mV.

The adsorption of the cationic polyelectrolyte could mainly be attributed to the electrostatic force, resulting in the charge neutralization. That explain the sharp decreasing in the zeta

potential by the addition of Zetag 7557, which neutralizing the negative charge of the suspended particle in the wastewater sample (i.e. decreasing the electrostatic repulsion between particles). As a result, the particles approached to closer distances and formed primary floc (microflocs). The adsorbed cationic polyelectrolyte (Zetag 7557) formed loops, trains and tails on primary floc surfaces (Langer et al., 1994; Somasundaran and Krishnakumar, 1997). Then by adding high-molecular anionic polyelectrolyte, they became adsorbed on the loops and tails of the cationic polyelectrolyte by hydrogen bonding and van der Waals force (Petzold et al., 2003; Lee and Liu, 2000). This results in formation of longer loops and tails on the surface, which enhances the formation of polymeric bridges between particles and, consequently, the efficiency of flocculation (i.e. smaller flocs will further aggregate into secondary bigger ones, which settle easily). As a result, the turbidity decreased sharply so as zeta potential till the selected optimal dose. Furthermore, another important reaction of pre-conditioning with the cationic polyelectrolyte was the efficient capture of some fine, dispersed particles. This is shown in the low residual turbidity of supernatant after 30 min of settling.

It is logical to suppose that in the case of polyelectrolyte mixture adsorption, the layer of the cationic polymer will be hidden inside (behind) the much more extended anionic polymer layer. Therefore, the latter will determine the properties of the peripheral part of the adsorbed layers that are responsible for the electrokinetic potential of particles bearing polymer mixture. This explains our results showing the decreasing of the zeta potential with increasing of the anionic polymer dose although this decrease does not reflect the expected proportion. The main reason was due to the hindrance and electrostatic repulsion; it was difficult for the anionic polyelectrolyte to adsorb on the loops, tails or surface of the particles at higher concentration after the selected optimum value.

The target zeta potential was selected corresponding to the minimum turbidity of the supernatant's water sample. The increase in turbidity after the optimal dose value was mainly due to the over dosing of anionic polymer, which inhibited the flocculation.

5.2.3. Settling Rate and Volume of the Sediment

The flocculation or settling rate was estimated by the observation of the displacement of the upper interface of the cell suspension with time through the naked eyes. This means that the movement of the layer between the clear solution and the layer of high suspension was monitored toward the bottom of the container.

The wastewater sample was left to settle without any addition of polyelectrolyte and the settling rate was 0.093 cm/min and sludge volume after 24 hrs of settling was 105 ml, which is about 42% of the total wastewater volume. The settling rate was 1.87 cm/min for wastewater sample conditioned with the pre-calculated optimum dose of Magnafloc 336 and Zetag 7555 and sludge volume after 30 min of settling was 32 ml. The settling rate of wastewater sample conditioned with the pre-calculated optimum dose of Magnafloc 919 and Zetag 7557 was 2.13 cm/min and sludge volume was 40ml, which was also measured after 30 min of settling.

Settleability has been used to investigate the floc structure and the sludge-water separation behaviours. The floc density and floc diameter are known to affect the settling behaviours. However, the floc size is relatively more significant in determining settling rate. The flocs that formed by the addition of Magnafloc 919 and Zetage 7557 were larger than that formed by the addition of Magnafloc 336, as evidenced by the faster settling rate. That was mainly cause of the ultra-high molecular weight of Magnafloc 919 polyelectrolyte.

When the wastewater was pre-conditioned with the cationic polyelectrolyte in dual polyelectrolyte conditioning, the cationic polyelectrolyte, through bridging effect, could increase rigidity of the flocs, which resulted in increased dimensions of loops and tails (Langer et al., 1994). Also, relatively more compact primary flocs were formed due to the electrostatic attraction between cationic polyelectrolyte and the negatively charged particle surfaces (Eriksson and Alm, 1993). The subsequent addition of the anionic polyelectrolyte then provided bridging of primary flocs into larger and stronger flocs.

The larger and stronger flocs thus resulted in an enhanced dewaterability. This is the reason of the small settled sludge volume of the wastewater conditioned with the polyelectrolyte.

It has been demonstrated in this work, that the results obtained from using of the dual polyelectrolyte system are superior in sludge dewaterability and fine particle capture efficiency.

5.2.4. Chemical Analysis of the Supernatant Water

The residual water produced from the enhanced sedimentation experiments pre-conditioned with the optimal dose of Magnafloc 336 and Zetag 7557, was chemically analysed; the results are shown in table 5.1.

Table 5.1: Chemical analysis of supernatant water.

Compositions	Concentrations (ppm)
Calcium ion, Ca^{2+}	140
Megnesium ion, Mg^{2+}	42
Sodium ion, Na^+	297
Potassium ion, K^+	7
Chloride ion, Cl^-	815
Sulfate ion, SO_4^{-2}	162
Phosphate ion, PO_4^{-3}	< 0.2
Bicarbonate ion, HCO_3^-	62
pH=7.1	

The phosphate ion concentration was decreased from 800 ppm in the wastewater sample to < 0.2 ppm after the enhanced sedimentation experiment, so the removal of phosphate ion is almost 100% by comparing between table 5.1 and table 3.1.

The supernatant water from the enhanced sedimentation experiment and a stock solution were used then in the ion exchange experiments, which is the second part of the present work.

5.3. Ion Exchange Experiments

By ion exchange, undesirable ions are replaced by others which don't contribute to contamination of the environment. The method is technologically simple and enables efficient removal of even traces of impurities from solutions.

In this study, batch and fixed bed ion exchange experiments, were studied to determine the effects of several parameters such as, initial solution concentration, flow rate (just in the column method), amount and types of adsorbent on chloride, sulphate and sodium removal from wastewater. Langmuir and Freundlich isotherm models were used for the evaluation of findings from the batch test.

5.3.1. Batch Studies

In the first phase of runs, batch ion exchange experiment were conducted using various amounts and types of resin with 100 ml of solutions containing single or multi ions of desired concentrations at constant temperature in 250 ml flasks. The sample were agitated at constant speed with magnetic stirrer and then filtered to get the clear solution, which was analyzed to determine its ions content.

The batch experiments were performed to investigate the effect of adsorbent quantity and initial ions concentrations as well as studying the batch adsorption isotherms for the removal of mono and multi ions.

5.3.1.1. Effect of Adsorbent Quantity and Initial Monocomponent Concentration

The effect of adsorbent quantity was examined by using various amounts of Purolite A400 resin. In the experiments, initial chloride concentration was kept constant. Then the experiments were repeated for various chloride concentrations while the resin amount was kept constant. The results are shown graphically in Fig. (5.6) and Fig. (5.7). Initial and final chloride concentrations were used to obtain the adsorption capacity (q), the amount of ions adsorbed per unit mass of adsorbent (mg/g) was given in Eq. 5.1, which was derived from Eqs. 2.7 and 2.8:

$$q = [(C_o - C)/m] \times V. \quad 5.1$$

Where C_o and C are the initial and final chloride concentration (mg/L) in the solution, m the amount of the adsorbent (resin) used (g) and V the volume of the aqueous phase (L). When the equilibrium is reached; $C = C_e$ and $q = q_e$, which was calculated using Eq. 5.1. The amount of chloride retained or the removal efficiency is given in eq. 5.2:

$$\text{Removal efficiency} = [(C_o - C)/C_o] \times 100. \quad 5.2$$

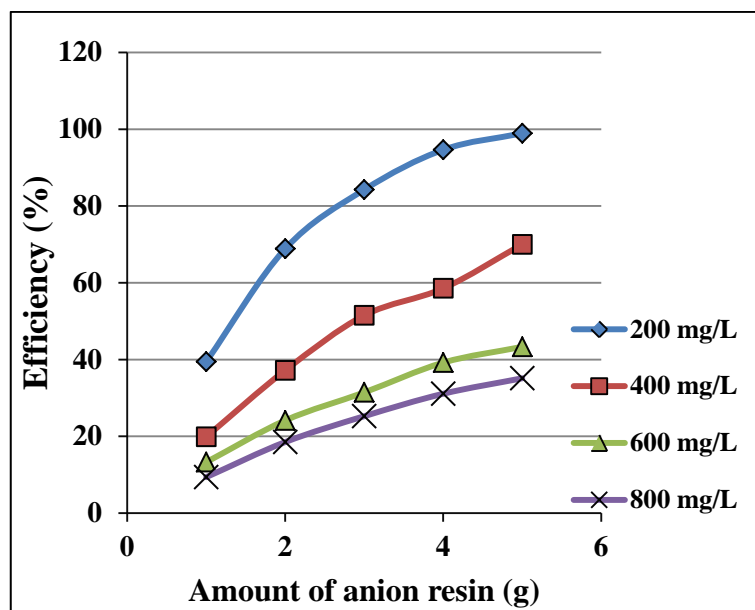


Figure 5.6: Effects of adsorbent amount and initial concentration on chloride removal efficiency

In Fig. (5.6), the retention of the chloride ions was examined in relation to amount of the resin. It shows that the removal efficiency of chloride is increased with increasing amount of adsorbent. It can also be seen that the efficiency is decreased with increasing chloride concentration. Maximum efficiency 98.95% was obtained by using 5 g adsorbent and 200 mg/l initial chloride concentration.

5.3.1.2. Adsorption Isotherm

The relation between the amount of chloride adsorbed and the chloride concentration remaining in solution is described by an isotherm as shown in Fig. (5.7), which demonstrated that the adsorption capacity increased with increasing the amount of adsorbent. While the equilibrium chloride concentration decrease with increasing adsorbent amount for a given initial chloride concentration.

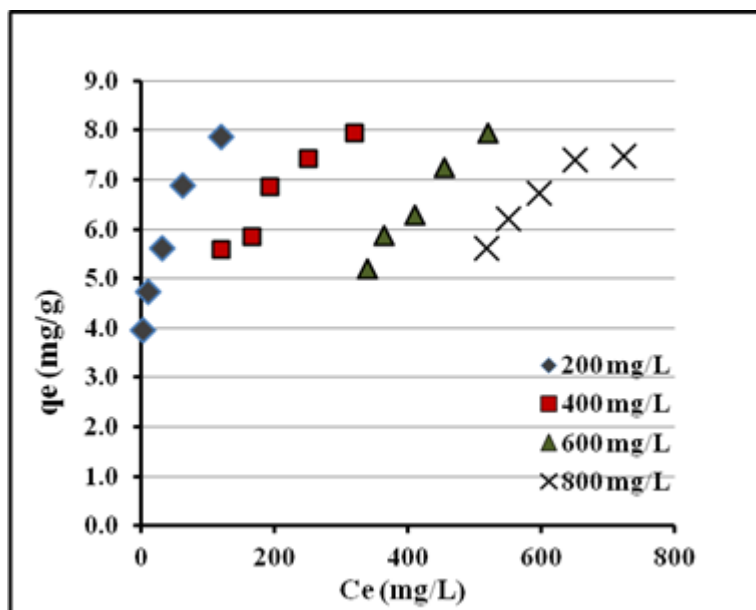


Figure 5.7: Cl^- adsorption isotherm (C_0 : 200-800 mg/l; m: 1-5 g)

These results in Figs. (5.6) and (5.7) show that the increasing in the resin/solution ratio, which means increasing of the resin-solution contact surface area and the amount of the exchangeable counterions (hydroxide ions) carried by ion exchange resin, that causes higher chloride removal efficiency, which means decreasing in the equilibrium chloride concentration for a fixed initial chloride concentration. These results were anticipated because from the practical point of view, an ion exchanger can be considered as a “reservoir” containing a constant amount of the exchangeable counterions, which can exchange with the chloride ions, therefore the increase in the initial chloride concentration, decrease the efficiency of removal at a fixed ion exchanger amount.

The same batch experiments were repeated by changing the chloride ion by sulphate ion. The same resin was used and the sulphate initial concentrations used were 100 and 200 ppm. Mixed ion exchange resin (Purolite® MB400) was used in the batch experimental test with sodium ions and the concentrations of sodium used were (178, 226, 306, 355, 436, 485, 568 and 615). From the above figures (i.e. Figs (5.6) and (5.7)) and the equilibrium data that were collected in Appendix A, we conclude that, percent adsorption is decreased with increase in initial ions concentration, but the actual amount of ions adsorbed per unit mass of resin is increased with increase in initial ions concentration. It

means that the adsorption is highly dependent on initial concentration of ions. It is because of that at lower concentration, the ratio of the initial number of ions to the available surface area is low subsequently the fractional adsorption becomes independent of initial concentration. However, at high concentration the available sites of adsorption becomes fewer and hence the percentage removal of ions is dependent upon initial concentration.

5.3.1.3. Equilibrium Studies

Experimental equilibrium data are important when judging the feasibility of the adsorption process for a given application. Moreover the isotherm plays a crucial role in the predictive modelling procedure for the analysis and design of the ions (i.e. chloride, sulphate and sodium) removal processes. Adsorption isotherm data of chloride ion on anion resin (Purolite®A400) are shown in Fig. (5.7). The experimental equilibrium data were correlated with Langmuir and Freundlich equation with two parameters to establish the most appropriate correlation for the experimental equilibrium curve. The two parameters of Langmuir were determined, as described briefly in section (2.11.1), by plotting $(1/q_e)$ versus $(1/C_e)$, which yields a straight line with intercept $(1/q_m)$ and a slope of $(1/q_m K_L)$. While the two Freundlich parameters were determined, as described in section 2.11.2, by plotting of $\log q_e$ versus $\log C_e$ gives a straight line with a slope equal $(1/n)$ and an intercept equal to $\log K_F$. The results were listed in table 5.2.

The experimental equilibrium data of sodium and sulphate were also correlated with Langmuir and Freundlich equations and the equations parameters were also determined as described above. The results were listed in tables 5.3 and 5.4.

Table 5.32: Langmuir and Freundlich models parameters for best fit and corresponding correlation coefficients with the experimental isotherm of chloride ion.

Co (mg/l)	Langmuir Isotherm			Freundlich Isotherm		
	$q_m(\text{mg/g})$	$K_L(\text{l/mg})$	R^2	$K_f(\text{mg/g})$	N	R^2
200	6.435	0.7099	0.7408	3.323	0.1708	0.963
400	10.672	0.0087	0.9087	0.8717	0.3847	0.935
600	24.39	8.98×10^{-4}	0.9437	0.0691	0.7566	0.955
800	66.67	0.0071	0.9217	0.026	0.8658	0.91

Table 5.3 Langmuir and Freundlich models parameters for best fit and corresponding correlation coefficients with the experimental isotherm of sulphate ion.

Co (mg/l)	Langmuir Isotherm			Freundlich Isotherm		
	$q_m(\text{mg/g})$	$K_L(\text{l/mg})$	R^2	$K_f(\text{mg/g})$	N	R^2
100	3.28	1.42	0.7667	1.9072	0.1727	0.9776
200	5.592	0.17	0.9499	2.655	0.1512	0.9606

Table 5.4: Langmuir and Freundlich models parameters for best fit and corresponding correlation coefficients with the experimental isotherm of sodium ion.

Co (mg/l)	Langmuir Isotherm			Freundlich Isotherm		
	$q_m(\text{mg/g})$	$K_L(\text{l/mg})$	R^2	$K_f(\text{mg/g})$	n	R^2
178	5.12	0.589	0.75	2.81	0.15	0.96
226	5.09	0.595	0.88	3.79	0.06	0.97
306	6.15	0.16	0.93	4.14	0.07	0.94
355	7.14	0.0135	0.91	1.13	0.29	0.92
436	5.77	0.0204	0.89	2.01	0.16	0.93
485	29.5	5.01×10^{-4}	0.92	0.023	0.89	0.92
568	35.97	2.41×10^{-4}	0.92	0.004	1.16	0.91
615	17.21	3.4×10^{-4}	0.91	0.002	1.25	0.92

According to the correlation coefficients of both isotherms models, Freundlich isotherm best represented the equilibrium adsorption of chloride, sulphate and sodium on the anion and cation ion exchange resin. That is mean that adsorption equilibrium data do not fit well on linear coordinates.

According to the Freundlich equation, the amount adsorbed increases infinitely with increasing concentration (Smith, 1981), This equation is, therefore, satisfactory for low concentration. And that coincides with our results because the correlation coefficients of Freundlich, which obtained of the lower concentration, were higher than that of the higher concentration.

5.3.2. Column Studies

Column techniques are used to achieve a completeness of ion exchange reactions because it carrying out a large number of successive batch operation in series, as described in section 2.8.2. Fixed-bed ion exchange (adsorption) has been used widely in separation and purification process. To design such an adsorption process, it is important to understand the thermodynamic and kinetic characteristics of the adsorbent and adsorbate(s). One way to grasp these characteristics is by examining the concentration-vs.-time curves of the effluent. These breakthrough curves are perhaps the most common basis for assessing the behaviour of adsorbers. Breakthrough curves depend on bed geometry, operating conditions, transport properties, and equilibrium adsorption isotherms.

In the present study a continuous ion exchange (adsorption) study in a fixed-bed column was carried out by using Purolite® A400 (anion resin) and Purolite® MB400 (mixed resin) as an adsorbent for the removal of chloride, sulphate, and sodium from the prepared water solution. Effect of the bed height, flow rate, resin type and initial concentration was studied. Two set of experiments were performed. In each set a different ion exchange resin in the fixed bed column, was used. The set of experiments are shown in Appendix A.

5.3.2.1. Effect of the Flow Rate on Breakthrough Curve

In the fixed bed ion exchange column of anion and mixed resin, the effect of flow rate (0.05 and 0.1 l/min) at constant bed depth and initial concentration was investigated respectively. The breakthrough curve of chloride, sulphide and sodium, which were plotted as the ratio of the effluent to influent concentration (C/C_0) versus run time, at various flow rates are shown in figures below.

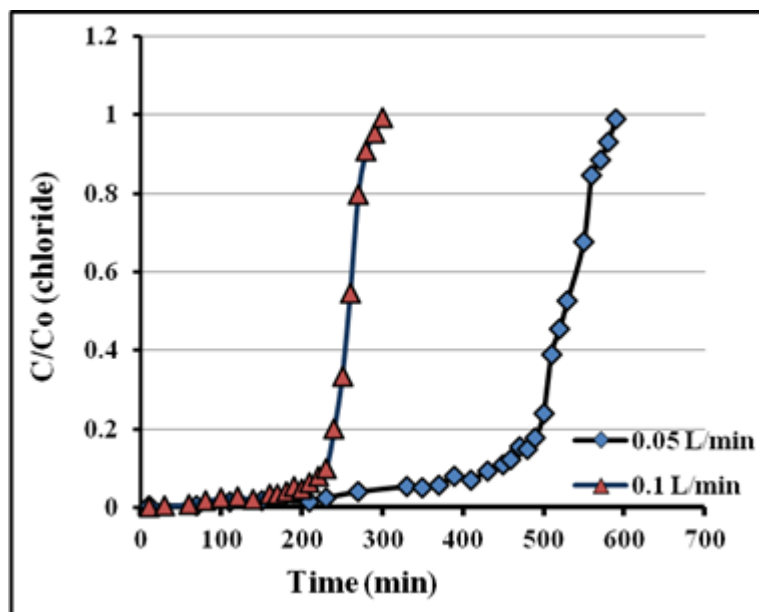


Figure 5.8: Effect of flow rate on the ion exchange breakthrough curve for Cl⁻ on anion resin at 20 cm bed depth and an initial chloride concentration of 200 mg/l.

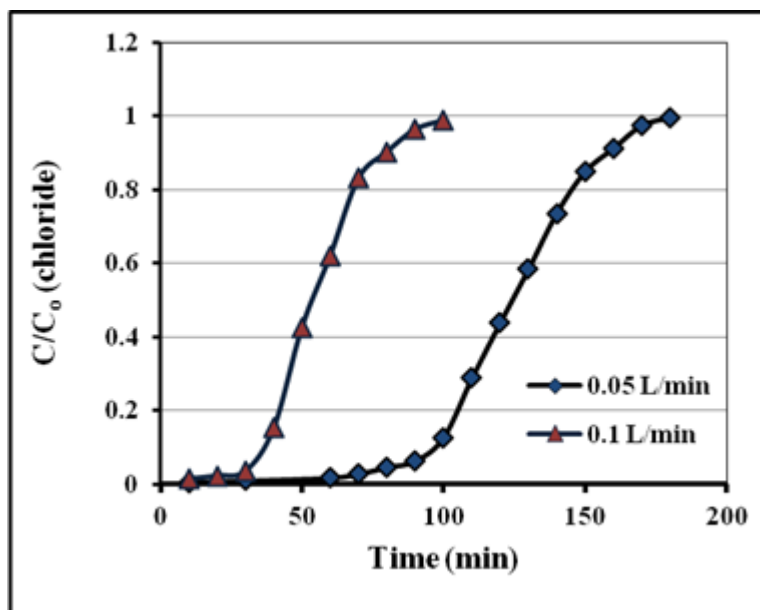


Figure 5.9: Effect of flow rate on the ion exchange breakthrough curve for Cl^- on anion resin at 10 cm bed depth and an initial chloride concentration of 400 mg/l.

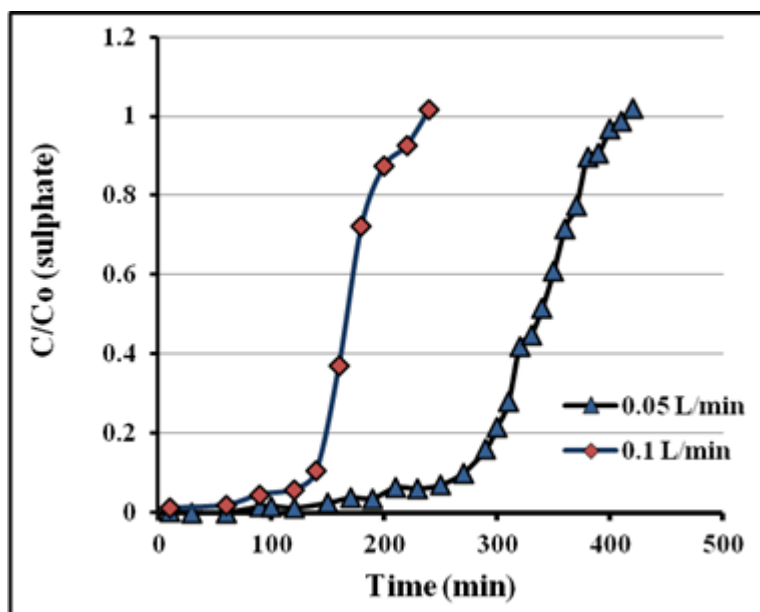


Figure 5.10: Effect of flow rate on the ion exchange breakthrough curve for SO_4^{2-} on anion resin at 10 cm bed depth and an initial sulphate concentration of 200 mg/l.

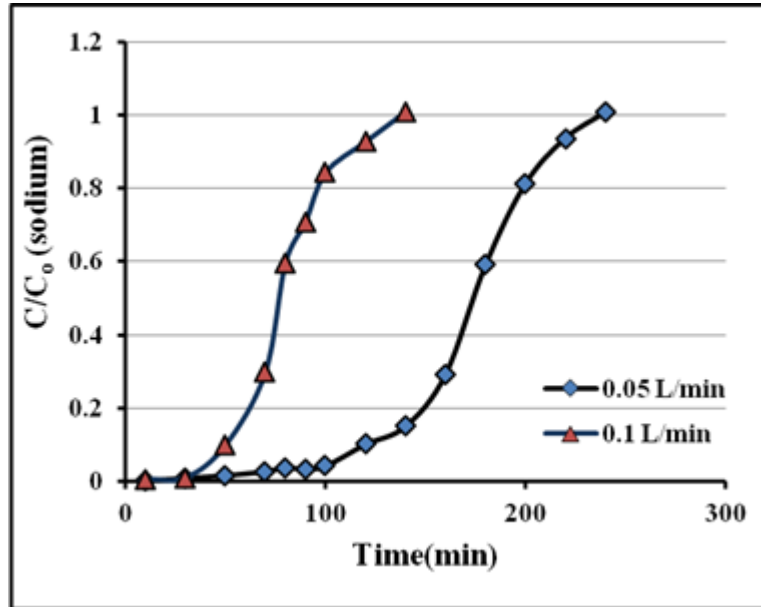


Figure 5.11: Effect of flow rate on the ion exchange breakthrough curve for Na^+ on mixed resin at 20 cm bed depth and an initial sodium concentration of 355 mg/l.

As described in section 2.10, when the adsorption zone moves down and the lower edge of this zone reaches the bottom of the column, the effluent concentration starts to rise rapidly (Zagorodni, 2007). This is called the breakthrough point (corresponding to $C/C_o = 0.1$). As seen in Fig. (5.8), which shows the breakthrough curve of chloride (at constant bed depth of 20 cm and at initial chloride concentration of 200 mg/l, the breakthrough time (t_{br}) occurred at 460 min and 230 min for flow rates of 0.05 and 0.1 l/min, respectively. The results indicate that an increase in flow rate at constant bed depth and feed concentration decreased the breakthrough time and maintains constant breakthrough volume (V_{br}). This is due to the increasing of the mass transfer coefficients of both ions as the flow rate increases, indicating that kinetics are controlled by film diffusion. Film diffusion is inferred to be the rate controlling mechanism because the film thickness decreases as flow rate increases leading to improved kinetics. In addition the removal efficiency here is not proportional to the flow rate as it does not increase with increasing the flow rate. The results also show that the shape of the breakthrough curve is saturated (exhaust time, $C/C_o = 0.9$) earlier at higher flow rates because the front of the sorption zone quickly reached the bottom of column.

Fig. (5.9), shows also the breakthrough curve of chloride at an initial concentration of 400 mg/L and a bed depth of 10 cm. The breakthrough time here occurred at 35 min and 95 min for flow rates of 0.05 and 0.1 l/min, respectively. The breakthrough volume and time decreased with increasing the flow rate due to decrease in the residence time through the bed resulting in higher ionic leakage. That can be due also to the increasing of the feed concentration to a double comparing with the results in Fig. (5.8), which can certainly alter the rate determining step (i.e. ion exchange mechanism) from the film diffusion to a particle diffusion. In this case the increasing in the flow rate decreased the removal efficiency of chloride (i.e. the increasing in the flow rate decreased the breakthrough volume). The decrease of the removal efficiency, due to a decrease in Empty Bed Contact Time (EBCT), which were 2.83 and 1.41 min for flow rates at 0.05 and 0.1 l/min respectively. The lower the EBCT, the less effective the diffusion process becomes, resulting in lower adsorption. Thus, the adsorbent needs more time to bond the removal ions efficiently (Sarin et al., 2006). Empty Bed Contact Time (EBCT) can be calculated as expressed in equation 5.3:

$$EBCT = \frac{V_{bed}}{Q_f} , \quad 5.3$$

where V_{bed} is the resin volume in the fixed bed column (cm^3) and Q_f is the water flow rate (cm^3/min), so that the EBCT is expressed in min. The EBCT is used as a measure of the duration of the contact between the resin granules and the water flowing through the bed. An increase in the EBCT means an increased time for the adsorption of dissolved matter onto the resin beads.

The breakthrough curve of sulphate and sodium are shown in Figs. (5.10) and (5.11), at a bed depth of 20 cm and at an initial concentration of 200 mg/l and 355 mg/l, respectively. The figures show that the breakthrough curve volume and time decreased with increasing the flow rate due to the reasons explained above, which are mainly due to the low EBCT value at a flow rate of 0.1 l/min.

5.3.2.2 Effect of Bed Height on Breakthrough Curve

The effect of a bed height of 10 and 20 cm on the breakthrough curve of chloride at a constant flow rate of 0.05 l/min was investigated (Fig. 5.12). The results show that the higher uptake of Cl^- was observed at the beginning of the fixed-bed column, but the concentration of Cl^- in the effluent rapidly increased after breakthrough volume or breakthrough time. The upper bed depth gets saturated earlier than lower bed depth at the bed height of 10 cm. As can be seen in Fig. (5.12), the breakthrough time (t_{br}) was 65 and 162 min at bed heights of 10 and 20 cm, respectively.

Figure (5.13); shows also the effect of the bed height on the breakthrough curve of chloride at a flow rate of 0.1 l/min. The breakthrough time (t_{br}) was 15 and 62 min at bed height of 10 and 20 cm, respectively. From these two figures we can conclude that the t_{br} or V_{br} increased when increasing the bed height. Similar results were obtained for SO_4^{2-} and Na^+ removal as shown in Fig. (5.14) and (5.15).

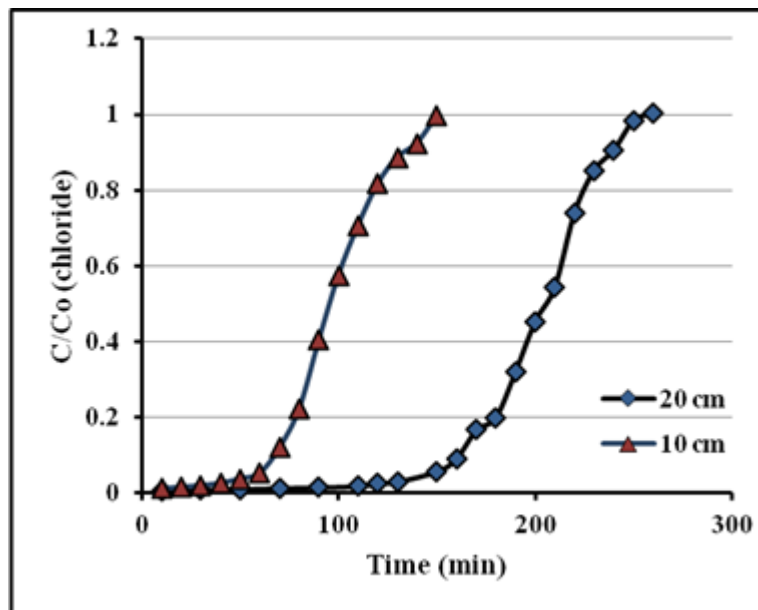


Figure 5.12: Effect of bed height on the ion exchange breakthrough curve for Cl^- on anion resin at 0.05 l/min flow rate and an initial chloride concentration of 600 mg/l.

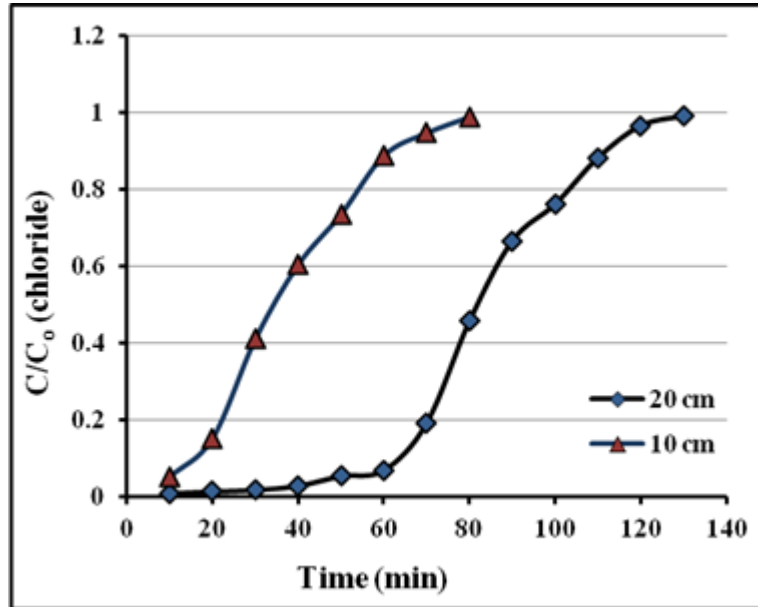


Figure 5.13: Effect of bed height on the ion exchange breakthrough curve for Cl^- on anion resin at 0.1 l/min flow rate and an initial chloride concentration of 600 mg/l.

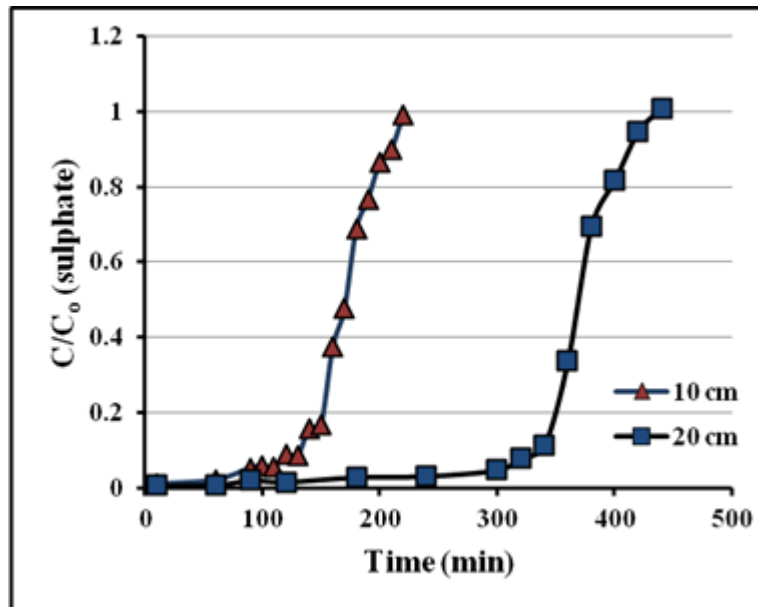


Figure 5.14: Effect of bed height on the ion exchange breakthrough curve for SO_4^{2-} on anion resin at 0.1 l/min flow rate and an initial sulphate concentration of 200 mg/l.

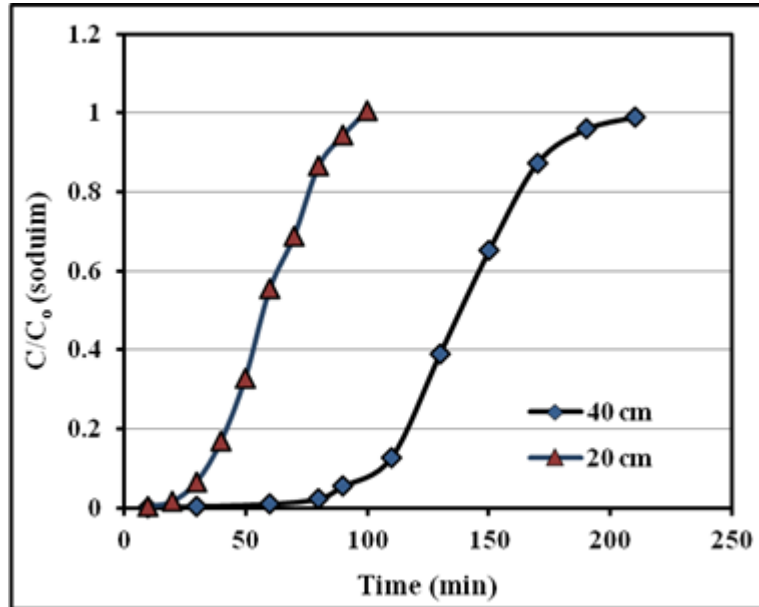


Figure 5.15: Effect of bed height on the ion exchange breakthrough curve for Na^+ on mixed resin at 0.1 /min flow rate and an initial sodium concentration of 485 mg/l.

From these results, it can be concluded that increase in the Cl^- , SO_4^{2-} and Na^+ uptake in a column with the increase of the bed height was due to an increase in longer contact time for ions adsorption (Kundu and Gupta, 2006). In another word, the increasing of the bed height means increasing in the bed volume, leads to increase in the EBCT, which in turn will increase the removal efficiency of the ions.

5.3.2.3 Effect of Initial Ion Concentration on Breakthrough Curve

In order to investigate the effect of initial chloride concentration in the feed solution on separation performance of chloride from water, the experiments were performed using various Cl^- concentrations of (200, 400, 600 and 800 mg/l) at 0.05 l/min and 20 cm bed height. Histories of change in chloride concentration at any time over initial feed concentration (C/C_0) using different initial concentration of chloride are given in Fig. (5.16). The breakthrough point for the 800 mg/l Cl^- concentration appeared much quickly than for 200 mg/l Cl^- concentration.

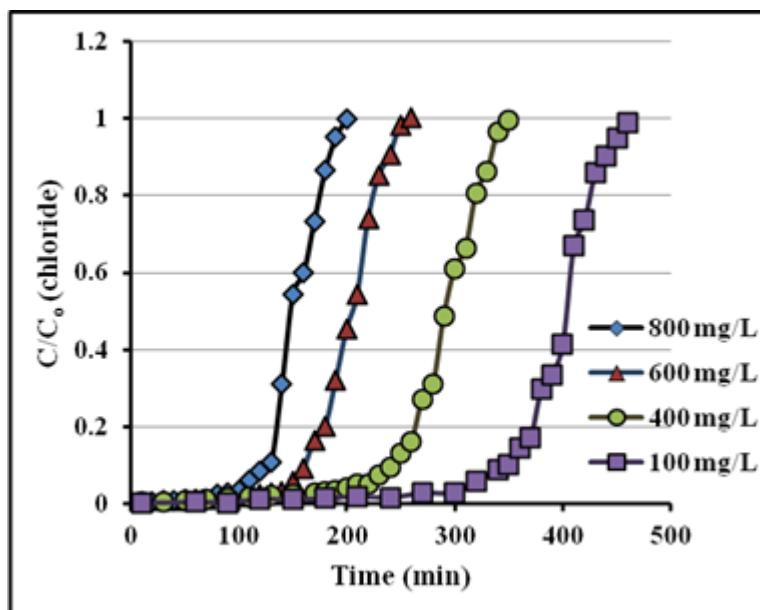


Figure 5.16: Effect of initial concentration on the ion exchange breakthrough curve for Cl^- on anion resin at 0.05 l/min flow rate and 20 cm bed height.

The change in inlet concentration markedly affects the shape and position of the breakthrough curve. The higher the inlet concentration, the faster the breakthrough is. In addition, the effluent concentration after the breakthrough point sharply increased on the higher inlet concentration comparing with the lower inlet concentration and the dynamic capacity or breakthrough volume (V_{br}) decreased with increasing the initial concentration. The quantity of solutions to be supplied is large when the inlet concentration is low. The results of the breakthrough behaviour experiment for a Cl^- concentration of 200 mg/l show that about 18 liter of feed solution could be passed through the resin with less than 20 mg/l of Cl^- ion in the effluent.

Figures (5.17) and (5.18) displays the effect of initial SO_4^{2-} and Na^+ concentrations on the breakthrough curve, where a same results as in Fig. (5.16) was obtained. From the above experimental results we conclude that on increasing the initial ion concentration, the breakthrough curves became steeper and breakthrough volume decreased because of the lower mass-transfer flux from the bulk solution to the particle surface due to the weaker driving force (Baek et al, 2007). At higher concentration, the availability of the desired removal molecules for the adsorption sites is more, which leads to higher uptake of them

at higher concentration even though the breakthrough time is shorter than the breakthrough time of lower concentrations.

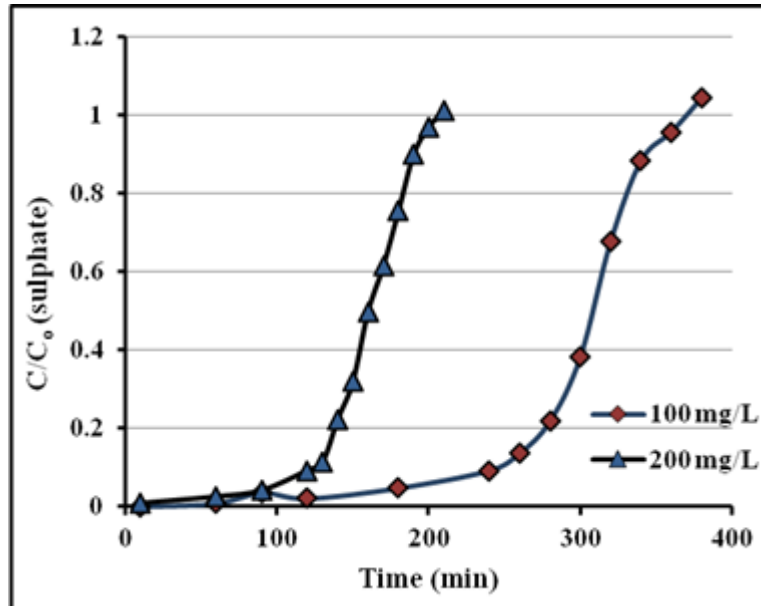


Figure 5.17: Effect of initial concentration on the ion exchange breakthrough curve for SO_4^{2-} on anion resin at 0.1 l/min flow rate and 10 cm bed height.

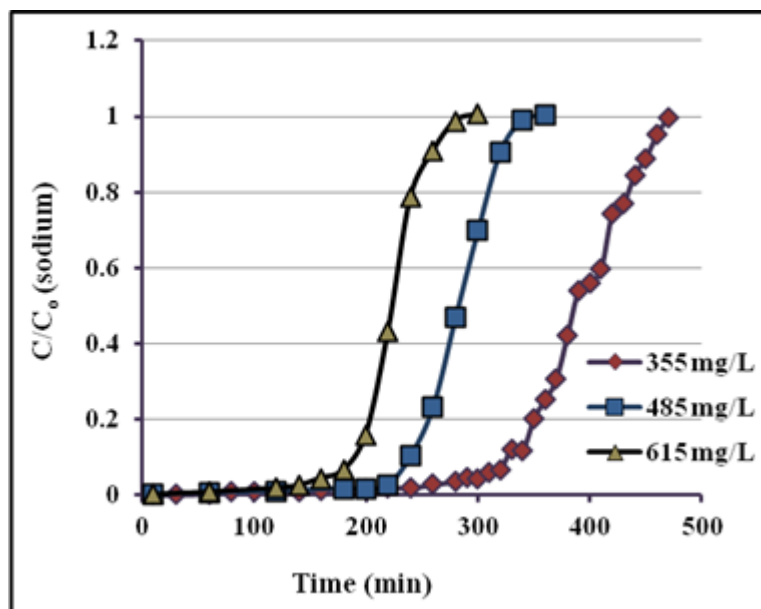


Figure 5.18: Effect of initial concentration on the ion exchange breakthrough curve for Na^+ on mixed resin at 0.05 l/min flow rate and 40 cm bed height.

5.3.2.4 Effect of Co-Ion on Breakthrough Curve for Cl^-

In order to investigate the effect of sulphate concentration on the Breakthrough curve for chloride (i.e. on the removal of chloride ions), the experiments were performed using 100 and 200 mg/L sulphate concentrations. The effects of SO_4^{2-} on the breakthrough curve for Cl^- are indicated in Fig. (5.19) and (5.20).

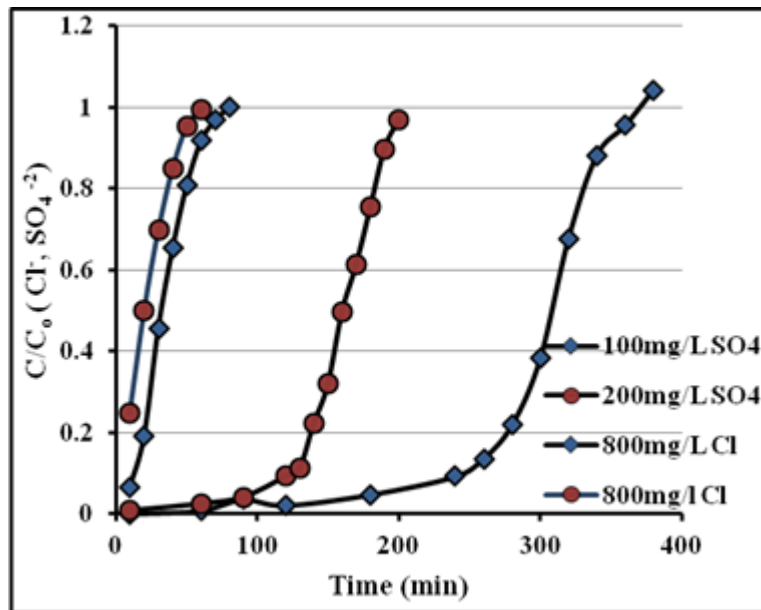


Figure 5.19: Effect of SO_4^{2-} initial concentration on the ion exchange breakthrough curve for Cl^- on anion resin at 0.1 l/min flow rate and 10 cm bed height.

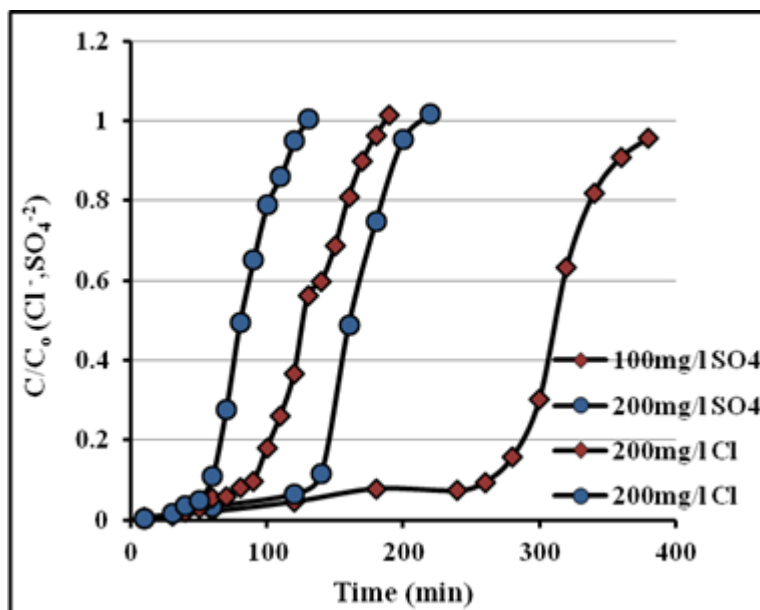


Figure 5.20: Effect of SO_4^{2-} initial concentration on the ion exchange breakthrough curve for Cl^- on anion resin at 0.1 l/min flow rate and 10 cm bed height.

The selectivity of the resin can be analyzed using the breakthrough results. Fig. (5.19), shows the ion exchange breakthrough curve for Cl^- and SO_4^{2-} using the anion resin. In these breakthrough curves the normalized concentration, defined as the measured concentration divided by the inlet concentration, is plotted against time in minutes. The SO_4^{2-} ions bind strongly to the ion exchange resin due to the high selectivity of the resin to SO_4^{2-} ions comparing with Cl^- ions, as described in section 2.7.4. So the SO_4^{2-} ions can also ion exchanging with Cl^- ion on the resin. In turn, the breakthrough curve for Cl^- became saturation before the appearance of the SO_4^{2-} ions in the effluent solution. In addition the decrease in the adsorption of Cl^- by the resin as the amount of SO_4^{2-} ions held by the resin increases can be a consequence of the loss of available exchange sites due to the presence of additional ions adsorbed into the ion exchange resin, therefore the increasing of SO_4^{2-} initial concentration from 100 to 200 mg/l strongly affected the removal of Cl^- ions as shown in Fig. (5.19).

The chloride breakthrough curve in Fig. (5.20) was also affected by the increasing of the sulphate concentration, but the changing was not much as in Fig. (5.20), due to the much high concentration of Cl^- comparing with SO_4^{2-} concentration. It can be conclude

from these results that the presence of SO_4^{2-} ions reduce the resin capacity and the Cl^- ions removal. The removal of sulphate ions before the ion exchange process is essential in order to increase the Cl^- removal.

5.3.2.5 The Effect of Mixed Bed Ion Exchange on Breakthrough Curve

All the experiments that preformed by using the anion exchange resin was repeated by changing the resin to a mixed exchange resin, in order to investigate the effect of it on the breakthrough curve.

Figures below shows the effect of flow rate, bed height and initial concentration on breakthrough curve for Cl^- on mixed and anion exchange resin. As seen in the figures, the breakthrough behavior is the same as for Cl^- on anion resin and the only different is in the breakthrough time and volume. For example, in Fig. (5.21), the breakthrough time occurred at 130 min and 65 min for flow rates of 0.05 and 0.1 l/min on the mixed exchange resin, while it occurred at 95 min and 35 min for flow rates of 0.05 and 0.1 l/min on the anion exchange resin, respectively.

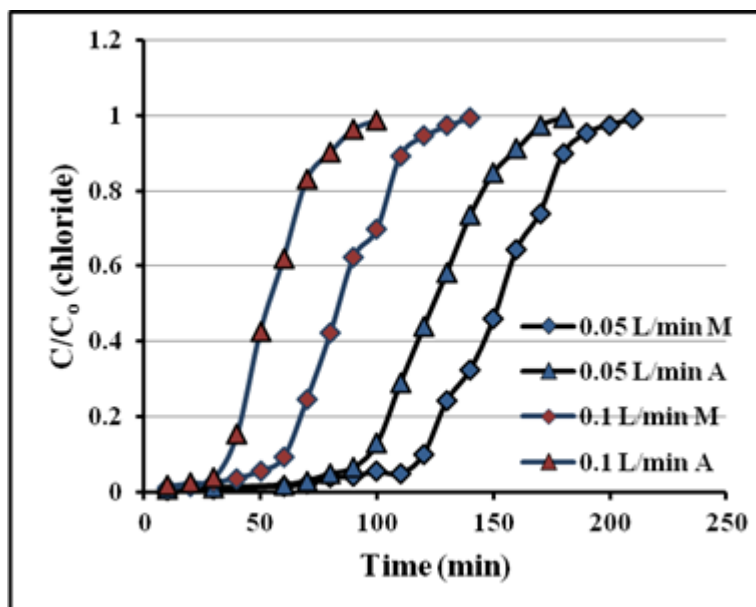


Figure 5.21: Effect of flow rate on the ion exchange breakthrough curve for Cl^- on mixed resin at 20 cm bed depth and an initial chloride concentration of 400 mg/l.

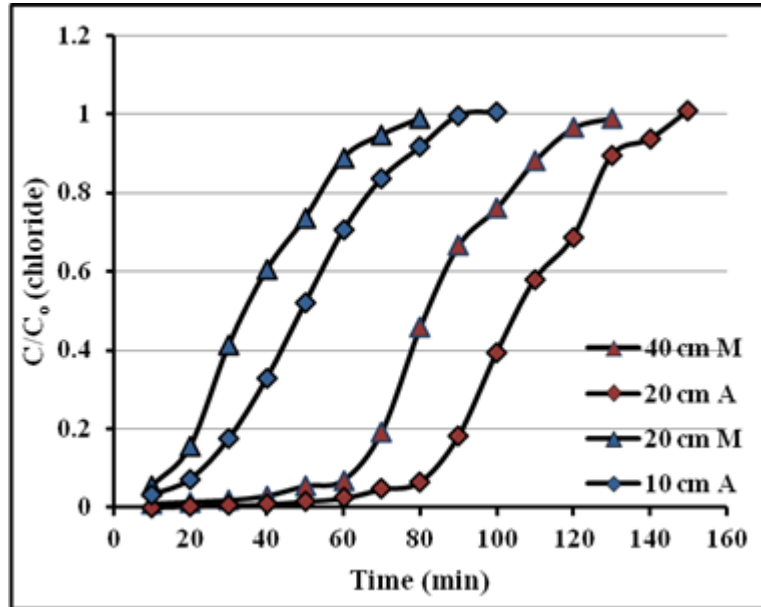


Figure 5.22: Effect of bed height on the ion exchange breakthrough curve for Cl^- on mixed resin at 0.1 l/min flow rate and an initial chloride concentration of 600 mg/l.

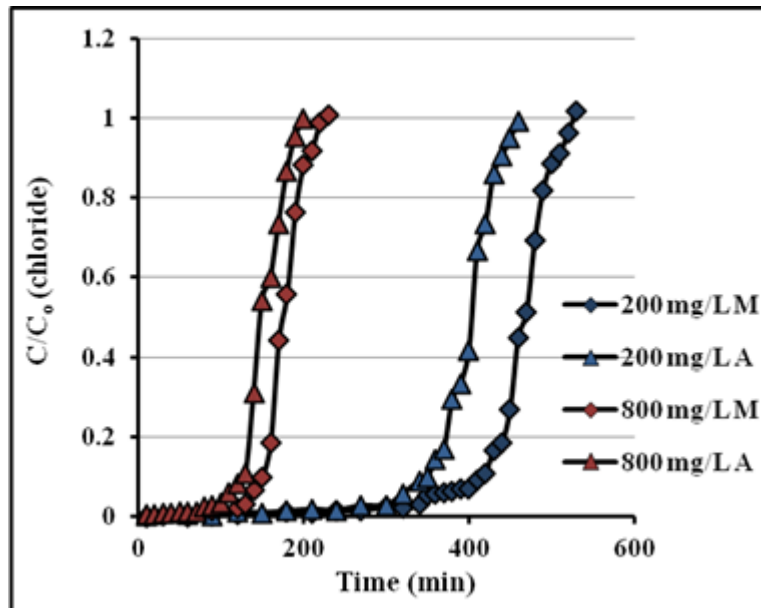


Figure 5.23: Effect of initial concentration on the ion exchange breakthrough curve for Cl^- on mixed resin at 0.05 l/min flow rate and 40 cm bed height.

In addition to the improving of the breakthrough time by using the mixed exchange resin, the removal efficiency also improved as representing by the increasing of the breakthrough volume.

For an anionic monobed, the OH^- concentration increases during exchange, and reaction continues in a more basic solution. In contrast, cationic monobed exchange occurs in a more acidic solution than a mixed bed due to the same phenomenon (as described in section 2.9). The mass transfer coefficient of anionic exchange are higher in acidic solution, while those for cationic exchange are higher in basic solution according to Harries (1991), who attributed the lower mass transfer coefficient of a monobed to solution pH. The higher mass transfer coefficients in mixed beds were explained by Haub and Foutch (1986) by considering neutralization in the bulk phase and liquid film. Since mass transfer coefficient is an overall system parameter, the ionic flux through the film is a complex function of all species present.

The mass transfer coefficients of cationic and anionic resin in monobeds are lower than the mass transfer coefficients in mixed beds which can be attributed to solution pH. The hydrogen and hydroxyl neutralization reaction in a mixed bed serves as a sink for maintaining the hydrogen and hydroxyl concentration gradients around the cation and anion resins respectively. This will keep the mass transfer coefficients in mixed beds in the high level, in turn the adsorption capacity or the removal efficiency of the mixed bed will increase.

5.3.2.6 Comparison between Model Predictions and Experimental Results

Figures (5.24) to (5.28) show a comparison between experimental results of breakthrough curve for Cl^- , SO_4^{2-} and Na^+ on the mixed exchange resin with theoretical ones which are calculated using the Matlab program. The theoretical results are given in tables in appendix A.

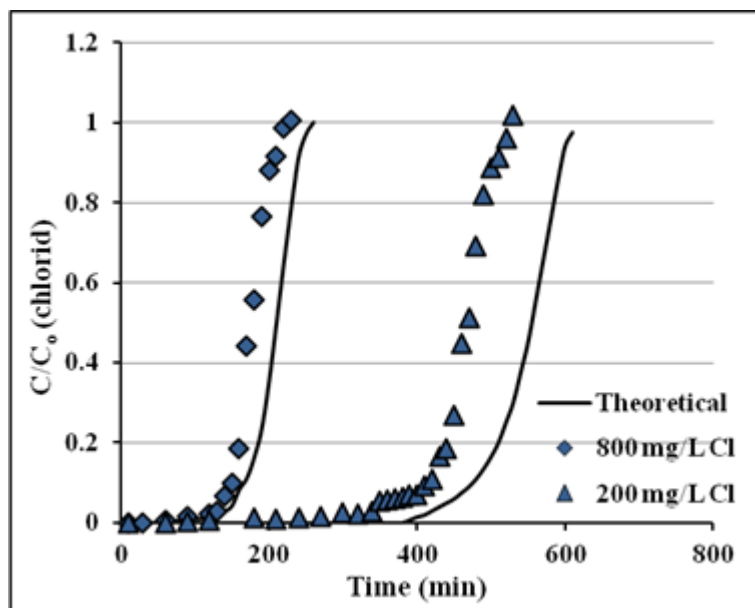


Figure 5.24: Comparison between experimental and theoretical breakthrough curve for Cl^- (flow rate 0.05 l/min and 40 cm bed height).

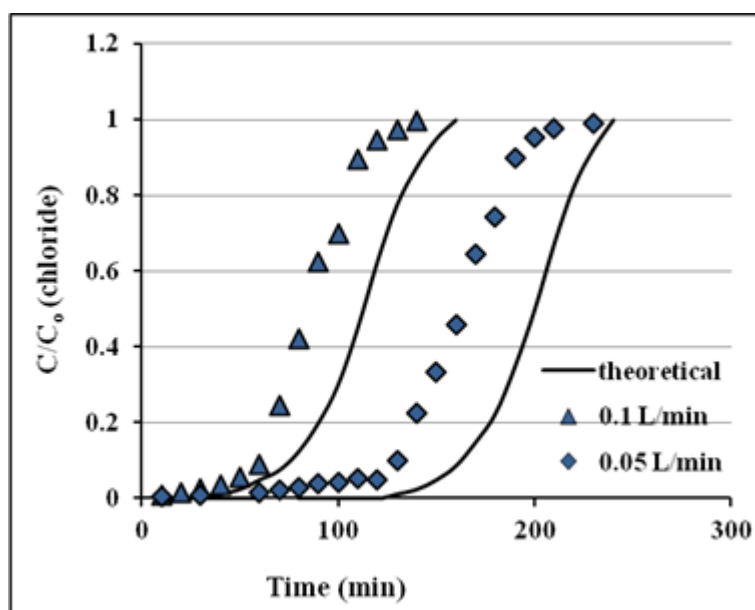


Figure 5.25: Comparison between experimental and theoretical breakthrough curve for Cl^- (20 cm bed height and 400 mg/l Cl^-).

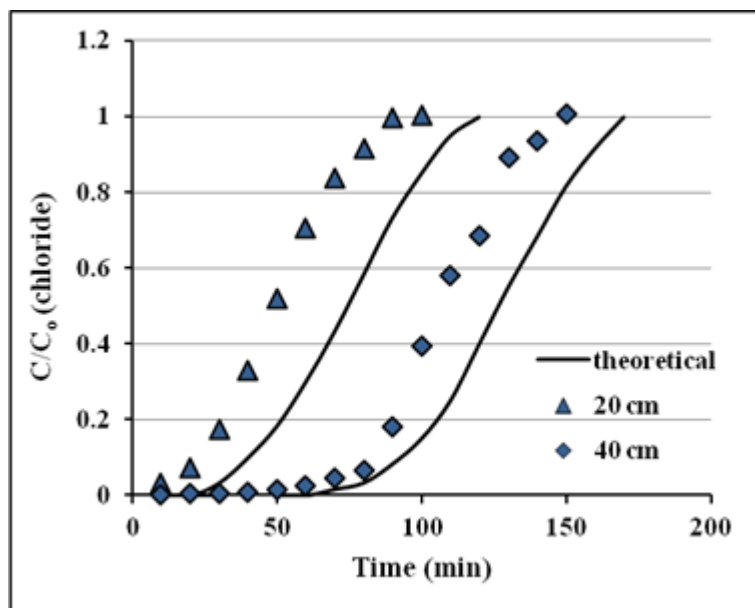


Figure 5.26: Comparison between experimental and theoretical breakthrough curve for Cl^- (flow rate 0.1 l/min and 600 mg/l Cl^-).

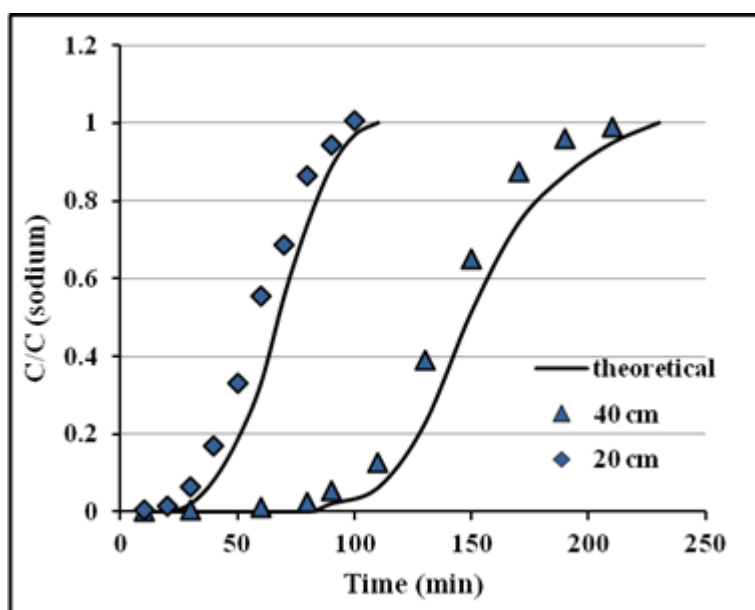


Figure 5.27: Comparison between experimental and theoretical breakthrough curve for Na^+ (flow rate 0.1 l/min and 485 mg/l Na^+).

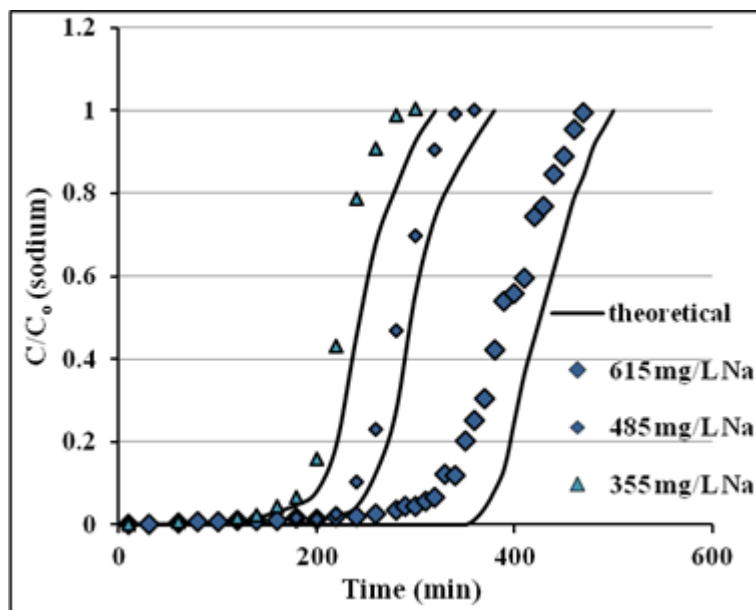


Figure 5.28: Comparison between experimental and theoretical breakthrough curve for Na^+ (flow rate 0.05 l/min and bed height 40 cm).

As can be seen from the figures, the experimental breakthrough points for chloride are not well close to the theoretical breakthrough curve while the experimental breakthrough points for sodium are well close to the theoretical breakthrough curve. Due to the effect of the bicomponent isotherm (chloride and sulphate isotherms), which was not taken in the computer simulation (the Freundlich monocomponent isotherm parameters was used in the program). In order to improve equilibrium relations and its predictions in a multicomponent exchange and applied to the divalent species (as described in section 4.1.3), batch adsorber experiments for the binary mixture (chloride and sulphate) at different concentrations and adsorbent amount, should be performed.

From the fixed bed experiments, one can conclude that higher flow rates than 0.1 l/min should be avoided since breakthrough would occur faster and with less sharpened boundaries. Flow rates lower than 0.05 l/min flow rates are expected to be beneficial on removal efficiency, leading however to practically too high retention times. In column studies the decrease of the flow rate resulted in the increase of the removal efficiency.

However, there is a need to balance between very low flows which are not practicable and high flows that reduce removal efficiencies. In addition at low initial concentration, breakthrough occurred late and the treated volume was higher since the lower concentration gradient caused a slower transport due to decreased diffusion coefficient or mass transfer coefficient. It was seen from the breakthrough curve that the slope of breakthrough curve a little decreased with increasing bed height. Because the increase in bed height the adsorbate has more time to contact with the resin, which in turn results into higher removal capacity and lower solute concentration in the effluent. Besides, at higher bed height the availability of the effective surface area of adsorbent is more which offers more active sites to adsorption and it also broadens the mass transfer zone length.

The mass transfer coefficients of cationic and anionic resin in monobeds are lower than that in the mixed beds which can be attributed to solution pH. The hydrogen and hydroxyl neutralization reaction in a mixed bed serves as a sink for maintaining the hydrogen and hydroxyl concentration gradients around the cation and anion resins respectively. The higher mass transfer coefficient improves the removal efficiency of the mixed bed ion exchange column.

Chapter Six

Conclusions and Recommendation for Future Work

6.1. Conclusions

1. The use of the dual polyelectrolyte system of the low-molecular weight cationic Zetage 7557 followed by high-molecular weight anionic Magnafloc 336 flocculants, produced excellent flocculation, when they added to the Eshidiya wastewater, resulting in an excellent dewaterability, very low turbidity value and almost a 100% removal of the phosphate ion.
2. The optimum dosage of the dual polyelectrolyte flocculants used to enhance sedimentation for Eshidiya wastewater is by combining 7 ppm of cationic Zetage 7557 polymer followed by 10 ppm of anionic Magnafloc 336 polymer, which gives a target Zeta potential of -5.6 mV.
3. The settling rate was increased 20 times by adding the optimum dose of the dual polyelectrolyte flocculants and the waste volume was decreased by 70% as compared to the natural settling rate and volume of the same waste.
4. Enhanced sedimentation rate was the obvious advantage of flocculation with flocculants, which significantly reduced the sedimentation time of the Eshidiya wastewater. Although the physical properties of the flocculants such as molecular weight play an important role in the performance of the flocculation process, through it is effect on the size of the flocs. As shown in the present work the ultra-high molecular weight anionic polyelectrolyte flocculent (Magnafloc 919) produced a super large flocs that settled faster than the flocs produced by the

addition of high molecular weight anionic polyelectrolyte flocculent (Magnafloc 336).

5. The anionic polyelectrolyte flocculent of the lower molecular weight gives a better dewaterability results. This is shown in the lower sludge volume after 30 min of settling.
6. The over dosing of the anionic polyelectrolyte inhibited the flocculation, resulting in increased the turbidity of the residual water.
7. When the wastewater is pre-conditioned with the cationic polyelectrolyte in dual polyelectrolytes conditioning. The fine and dispersed particles were efficiently captured, which is shown clearly by the sharp decreasing of turbidity after 30 min of settling.
8. The batch experimental study show that the chloride removal decrease with increasing chloride concentration. Maximum chloride removal was obtained with minimum solution concentration (200 mg/l) with 98.95% yield. The other removal yields for initial solution concentration 400 mg/l, 600 mg/l and 800 mg/l are 70%, 43.3% and 35.1%, respectively. Amount of resin is proportional with chloride removal efficiency due to increase in the resin surface area.
9. The data obtained from batch studies were applied to Langmuir and Freundlich isotherm. The Freundlich isotherm gives an adequate correlation coefficient value compared to the Langmuir isotherm correlation isotherm.
10. The ion exchange (adsorption) of Cl^- , SO_4^{2-} and Na^+ is dependent on the bed depth, flow rate, and initial concentration. A shorter breakthrough time (t_{br}) and lower breakthrough volume (V_{br}) is observed at decreasing bed depth, and increasing flow rate and initial concentration. Removal capacity are observed at highest bed depth of 20 cm in anionic monobed, 40 cm in mixed bed, lowest flow rate of 0.05 l/min, and lowest initial concentration of 200 mg/l Cl^- .
11. Mechanism of the system, which was studied in this work, is mixed diffusion mechanism. Because in low solution concentration its film diffusion control, while it became particle diffusion control with increasing the solution concentration. In another word the studied system is intermediate between film and particle diffusion control.

6.2. Recommendations for future work

From the present study it was noticed that further studies in the following areas would be desirable:

1. The possible superiority of the dual polyelectrolyte system is not ruled out. Research work on another dual system and compare with the present study to find the much more efficient and cost-effective.
2. Studying the effect of mixing speed on coagulation. By applying a different mixing speed to the Eshidiya wastewater conditioned with the optimum dosage of the dual polyelectrolyte system to determine the best mixing speed in the coagulation stage using turbidity as a criterion.
3. Studying the effect of temperature on the ion exchange capacity and adsorption isotherms. Variation of these values with changes in service water temperature has to be determined and incorporated into the model.
4. Studying the effect of resin ratios (cation/anion) in the mixed bed on the predicted effluent
5. There is a need to balance between very low flows which are not practicable and high flows that reduce removal efficiencies of the mixed bed ion exchange, which need to perform more experiments at a flow rate below 0.05 l/min.

References

- Acrivos, A., "On the combined effect of longitudinal diffusion and external mass transfer resistance in fixed bed operations," Chem. Eng. Sci., Vol. 13, 1960.
- Baek, K.; Song, S.; Kang, S.; Rhee, Y.; Lee, C.; Lee, B.; Hudson, S.; & Hwang, T., Adsorption kinetics of boron by anion exchange resin in packed column bed," J. Ind. Eng. Chem., Vol. 13,(2007).
- Bennett, A. (2004). "Advances in high purity water filtration technologies," Filtration & Separation, Vol. 41, 2004.
- Bernahl, W. E., and C.E. Rossow, "Current Trends in Ion Exchange Operations-What the Resins are Telling Us," Water Quality Products, Vol. 8, 2003.
- Bohm N.; Kulicke W.M., (1997) "Optimization of the Use of Polyelectrolytes for Dewatering Industrial Sludge of Various Origins," Colloid Polymer Sci., Vol. 275, 1997.
- Bratby, J., "Coagulation and Flocculation in Water and Wastewater Treatment," IWA publishing, London UK, 2006.
- Bronwell, L.G., Oxford T.P., "Waste clay and disposal, Geotechnical practice for disposal of solid waste materials," ASCE, New York, 1977.
- CH.Sheindorf; M. Rebhun; M. Sheintuch, "A Freundlich-type multicomponent isotherm," Journal of Colloid and Interface Science, Vol. 79, 1981.
- Christensen J. R.; Sorensen P. B.; Christensen G. L.; Hansen J. A., "Mechanisms for overdosing in sludge conditioning," J. Environ. Eng. ASCE, Vol. 119, 1993.
- Colwell, C. J.; Dranoff, J. S., "Nonlinear Equilibrium and Axial Mixing Effects in Intraparticle Diffusion-Controlled Sorption by Ion Exchange Resin Beds, Experimental Study," Ind. Eng. Chem. Fundamen., Vol. 10, 1971.
- Cooney, D. O., "Comparison of simple adsorber breakthrough curve method with exact solution," AIChE Journal, Vol. 39, 1993.
- Cooney, D. O., "External film and particle phase control of adsorber breakthrough behavior," AIChE Journal, Vol. 36, 1990.
- David H. Bache, Ross Gregory,"Flocs in Water Treatment," IWA Publishing, London, UK, 2007.

- David J. Raden, "Current Problems in Beneficiation of Phosphate Fines, in: Beneficiation of Mineral Fines, problems and research needs," American Institute of Mining, Metallurgical, and Petroleum Engineers, New York, 1978.
- Dorfner, K., "Ion Exchangers (Ed. Dorfner K.)," Walter de Grauter, Berlin and New York, 1991.
- Ebeling, J.M.; Ogden, S.; Sibrell, P.L.; Rishel, K. L., "Application of chemical coagulation aids for the removal of suspended solids and phosphorus from the microscreen effluent discharge of an intensive recirculating aquaculture system", J. of North American Aquaculture, Vol. 66, 2004.
- Eriksson L.; Alm B., "Characterization of activated sludge and conditioning with cationic polyelectrolyte," Water. Sci. Tech., Vol. 28, 1993.
- Ernest, M. V.; Bibler, J. P.; Whitley, R. D.; Wang, N. H. L., "Development of a Carousel Ion-Exchange Process for Removal of Cesium," Industrial & engineering Chemistry Research, Vol. 36, 1997.
- Faust, A.D.; Aly, O.M., "Chemistry of Water Treatment," Butterworths, Boston, 1983.
- Fourest, E.; Canal, C.; Roux, J., "Improvement of heavy metal biosorption by mycelial dead biomasses (*Rhizopusarrhizus*, *Mucormiehei* and *Penicilliumchrysogenum*): pH control and cationic activation," FEMS Microbiol Rev, Vol. 14, 1994.
- Freger, V., "Elastic energy in microscopically phase-separated swollen polymer networks," Polymer, Vol. 43, 2002.
- Gantman, A. I. "Basic characteristics of the sorption of water by polymeric ion exchangers" Russian journal of physical chemistry Y, vol. 66, 1992.
- George Tchobanoglous, Franklin Louis Burton, H. David Stensel, "Wastewater Engineering: Treatment, Disposal and Reuse," 4th Edition, McGraw-Hill, Boston, 2003.
- Gregory, J., "Flocculation by inorganic salts," The Scientific basis of flocculation, K. J. Ives, ed., Sijthoff and Noordhoff, Amsterdam, Netherlands, 1978.
- Gregory, J., "Stability and Flocculation of Suspensions" in: "Processing of Solid-Liquid Dispersions" (Edited by Shamlou, P.A.), Butterworth-Heinemann Ltd, Oxford UK, 1993.
- Hall, K.R.; Eagletow, L.C.; Acrivers, A.; Vermenlem, T., "Pore and Solid kinetics in fixed-bed adsorption under constant pattern condition," Ind. Eng. Chem. Fund., Vol.5, 1966.

- Halverson, F.; Panzer, H.P., "Flocculating Agents," in: "Encyclopedia of Chemical Technology (Edited by I. Kirk and D.F. Othmer)," John Wiley & Sons, New York, USA, 1980.
- Harries, R. R., "Ion exchange kinetics in ultrapure water systems," J. Chern. Tech. Biotechnol., Vol. 51, (1991).
- Hashimoto K.; Miura, K.; Tsukano, M., "Experimental verification of design methods for liquid phase fixed-bed adsorbers," J. Chem. Eng. Japan, Vol. 10, 1977.
- Haub, C. E. and Foutch, G. L., "Mixed-bed ion exchange at concentrations approaching the dissociation of water 2. Column model applications," Ind. Eng. Chem. Fund., Vol. 25, (1986a).
- Haub, C. E. and Foutch, G. L., "Mixed-bed ion exchange at concentrations approaching the dissociation of water 2. Column model applications," Ind. Eng. Chem. Fund., Vol. 25, (1986b).
- Helfferich, F. G., "Models and physical Reality in ion-exchange kinetics," Reactive Polymers, Vol. 13, (1990).
- Helfferich, F. G., "In Mass Transfer and Kinetics of Ion Exchange (L. Liberti, F. G. Helfferich, eds.)," 157, Martinus Nijhoff Publishers, Hague, 1983.
- Helfferich, F. G.; Hwang, Y.-L., "In Ion Exchangers (K. Dorfner, ed.)," 1277, Walter de Gruyter, Berlin, 1991.
- Helfferich, F.G., "Ion Exchange," McGraw Hill Book Company, New York, 1962.
- Hendricks, D., "Fundamentals of Water Treatment Unit Processes: Physical, Chemical, and Biological," Taylor & Francis Group, USA, 2011.
- Hogg, R., "Flocculation problems in the coal industry, in Fine Particles Processing, "Somasundaran, P. (ed.) (AIME), 1980.
- http://www.outreach.canterbury.ac.nz/chemistry/chloride_mohr.shtml
- Hughes, M.A., "Coagulation and Flocculation," in: "Solid-Liquid Separation (Edited by Ladislav Svarovsky)," Butterworth-Heinemann Ltd, Oxford UK, 2000.
- Hunter, R.J., "Foundations of Colloid Science," Oxford University Press, Oxford, UK, 2001.
- Irving, J., "In Ion Exchange at the Millennium (J. A. Greig, ed.)," Imperial College Press, London, 2000.

- Jones, M., Stephenson, T., "The effect of temperature on enhanced biological phosphate removal," *Environ. Technol.*, Vol. 17, 1996.
- Kamiyango, M. W.; Masamba, W. R. L.; Sajidu, S. M. I; Fabiano, E., "Phosphate removal from aqueous solutions using kaolinite obtained from linthipe, Malawi," *Phys. Chem. Earth*, Vol. 34, 2009.
- Kirby, B.J., "Micro- and Nanoscale Fluid Mechanics: Transport in Microfluidic Devices," Cambridge University Press, Cambridge, UK, 2010.
- Kruyt, H. R., "Colloid Science," Volume 1, Elsevier Science, Amsterdam, 1995.
- Kundu, S.; Gupta, A. K. "As (III) Removal from Aqueous Medium in Fixed Bed Using Iron Oxide-Coated Cement (IOCC): Experimental and Modelling Studies," *Chemical Engineering Journal*, Vol. 122, 2006.
- Langer, S.; Klute, R.; Hahn, H. H., "Mechanisms of floc formation in sludge conditioning with polymers," *Water Sci. Tech.*, Vol. 30, 1994.
- Laurier Lincoln Schramm, "Emulsions, Foams and Suspensions," WILEY-VCH Verlag GmbH & Co. KGaA, Weinheim, Germany, 2005.
- Lawrence K. Wang; Yung-Tse Hung; Nazih K. Shamas, "Handbook of Environmental Engineering: Physicochemical Treatment Processes," Humana Press Inc., Totowa, New Jersey, 2005.
- Lee C.H.; Liu J.C., "Enhanced sludge dewatering by dual polyelectrolytes conditioning," *Water Research*, Vol. 34, 2000.
- Lehto, J. and Harjula, R., "Experimentation in ion exchange studies - the problem of getting reliable and comparable results," *Reactive & Functional Polymers*, Vol.27, 1995.
- Lehto, J.; Brodtkin, L.; Harjula, R.; Tusa, E., "Separation of Radioactive Strontium from Alkaline Nuclear Waste Solutions with the Highly Effective Ion Ex-changer SrTreat," *Nuclear Technology*, Vol. 127, 1999.
- Malykhin, M. D.; Shaposhnik, V. A.; Kuzminykh, V. A., "Diffusion boundary layers at a boundary with a cation-exchanger granule," *Russian Journal of Physical Chemistry*, Vol. 66, 1992.
- McFarlin, R. F.; El-Shall, H., "A Rapid Phosphatic Clay Dewatering Scheme,in: Beneficiation of Phosphate: Theory and Practice (H. El-Shall, B. M. Moudgil, R.

- Wiegel, Eds.),” Society of Mining Metallurgy and Exploration, Inc, Littleton (Colorado), 1993.
- Montgomery, J.M. (1985), “Water Treatment Principles and Design”, John Wiley & Sons, New York.
 - Moses Road, E., “Role of Weak Acid Cation Resin in Water Treatment,” Ion Exchange (India) Ltd., Mumbai, India, 2004.
 - Nicholas P. Cheremisinoff,”Handbook of Water and Wastewater Treatment Technologies” Butterworth-Heinemann, USA, 2002.
 - Nozaic, D.J.; Freese, S.D.; Thompson, P., “Long Term Experience in the Use of Polymeric Coagulants at Umgeni Water,” Water Sci. Technol.: Water Supply, Vol. 1, 2001.
 - Packham,R.F., ”Some studies of the coagulation of dispersed clays with hydrolyzing salts,” J. Colloid Sci., Vol. 20, 1965.
 - Patrick Zhang et al.; Karen Swager; Laurindo Leal filho; Hassan El-shall, “Beneficiation OF Phosphates: Technology Advance and Adoption,” Society for Mining, Metallurgy, and Exploration, Inc. (SME), USA, 2010.
 - Perry, R.H.; Green, D., “Perry’s Chemical Engineers’ Handbook,” 8th Edition, McGraw-Hill, International Editions, 1999.
 - Petzold, G.; Mende, M.; Lunkwitz, K.; Schwarz, S.; Buchhammer, H., ”Higher efficiency in the flocculation of clay suspensions by using combinations of oppositely charged polyelectrolytes,” Colloids Surfaces, Vol. 218, 2003.
 - Regory, J., ”Particles in Water: Properties and Processes,” London:CRC Press, Taylor & Francis Group, UK, 2006.
 - Rout, D.; Verma, R.; Agarwal, S.K., “Polyelectrolyte Treatment-an approach for water quality improvement,” Water Sci. Technol., Vol. 6, 1999.
 - Russel, W.B.; Saville, D.A.; Schowalter, W.R, “Colloidal Dispersions”, Cambridge University Press, Cambridge, UK, 1995.
 - Ruthven, D.M., “Principles of Adsorption and Adsorption Processes,” Wiley, New York, 1984.
 - Sarin, V.; Singh, T. S.; Pant, K. K., “Thermodynamic and Breakthrough Column Studies for the Selective Sorption of Chromium from Industrial Effluent on Activated Eucalyptus Bark,” Bioresource Technology, Vol. 97, 2006.

- Schwartz, C. E., Smith, J. M., "Flow Distribution in Packed Beds," Journal of Industrial and Engineering Chemistry, Vol. 45, 1953.
- Selemeney, V. F.; Slavinskaya, G. V.; Khokhlov, V. Y.; Ivanov, V. A.; Gorshkov, V. I.; Timofeevskaya, V. D. "Practical Course in Ion Exchange, Voronezh State University Voronezh, 2004.
- Seung-Hyun, K.; Baumann, E. R., "Investigation of chemical Phosphate Removal from an Oxidation Ditch by Field Evaluation," Environ. Eng. Rrs., Vol. 2, 1997.
- Shaposhnik, V. A.; Vasileva, V. I.; Grigorchuk, O. V., "Transport Phenomena in Ion Exchange Membranes (Yavleniya perenisa v ionoobmennyyh membranah)", Moscow Physico- Technical Institute, Moscow, 2001.
- Slater, M. J., "Principles of Ion Exchange Technology," Butterworth-Heinemann, Oxford, 1991.
- Smith, J.M., "Chemical Engineering Kinetics," 3rd Edition., McGraw-Hill, New York, USA, 1981
- Smith, R.W.; Misra, M.; Dubel, J., "Bacterial flocculation of phosphate wastes using a hydrophobic bacterium," Mineral Processing and Extractive Metallurgy Review: An International Journal, Vol. 12, 1993.
- Somasundaran, P.; Krishnakumar, S., "Adsorption of surfactant and polymer at the solid-liquid interface," Colloids Surfaces, Vol. 123, 1997.
- Stanley, E. M., "Fundamentals of environmental chemistry," CRC Press, London, 2001.
- Streat, M., "Ion Exchange: A Technologist's Perspective of the 20th Century," in "Advances in Ion Exchange For Industry and Research," Edited by Williams, P.A., and Dyer, Q., The Royal Society of Chemistry, Cambridge, U.K., 1999.
- Tambo, N.; Hozumi, H., "Physical characteristics of flocs - II. Strength of floe," Water Research, Vol. 13, 1979.
- Van Loosdrecht, M.C.M.; Hooijmans, C.M.; Brdjanovic, D.; Heijnen, J.J., "Biological phosphate removal processes", Appl. Microbiol Biotechnol, Vol. 48, 1997.
- Vassilis J. Inglezakis, Stavros, G. Pouloupoulos, "Adsorption, Ion Exchange and Catalysis: Design of Operations and Environmental Applications "Elsevier Science, 2006.

- Wang, X. J.; Xia, S. Q.; Chen, L.; Zhao, J. F.; Renault, N. J.; Chovelon, J. M., "Nutrients removal from municipal wastewater by chemical precipitation in a moving bed bio film reactor," Proc. Bio Chem., Vol. 41, 2006.
- Zagorodni, A.A., "Ion Exchange Materials: Properties and Applications" 1st edition, Elsevier BV, Amsterdam, 2007.
- Zhang J., "Phosphate Beneficiation Trends of the 90's, in: Beneficiation of Phosphate: Theory and Practice, (H. El-Shall, B. M. Moudgil, R. Wiegel, Eds.) Society of Mining Metallurgy and Exploration," Inc, Littleton, Colorado, 1993.

Appendix A

Experimental Results

A1- Sedimentation experiment:

A1-1: The turbidity of waste water with time during sedimentation.

Time (hr)	Turbidity (NTU)
1	49.8
2	38.2
3	28.4
6	19.1
9	15.2
12	10.4
15	8.5
18	6.2
21	5.1
24	4.7
27	4.7
30	4.6

A2- Enhanced sedimentation experiments results:

A2-1: Zeta potential and turbidity results from the addition of Magnafloc 919 and Zetag 7557 to the tested water.

7 ppm cationic polymer			
Anion Polymer Dosage(ppm)	Zeta Potential (mV)	Standard Deviation (mV) of Zeta Potential	Turbidity (NTU)
0	-26.4	0.23	49.8
5	-12.8	0.65	15
7	-7.3	0.23	7.6
10	-5.6	0.32	3.3
15	-5.1	0.39	3.2
20	-7.6	0.25	3.9
25	-8.3	0.22	4.6
30	-8.5	0.33	5.5

A2-2: Zeta potential and turbidity results from the addition of Magnafloc 919 and Zetag 7557 to the tested water.

7 ppm cationic polymer			
Anion Polymer Dosage(ppm)	Zeta Potential (mV)	Standard Deviation (mV) of Zeta Potential	Turbidity (NTU)
0	-26.4	0.23	49.8
5	-14.3	0.31	16.3
7	-8.5	0.11	9.2
10	-7.7	0.45	3.9
15	-7.3	0.32	4.1
20	-9.4	0.22	5.4
25	-10.1	0.63	6.1
30	-10.4	0.21	6.9

A2-3: Zeta potential and turbidity results from the addition of Magnafloc 336 and Zetag 7557 to the tested water.

5 ppm cationic polymer			
Anion Polymer Dosage(ppm)	Zeta Potential (mV)	Standard Deviation (mV) of Zeta Potential	Turbidity (NTU)
0	-26.4	0.23	49.8
5	-12.4	0.29	14.5
7	-9.3	0.37	7.2
10	-8.2	0.19	4.2
15	-9.8	0.17	4.9
20	-10.4	0.72	5.6
25	-11.2	0.35	6.2
30	-11.5	0.43	7

A2-4: Zeta potential and turbidity results from the addition of Magnafloc 336 and Zetag 7557 to the tested water.

5 ppm cationic polymer			
Anion Polymer Dosage(ppm)	Zeta Potential (mV)	Standard Deviation (mV) of Zeta Potential	Turbidity (NTU)
0	-26.4	0.23	49.8
5	-14	0.15	15.8
7	-11.4	0.21	8.7
10	-10.1	0.15	4.9
15	-10.9	0.62	5.6
20	-11.8	0.52	6.4
25	-12.9	0.16	7.2
30	-13	0.71	8.3

A3- Batch ion exchange experiments results

A3-1: Results of the batch ion exchange study for chloride removal.

m(g)	200 mg/l Chlorid			400 mg/l Chlorid		
	C _e (mg/l)	q _e (mg/g)	Eff. %	C _e (mg/l)	q _e (mg/g)	Eff. %
1	121.2	7.88	39.4	320.6	7.94	19.85
2	62.3	6.89	68.85	251.3	7.44	37.18
3	31.5	5.62	84.25	194	6.87	51.5
4	10.7	4.73	94.65	165.8	5.86	58.55
5	2.1	3.96	98.95	120	5.6	70
m(g)	600 mg/l Chlorid			800 mg/l Chlorid		
	C _e (mg/l)	q _e (mg/g)	Eff. %	C _e (mg/l)	q _e (mg/g)	Eff. %
1	520.5	7.95	13.25	725.2	7.48	9.35
2	455.2	7.24	24.13	652	7.4	18.5
3	411.4	6.29	31.43	598.1	6.73	25.24
4	364.8	5.88	39.2	551.3	6.22	31.09
5	320.1	5.6	46.65	519	5.62	35.12

A3-2: Results of the batch ion exchange study for sulphate removal

m(g)	100 mg/l Sulphate			200 mg/l Sulphate		
	C _e (mg/l)	q _e (mg/g)	Eff. %	C _e (mg/l)	q _e (mg/g)	Eff. %
1	143.7	5.63	28.15	61.3	3.87	38.7
2	96	5.2	52	29.1	3.55	70.9
3	56.4	4.79	71.8	13.6	2.88	86.4
4	22.1	4.45	88.95	5.4	2.37	94.6
5	12.3	3.75	93.85	1.2	1.98	98.8

A3-3: Results of the batch ion exchange study for sodium removal

m(g)	178 mg/l Sodium			226 mg/l Sodium		
	C _e (mg/l)	q _e (mg/g)	Eff. %	C _e (mg/l)	q _e (mg/g)	Eff. %
1	119.8	5.82	32.7	174.2	5.18	22.92
2	71.1	5.35	60.06	123.6	5.12	45.31
3	38.5	4.65	78.37	80.7	4.84	64.29
4	17.2	4.02	90.33	36.1	4.75	84.03
5	3.4	3.49	98.09	9.3	4.33	95.89
m(g)	306 mg/l Sodium			355 mg/l Sodium		
	C _e (mg/l)	q _e (mg/g)	Eff. %	C _e (mg/l)	q _e (mg/g)	Eff. %
1	244.4	6.06	19.87	295.5	5.95	16.76
2	184.8	6.01	39.41	239.2	5.79	32.62
3	133	5.73	56.39	201.8	5.11	43.16
4	77.1	5.70	74.72	155.1	5.00	56.31
5	39.3	5.31	87.12	123.3	4.63	65.27
m(g)	436 mg/l Sodium			485 mg/l Sodium		
	C _e (mg/l)	q _e (mg/g)	Eff. %	C _e (mg/l)	q _e (mg/g)	Eff. %
1	384.4	5.16	11.84	429.9	5.51	11.36
2	334.6	5.07	23.26	390.5	4.73	19.49
3	290.1	4.86	33.46	355.2	4.33	26.76
4	246.6	4.74	43.44	325.3	3.99	32.99
5	201.2	4.7	53.85	290.7	3.89	40.06
m(g)	568 mg/l Sodium			615 mg/l Sodium		
	C _e (mg/l)	q _e (mg/g)	Eff. %	C _e (mg/l)	q _e (mg/g)	Eff. %
1	514	5.4	9.51	572.2	4.28	6.96
2	479.3	4.44	15.67	537.3	3.89	12.63
3	440.7	4.24	22.41	510	3.5	17.07
4	411.2	3.92	27.61	483.8	3.28	21.33
5	382.1	3.72	32.73	452.7	3.25	26.39

A4- Fixed bed ion exchange column experiment results

A4-1Set of experiments preformed by using anion resin

exp no	l/min flow	cm hight	mg/l Cl	mg/l SO4
1	0.05	10	200	100
2			200	200
3			400	100
4			400	200
5			600	100
6			600	200
7			800	100
8			800	200
9	0.05	20	200	100
10			200	200
12			400	200
13			600	100
14			600	200
16			800	200
17	0.1	10	200	100
18			200	200
20			400	200
22			600	200
23			800	100
24			800	200
25	0.1	20	200	100
26			200	200
27			400	100
28			400	200
29			600	100
30			600	200
32			800	200

Exp. 1(Chloride)		Exp.2(Chloride)		Exp.3(Chloride)		Exp. 4(Chloride)	
Time(min)	C/C _o	Time(min)	C/C _o	Time(min)	C/C _o	Time(min)	C/C _o
10	0.001	10	0.003	10	0.005	10	0.004
30	0.005	30	0.007	30	0.012	30	0.009
50	0.006	60	0.010	50	0.017	60	0.015
70	0.011	80	0.017	70	0.024	70	0.021
90	0.015	100	0.026	80	0.027	80	0.029
110	0.015	110	0.032	90	0.029	90	0.037
120	0.023	120	0.040	100	0.057	100	0.042
130	0.026	130	0.048	110	0.079	110	0.054
140	0.031	140	0.056	120	0.204	120	0.050
150	0.036	150	0.107	130	0.337	130	0.099
160	0.037	160	0.251	140	0.520	140	0.224
170	0.041	170	0.391	150	0.638	150	0.334
180	0.053	180	0.495	160	0.737	160	0.459
190	0.074	190	0.575	170	0.836	170	0.645
200	0.113	200	0.680	180	0.905	180	0.741
210	0.154	210	0.750	190	0.971	190	0.899
220	0.264	220	0.847	200	1.005	200	0.954
230	0.410	230	0.927			210	0.976
240	0.512	240	0.952			230	0.991
250	0.601	250	0.997				
260	0.724						
270	0.856						
280	0.920						
290	0.960						
300	0.996						

Exp.5(Chloride)		Exp.6(Chloride)		Exp. 7(Chloride)		Exp.8(Chloride)	
Time(min)	C/C _o	Time(min)	C/C _o	Time(min)	C/C _o	Time(min)	C/C _o
10	0.007	10	0.010	10	0.010	0.009706	10
30	0.014	20	0.014	30	0.014	0.017371	20
50	0.026	30	0.018	40	0.031	0.028146	30
60	0.034	40	0.025	50	0.056	0.080189	40
70	0.052	50	0.036	60	0.127	0.176891	50
80	0.124	60	0.052	70	0.367	0.378324	60
90	0.200	70	0.119	80	0.527	0.524193	70
100	0.334	80	0.221	90	0.664	0.683975	80
110	0.498	90	0.403	100	0.781	0.823646	90
120	0.648	100	0.575	110	0.862	0.910204	100
130	0.811	110	0.706	120	0.917	0.979976	110
140	0.884	120	0.816	130	0.962	1.002415	120
150	0.960	130	0.886	140			
160	1.004	140	0.924				
		150	0.995				

Exp. 9(Chloride)		Exp.10(Chloride)		Exp.12(Chloride)		Exp. 13(Chloride)		Exp.14(Chloride)	
Time(min)	C/C _o	Time(min)	C/C _o	Time(min)	C/C _o	Time(min)	C/C _o	Time(min)	C/C _o
10	0.001	10	0.001	10	0.004	10	0.005	10	0.006
70	0.004	60	0.004	30	0.006	30	0.008	30	0.008
110	0.006	90	0.003	50	0.008	50	0.010	50	0.009
150	0.013	120	0.007	70	0.011	70	0.011	70	0.012
210	0.018	150	0.010	90	0.015	90	0.012	90	0.014
230	0.014	180	0.014	110	0.018	110	0.015	110	0.018
270	0.024	210	0.018	130	0.022	130	0.023	120	0.024
330	0.039	240	0.017	150	0.024	150	0.026	130	0.030
350	0.052	270	0.023	170	0.030	160	0.027	140	0.033
370	0.049	300	0.029	180	0.037	170	0.036	150	0.056
390	0.056	320	0.053	190	0.044	180	0.075	160	0.091
410	0.078	340	0.079	200	0.049	190	0.141	170	0.166
430	0.070	350	0.125	210	0.057	200	0.289	180	0.199
450	0.092	360	0.275	220	0.080	220	0.551	190	0.321
460	0.108	370	0.396	230	0.187	230	0.744	200	0.453
470	0.123	380	0.499	240	0.305	240	0.853	210	0.544
480	0.153	390	0.705	250	0.488	250	0.905	220	0.740
490	0.148	400	0.889	260	0.610	260	0.952	230	0.852
500	0.176	410	0.949	270	0.737	270	0.989	240	0.905
510	0.238	420	0.986	280	0.807			250	0.983
520	0.391			290	0.862			260	1.002
530	0.453			300	0.965				
550	0.527			310	0.995				
560	0.676								
570	0.846								
580	0.886								
590	0.930								
600	0.991								

Exp.16(Chloride)		Exp. 17(Chloride)		Exp.18(Chloride)		Exp. 20(Chloride)	
Time(min)	C/C _o	Time(min)	C/C _o	Time(min)	C/C _o	Time(min)	C/C _o
10	0.005	10	0.003	10	0.006	10	0.016
20	0.006	30	0.009	30	0.016	20	0.024
30	0.008	40	0.020	40	0.036	30	0.037
40	0.009	50	0.031	50	0.049	40	0.154
50	0.010	60	0.055	60	0.111	50	0.427
60	0.013	70	0.068	70	0.278	60	0.621
70	0.012	80	0.105	80	0.494	70	0.832
80	0.023	90	0.163	90	0.651	80	0.903
90	0.030	100	0.281	100	0.789	90	0.964
100	0.036	110	0.427	110	0.861	100	0.989
110	0.062	120	0.518	120	0.950		
120	0.083	130	0.607	130	1.006		
130	0.108	140	0.718				
140	0.312	150	0.861				
150	0.543	160	0.914				
160	0.599	170	0.909				
170	0.734	180	0.964				
180	0.865	190	1.015				
190	0.951						
200	0.998						

Exp.22(Chloride)		Exp.23(Chloride)		Exp.24(Chloride)	
Time(min)	C/C _o	Time(min)	C/C _o	Time(min)	C/C _o
10	0.056	10	0.065	10	0.087
20	0.156	20	0.191	20	0.248
30	0.411	30	0.457	30	0.500
40	0.605	40	0.654	40	0.698
50	0.735	50	0.810	50	0.851
60	0.888	60	0.918	60	0.955
70	0.947	70	0.970	70	0.993
80	0.988	80	1.002		

Exp.25(Chloride)		Exp. 26(Chloride)		Exp.27(Chloride)		Exp.28 (Chloride)	
Time(min)	C/C _o	Time(min)	C/C _o	Time(min)	C/C _o	Time(min)	C/C _o
10	0.002	10	0.003	10	0.003	10	0.006
30	0.004	30	0.007	30	0.005	30	0.012
60	0.008	50	0.012	50	0.009	50	0.017
80	0.018	70	0.022	70	0.015	60	0.022
100	0.023	90	0.031	90	0.021	70	0.032
120	0.027	110	0.040	100	0.027	80	0.037
140	0.021	120	0.047	110	0.033	90	0.082
160	0.035	130	0.055	120	0.138	100	0.139
170	0.032	140	0.058	130	0.248	110	0.332
180	0.041	150	0.100	140	0.496	120	0.530
190	0.063	160	0.233	150	0.624	130	0.722
200	0.046	170	0.316	160	0.735	140	0.855
210	0.063	180	0.534	170	0.854	150	0.905
220	0.069	190	0.713	180	0.907	160	0.961
230	0.099	200	0.780	190	0.970	170	1.007
240	0.200	210	0.869	200	0.989		
250	0.384	220	0.934				
260	0.648	230	0.984				
270	0.848						
280	0.908						
290	0.953						
300	0.993						

Exp.29(Chloride)		Exp.30(Chloride)		Exp.32(Chloride)	
Time(min)	C/C _o	Time(min)	C/C _o	Time(min)	C/C _o
10	0.008	10	0.010	10	0.013
20	0.011	20	0.014	20	0.021
30	0.016	30	0.018	30	0.057
40	0.020	40	0.029	40	0.112
50	0.025	50	0.054	50	0.262
60	0.046	60	0.070	60	0.485
70	0.066	70	0.193	70	0.688
80	0.163	80	0.458	80	0.837
90	0.340	90	0.666	90	0.903
100	0.525	100	0.761	100	0.977
110	0.743	110	0.882	110	0.992
120	0.843	120	0.965		
130	0.909	130	0.990		
140	0.966				
150	1.005				

Exp.4(Sulphate)		Exp. 17(Sulphate)		Exp.18(Sulphate)		Exp. 20(Sulphate)	
Time(min)	C/C _o	Time(min)	C/C _o	Time(min)	C/C _o	Time(min)	C/C _o
10	0.000	10	0.007	10	0.005	10	0.011
30	0.001	60	0.022	60	0.034	60	0.019
60	0.001	120	0.046	120	0.066	90	0.046
90	0.015	180	0.079	140	0.117	120	0.058
100	0.017	240	0.074	160	0.488	140	0.106
120	0.012	260	0.095	180	0.748	160	0.369
150	0.024	280	0.157	200	0.953	180	0.723
170	0.037	300	0.301	220	1.019	200	0.875
190	0.036	320	0.632			220	0.927
210	0.063	340	0.818			240	1.018
230	0.060	360	0.909				
250	0.069	380	0.957				
270	0.100						
290	0.159						
300	0.215						
310	0.280						
320	0.420						
330	0.448						
340	0.516						
350	0.608						
360	0.716						
370	0.773						
380	0.898						
390	0.906						
400	0.968						
410	0.987						
420	1.018						

Exp.22(Sulphate)		Exp.23(Sulphate)		Exp.24(Sulphate)	
Time(min)	C/C _o	Time(min)	C/C _o	Time(min)	C/C _o
10	0.010	10	0.000	10	0.009
60	0.021	60	0.008	60	0.026
90	0.053	90	0.036	90	0.042
100	0.059	120	0.021	120	0.093
110	0.055	180	0.047	130	0.113
120	0.089	240	0.092	140	0.222
130	0.085	260	0.136	150	0.319
140	0.158	280	0.218	160	0.498
150	0.168	300	0.382	170	0.613
160	0.374	320	0.677	180	0.755
170	0.477	340	0.883	190	0.899
180	0.689	360	0.956	200	0.969
190	0.769	380	1.043	210	1.011
200	0.864				
210	0.901				
220	0.994				

A4-2Set of experiments preformed by using mixed ion exchange resin

exp no	l/min flow	cm hight	mg/l Cl	mg/l SO4	mg/l Na
1M	0.05	20	200	100	178
2M			200	200	226
3M			400	100	306
4M			400	200	355
5M			600	100	436
6M			600	200	485
7M			800	100	568
8M			800	200	615
10M			200	200	226
12M			400	200	355
13M			600	100	436
14M			600	200	485
16M			800	200	615
17M	0.1	20	200	100	178
18M			200	200	226
20M			400	200	355
22M			600	200	485
23M			800	100	568
24M			800	200	615
30M	0.1	40	600	200	226

Exp.1M (Chloride)		Exp.2M(Chloride)		Exp.3M(Chloride)		Exp. 4M(Chloride)	
Time(min)	C/C _o	Time(min)	C/C _o	Time(min)	C/C _o	Time(min)	C/C _o
10	0.000	10	0.000	10	0.000	10	0.004
60	0.000	60	0.000	60	0.004	30	0.009
120	0.007	120	0.012	90	0.014	60	0.015
180	0.037	140	0.030	120	0.067	70	0.021
200	0.034	160	0.060	140	0.152	80	0.029
220	0.059	180	0.099	160	0.352	90	0.037
240	0.093	200	0.148	180	0.578	100	0.042
260	0.203	220	0.264	200	0.729	110	0.054
280	0.288	240	0.490	220	0.912	120	0.050
300	0.559	260	0.740	240	1.009	130	0.099
320	0.789	280	0.884			140	0.224
340	0.919	300	0.953			150	0.334
360	1.012	320	1.029			160	0.459
						170	0.645
						180	0.741
						190	0.899
						200	0.954
						210	0.976
						230	0.991

Exp.5M(Chloride)		Exp.6M(Chloride)		Exp. 7M(Chloride)		Exp.8M(Chloride)	
Time(min)	C/C _o	Time(min)	C/C _o	Time(min)	C/C _o	Time(min)	C/C _o
10	0.000	10	0.002	10	0.005	10	0.005
60	0.026	30	0.011	30	0.013	30	0.016
80	0.034	60	0.033	60	0.072	50	0.095
100	0.111	80	0.067	80	0.191	70	0.339
120	0.326	100	0.202	100	0.526	90	0.600
140	0.631	120	0.408	120	0.754	110	0.817
160	0.835	140	0.701	140	0.903	130	0.928
180	0.949	160	0.898	160	0.999	150	0.995
200	1.006	180	1.003				

Exp.10M(Chloride)		Exp.12M(Chloride)		Exp. 13M(Chloride)		Exp.14M(Chloride)	
Time(min)	C/C _o	Time(min)	C/C _o	Time(min)	C/C _o	Time(min)	C/C _o
10	0.000	10	0.000	10	0.000	10	0.000
60	0.000	60	0.000	60	0.004	60	0.002
90	0.003	120	0.003	120	0.011	120	0.009
120	0.006	180	0.011	180	0.038	140	0.018
180	0.012	240	0.030	200	0.078	160	0.032
210	0.009	260	0.037	220	0.368	180	0.081
240	0.014	280	0.054	240	0.618	200	0.116
270	0.016	300	0.127	260	0.851	220	0.326
300	0.024	320	0.331	280	0.951	240	0.523
320	0.021	340	0.467	300	1.006	260	0.762
340	0.030	360	0.649			280	0.844
350	0.054	380	0.929			300	0.993
360	0.058	400	1.012				
370	0.059						
380	0.064						
390	0.069						
400	0.071						
410	0.091						
420	0.109						
430	0.165						
440	0.184						
450	0.269						
460	0.449						
470	0.514						
480	0.693						
490	0.819						
500	0.886						
510	0.912						
520	0.962						
530	1.018						

Exp.16M(Chloride)		Exp. 17M(Chloride)		Exp.18M(Chloride)		Exp. 20M(Chloride)	
Time(min)	C/C _o	Time(min)	C/C _o	Time(min)	C/C _o	Time(min)	C/C _o
10	0.000	10	0.000	10	0.000	10	0.009
30	0.001	60	0.038	30	0.013	20	0.015
60	0.006	80	0.058	50	0.043	30	0.024
90	0.014	100	0.099	70	0.060	40	0.035
120	0.023	120	0.270	90	0.183	50	0.054
130	0.030	140	0.443	110	0.508	60	0.091
140	0.068	160	0.614	130	0.703	70	0.246
150	0.098	180	0.853	150	0.924	80	0.421
160	0.185	200	0.948	170	1.019	90	0.624
170	0.442	220	1.019			100	0.699
180	0.557					110	0.894
190	0.765					120	0.946
200	0.881					130	0.973
210	0.917					140	0.997
220	0.987						
230	1.007						

Exp.4M(Sodium)		Exp.12M(Sodium)		Exp.14M(Sodium)		Exp.16M(Sodium)	
Time(min)	C/C ₀	Time(min)	C/C ₀	Time(min)	C/C ₀	Time(min)	C/C ₀
10	0.003	10	0.000	10	0.000	10	0.000
30	0.010	30	0.000	60	0.005	60	0.007
50	0.017	60	0.003	120	0.009	120	0.017
70	0.028	80	0.008	180	0.016	140	0.024
80	0.039	100	0.007	200	0.014	160	0.043
90	0.034	120	0.011	220	0.026	180	0.065
100	0.043	140	0.010	240	0.102	200	0.158
120	0.102	160	0.011	260	0.232	220	0.432
140	0.151	180	0.017	280	0.467	240	0.787
160	0.293	200	0.015	300	0.697	260	0.908
180	0.591	220	0.020	320	0.906	280	0.988
200	0.813	240	0.018	340	0.991	300	1.006
220	0.937	260	0.027	360	1.002		
240	1.008	280	0.035				
		290	0.045				
		300	0.044				
		310	0.057				
		320	0.067				
		330	0.121				
		340	0.118				
		350	0.201				
		360	0.252				
		370	0.305				
		380	0.422				
		390	0.540				
		400	0.559				
		410	0.596				
		420	0.743				
		430	0.769				
		440	0.846				
		450	0.889				
		460	0.954				
		470	0.996				

Exp.20M(Sodium)		Exp.22M(Sodium)		Exp.30M(Sodium)	
Time(min)	C/C _o	Time(min)	C/C _o	Time(min)	C/C _o
10	0.006	10	0.003	10	0.002
30	0.009	20	0.016	30	0.005
50	0.098	30	0.066	60	0.011
70	0.298	40	0.168	80	0.024
80	0.596	50	0.330	90	0.055
90	0.709	60	0.554	110	0.128
100	0.844	70	0.688	130	0.391
120	0.928	80	0.865	150	0.651
140	1.010	90	0.944	170	0.874
		100	1.007	190	0.959
				210	0.991

Exp.4M(Sulphate)		Exp.20M(Sulphate)		Exp.22M(Sulphate)		Exp.23M(Sulphate)	
Time(min)	C/C _o	Time(min)	C/C _o	Time(min)	C/C _o	Time(min)	C/C _o
10	0.000	10	0.000	10	0.000	10	0.000
30	0.001	60	0.013	60	0.012	60	0.000
60	0.001	90	0.021	90	0.008	90	0.008
120	0.004	120	0.063	100	0.023	120	0.013
180	0.020	140	0.055	110	0.020	180	0.019
240	0.027	160	0.134	120	0.038	240	0.037
270	0.069	180	0.298	130	0.061	260	0.052
290	0.084	200	0.534	140	0.064	280	0.086
310	0.093	220	0.791	150	0.078	300	0.079
330	0.108	240	0.893	160	0.150	320	0.112
350	0.233	260	0.969	170	0.329	340	0.139
370	0.464	270	1.009	180	0.463	360	0.195
390	0.666			190	0.592	380	0.277
410	0.724			200	0.673	400	0.496
430	0.809			210	0.893	420	0.585
450	0.902			220	0.984	440	0.768
470	0.969			240	1.015	460	0.916
490	0.998					480	0.984

Exp.24M(Sulphate)		Exp.30M(Sulphate)	
Time(min)	C/C _o	Time(min)	C/C _o
10	0.000	10	0.000
60	0.000	60	0.004
90	0.012	90	0.009
110	0.025	120	0.013
130	0.046	180	0.027
150	0.089	240	0.024
170	0.084	300	0.038
190	0.108	320	0.053
210	0.119	340	0.063
230	0.498	360	0.058
250	0.650	380	0.100
270	0.893	400	0.259
290	0.977	420	0.569
310	1.019	440	0.774
		460	0.867
		480	0.924
		500	0.974
		520	1.018

Appendix B

CATIONIC AND ANIONIC POLYELECTROLYTES SPECIFICATIONS

PRODUCT DATA



PRODUCT NAME:

Zetag 7557

DESCRIPTION:

Zetag 7557 is a medium molecular weight, polyacrylamide based flocculant, which exhibits a high degree of cationic charge. Once hydrated in water, reacts readily to provide superior floc formation and performance in a variety of solids/liquid separation processes. Zetag 7557 is supplied in a unique micro bead form, which renders the product free flowing and essentially non-dusting.

PROPERTIES:

<u>Physical</u>		<u>Chemical</u>	
Appearance:	Solid, white granular	Type:	Co-polymer of a quarternary acrylate salt and acrymalide
Specific Gravity:	0.75	Solubility:	Soluble
Melting Point:	N/A	pH:	3.8 (1% solution)
Flash Point:	N/A	Microtox:	Not controlled

APPLICATION:

Zetag 7557 has been designed as a flocculant for a variety of municipal and industrial waste substrates. It has been proven especially effective for conditioning these substrates for solids sedimentation, thickening and dewatering processes.

Zetag 7557 offers greatly improved solid/liquid separation efficiencies over a wide range of pH and is available in 25 kg bags for ease of handling and safety. Corrosion towards most standard materials of construction is very low. Stainless steel, fiberglass, polyethylene, polypropylene and rubberized surfaces are recommended. In some cases, aluminum and galvanized surfaces can be adversely affected.

MIXING AND HANDLING:

Recommended solution concentration:

Stock Solution: 0.25-0.5%

Feed Solution 0.05-0.25%

Recommended Storage Periods:

Product as supplied: Up to 2 years

Stock: 2-5 days

Feed: 1-3 days

Product should be stored in a cool, dry place and conditions of high temperature and high humidity should be avoided. Under such conditions, the hygroscopic nature of the product may result in excessive moisture and product caking.

Zetag 7557 is a D-2-B controlled product using the WHMIS classification.

Refer to MSDS information of specific precautions and handling.

WHMIS: D-2-B (See MSDS)

TDG: Not Regulated

PACKAGING: 25 kg sacks



Ciba[®] MAGNAFLOC[®] 336

Anionic flocculant

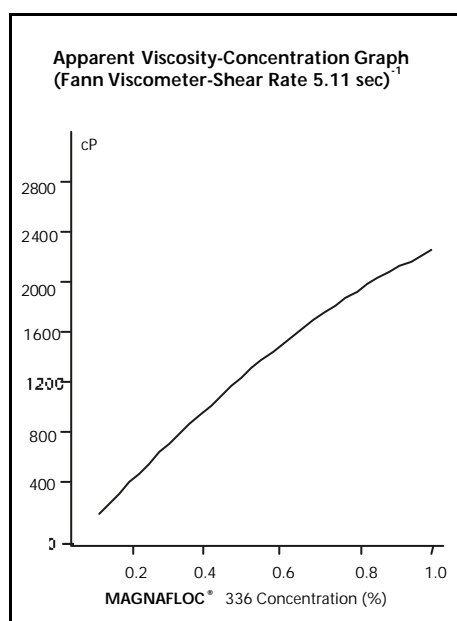
Description **MAGNAFLOC[®] 336** is a high molecular weight anionic polyacrylamide flocculant supplied as a free flowing granular powder.

Principal Uses **MAGNAFLOC[®] 336** has found application in a wide variety of mineral processing operations including the following:

1. Base metal sulphide and oxide concentrates thickening and filtration
2. Sedimentation of coal tailings
3. Sedimentation of coal fines
4. Filtration of coal fines
5. Sedimentation and filtration of metal hydroxides
6. Sedimentation of fine sands and clays
7. Tailings dewatering
8. Brine clarification
9. Phosphate slimes thickening

Dosage depends on application but normally lies in the range 50-200 g/tonne of dry substrate flocculated

Typical Properties	Physical Form	Off-white granular powder
	Particle Size	98% < 1000 μm
	Bulk Density	0.75g/cm ³
	pH of 1% solution at 25°C	7.0
	Viscosity at 25°C	See graph and table



Application & Storage	Recommended solution concentrations:	
	Stock solution	0.25 - 0.5% max
	Feed solution	0.025 - 0.1% max

Recommended storage periods:

Shelf Life	2 years from receipt of goods	
	Stock solution	1-2 days

Storage of polymer should be in a cool, dry place.

Details on preparation and feeding can be obtained from a Ciba Representative.

Solution viscosity data (Fann viscometer – 25°C – solvent – deionised water)						
MAGNAFLOC® 336 concentration (%)	Shear rate (sec ⁻¹)					
	5.11	10.22	170	340	511	1022
	Viscosity (cP)					
1.0	2300	1300	180	120	60	38
0.5	950	550	78	62	49	41
0.25	450	255	44	33	26	22
0.10	180	125	22	17	14	11

Packaging **MAGNAFLOC® 336** is supplied in 25kg nett plastic bags shrinkwrapped onto a pallet suitable for export shipment. The product can also be supplied via intermediate big bags or bulk tanker. Specific details of bag and tanker sizes can be obtained on request.

Corrosivity towards most standard materials of construction is low, but aluminium and galvanised equipment should be avoided.

MAGNAFLOC® 336 spills are a hazard due to the inherent slipperiness of this type of product. Spills should be cleaned up immediately. Dry spills should be left dry and swept up. If the polymer becomes wet, an absorbent material should be applied to the spill, then swept up and discarded.

Technical Service Advice and assistance in the running of laboratory and plant tests to select the correct flocculant and determine the best application is given by representatives of Ciba, who are experienced in mineral processing applications.

Health and Safety **MAGNAFLOC® 336** has a low order of oral toxicity and does not present any abnormal handling problems.

Detailed information on handling and any precautions to be observed in the use of the product(s) described in this leaflet can be found in our relevant Health and Safety information sheet.

Important

Copyright © 2007 Ciba. All rights reserved.

All trademarks mentioned are either property of or licensed to Ciba and registered in relevant countries.

IMPORTANT: The following supersedes Buyer's documents. SELLER MAKES NO REPRESENTATION OR WARRANTY, EXPRESS OR IMPLIED, INCLUDING OF MERCHANTABILITY OR FITNESS FOR A PARTICULAR PURPOSE. No statements herein are to be construed as inducements to infringe any relevant patent. Under no circumstances shall Seller be liable for incidental, consequential or indirect damages for alleged negligence, breach of warranty, strict liability, tort or contract arising in connection with the product(s). Buyer's sole remedy and Seller's sole liability for any claims shall be Buyer's purchase price. Data and results are based on controlled or lab work and must be confirmed by Buyer by testing for the intended conditions of use. The product(s) has (have) not been tested for, and is (are) therefore not recommended for, uses for which prolonged contact with mucous membranes, abraded skin, or blood is intended; or for uses for which implantation within the human body is intended. *Please note that products may differ from country to country.*

® indicates a registered trademark

™ indicates a trade mark

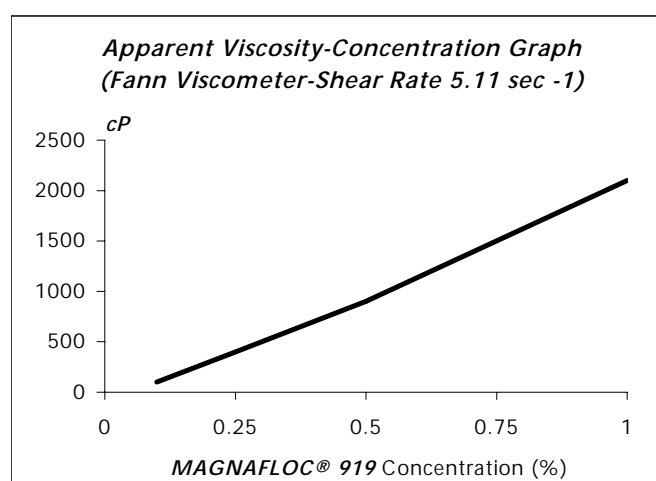
For further information, contact your regional office, details on : www.ciba.com, alternatively e.mail: extractives@ciba.com



Ciba[®] MAGNAFLOC[®] 919

Anionic flocculant

Description	MAGNAFLOC[®] 919 is an ultra high molecular weight anionic polyacrylamide flocculant supplied as a free flowing granular powder.	
Principal Uses	MAGNAFLOC[®] 919 has found application in a wide variety of mineral processing operations including the following: <ol style="list-style-type: none"> 1. Coal tailings clarification. 2. Copper tailings clarification. 3. Iron ore tailings clarification. 4. Gold cyanidation, C.C.D. washing. 5. Centrifugation of many mineral slurries including clays etc. <p>Dosage depends on application but normally lies in the range 2g to 200g per tonne of dry substrate flocculated.</p>	
Typical Properties	Physical Form	Off-white granular powder
	Particle Size	98% < 1000 µm
	Bulk Density	0.75g/cm ³
	PH of 1% solution at 25°C	7.0
	Viscosity at 25°C	See graph and table



Application & Storage Recommended solution concentrations:

Stock solution	0.25 - 0.5% max
Feed solution	0.025 - 0.1% max

Recommended storage periods:

Shelf Life 2 years from receipt of goods

Stock solution 1-2 days

Storage of polymer should be in a cool, dry place.

Details on preparation and feeding can be obtained from a Ciba Specialty Chemicals Representative

Solution viscosity data (Fann viscometer – 25°C - solvent - deionised water)						
MAGNAFLOC® 919 concentration (%)	Shear rate (sec⁻¹)					
	5.11	10.22	170	340	511	1022
	Viscosity (cP)					
1.0	2100	1250	204	146	128	99
0.5	900	630	75	65	60	45
0.25	400	300	42	38	32	24
0.10	100	75	18	15	12	9

Shipping and Handling **MAGNAFLOC® 919** is supplied in 25kg nett plastic bags shrinkwrapped onto a pallet suitable for export shipment. The product can also be supplied via intermediate big bags or bulk tanker. Specific details of bag and tanker sizes can be obtained on request.

Corrosivity towards most standard materials of construction is low, but aluminium and galvanised equipment should be avoided.

Technical Service Advice and assistance in the running of laboratory and plant tests to select the correct flocculant and determine the best application is given by representatives of Ciba Specialty Chemicals, who are experienced in mineral processing applications.

Health and Safety **MAGNAFLOC® 919** exhibits a very low order of oral toxicity and does not present any abnormal problems in its handling or general use.

Detailed information on handling and any precautions to be observed in the use of the product(s) described in this leaflet can be found in our relevant Health and Safety information sheet.

Important

Copyright © 2002 Ciba Specialty Chemicals. All rights reserved.

All trademarks mentioned are either property of or licensed to Ciba Specialty Chemicals and registered in relevant countries.

IMPORTANT: The following supersedes Buyer's documents. SELLER MAKES NO REPRESENTATION OR WARRANTY, EXPRESS OR IMPLIED, INCLUDING OF MERCHANTABILITY OR FITNESS FOR A PARTICULAR PURPOSE. No statements herein are to be construed as inducements to infringe any relevant patent. Under no circumstances shall Seller be liable for incidental, consequential or indirect damages for alleged negligence, breach of warranty, strict liability, tort or contract arising in connection with the product(s). Buyer's sole remedy and Seller's sole liability for any claims shall be Buyer's purchase price. Data and results are based on controlled or lab work and must be confirmed by Buyer by testing for the intended conditions of use. The product(s) has (have) not been tested for, and is (are) therefore not recommended for, uses for which prolonged contact with mucous membranes, abraded skin, or blood is intended; or for uses for which implantation within the human body is intended. *Please note that products may differ from country to country.*

© Ciba Specialty Chemicals PLC, 1998

® indicates a registered trademark

™ indicates a trade mark

For further information, contact your regional office, details on : www.cibasc.com, alternatively e.mail: extractives@cibasc.com

Appendix C

ION EXCHANGE RESIN SPECIFICATIONS

Purolite® MB400

Mixed Bed Resin - Self Indicating

Purolite MB400 is a high quality resin mixture for direct purification of water. It is suitable for use in regenerable or non-regenerable cartridges and in large ion exchange units. Passage of water at recommended flow rates through the resin as supplied can achieve almost complete reduction of total dissolved solids. The residuals produce average conductivity values of about 0.1 $\mu\text{S cm}^{-1}$ for a major portion of the service run which may be extended depending upon the final water quality acceptable. Equivalent volumes of ultra pure water may be obtained after regeneration but only if sufficient regenerant quantities are employed to achieve the percentage conversion levels equivalent to those of the "as supplied" resin. Generally acceptable capacity and quality is obtained economically at lower regeneration.

BASIC FEATURES:

Application - Demineralization - High quality; general purpose

Polymer Structure - Gel polystyrene crosslinked with divinylbenzene

Appearance - Spherical beads

Functional Group - Sulfonic Acid and Type 1 Quaternary Ammonium

Ionic Form as Shipped - H^+ / OH^-

Product Information

	Cation	Anion
Component	Gel strong acid cation	Gel type 1 strong base anion
Cation / Anion Volumetric Ratio	50 %	50 %
Moisture Content	65 % (max)	
Particle Size Range	300 - 1200 μm	
Uniformity Coefficient (max.)	1.7	
<300 μm (max.)	1 %	
Temp Limit, Non-Regenerable Bed	100°C (212°F)	
Temp Limit, Regenerable Bed	60°C (140°F)	
Shipping Weight (approx.)	705 - 740 g/l (44.1 - 46.3 lb/ft ³)	

Purolite® A400

Gel Type 1 Strong Base Anion Exchange Resin

Purolite A400 is a clear gel Type 1 strong-base anion exchanger with both high operating capacity and the ability to achieve low residual silica levels. Minimal quantities of caustic soda are required compared with those typical of the classical Type 1 (Purolite A600) quaternary ammonium structure based on polystyrene. It has a clear gel structure, showing excellent regeneration efficiency and rinse characteristics. Purolite A400 functions well both in mixed bed and layered bed demineralizer systems, where specially tailored particle size ranges result in achieving or maintaining good separations. Purolite A400 has exceptional physical stability for a conventional gel-type resin which permits a long life without the development of excessive pressure drop; it also shows good kinetics of exchange, enabling very low concentration levels of both strong and weak acid anions to be achieved at practical flowrates.

BASIC FEATURES:

Application - Regeneration Efficient Demineralization / Silica Removal

Polymer Structure - Gel polystyrene crosslinked with divinylbenzene

Appearance - Spherical beads

Functional Group - Type 1 Quaternary Ammonium

Ionic Form as Shipped - Cl⁻

Product Information

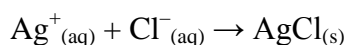
Total Capacity (min.)	1.3 eq/l (28.4 Kgr/ft ³) (Cl ⁻ form)	
Moisture Retention, Cl ⁻ Form	48 - 54 %	
Particle Size Range	300 - 1200 µm	
<300 µm (max.)		
Uniformity Coefficient (max.)	1.7	
Reversible Swelling, Cl ⁻ → OH ⁻ (max.)	20 %	
Specific Gravity	1.08	
Shipping Weight (approx.)	680 - 715 g/l (42.5 - 44.7 lb/ft ³)	
Temp Limit, Cl ⁻ Form	100°C (212°F)	
Temp Limit, OH ⁻ Form	60°C (140°F)	

Appendix D

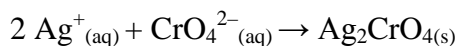
Determination of Chloride Ion Concentration by Titration (Mohr's Method)

Introduction

This method determines the chloride ion concentration of a solution by titration with silver nitrate. As the silver nitrate solution is slowly added, a precipitate of silver chloride forms.



The end point of the titration occurs when all the chloride ions are precipitated. Then additional chloride ions react with the chromate ions of the indicator, potassium chromate, to form a red-brown precipitate of silver chromate.



This method can be used to determine the chloride ion concentration of water samples from many sources such as seawater, stream water, river water and estuary water.

Equipment Needed

Burette and stand

10 and 20 ml pipettes

100 ml volumetric flask

250 ml conical flasks

10 ml and 100 ml measuring cylinders

Solutions Needed

Silver nitrate solution: 0.1 mol l^{-1} , accurately 4.25g was weight of solid AgNO_3 and dissolved in 250 ml of distilled water in a conical flask.

Potassium chromate indicator solution: (approximately 0.25 mol l^{-1}) 1g of K_2CrO_4 was weighed and dissolved in 20 ml of distilled water in a conical flask.

Method

1. 2-3 drops of chromate indicator was added to 10 ml water sample, which want to find its chloride concentration, in a conical flask.
2. The sample was titrated with 0.1 mol l^{-1} silver nitrate solution. Although the silver chloride that forms is a white precipitate, the chromate indicator initially gives the cloudy solution a faint lemon-yellow colour. The endpoint of the titration is identified as the first appearance of a red-brown colour of silver chromate. If addition of Ag^+ is continued past the endpoint, further silver chromate precipitate is formed and a stronger red-brown colour results.
3. The titration should be stopped when the first trace of red-brown colour is observed. Using an incompletely titrated reference flask for comparison is a helpful way to identify the first appearance of red-brown colouration.
4. The titration was repeated with further 10 ml water sample to make sure of the first end point we obtained.

الخلاصة

يتناول هذا العمل معالجة مياه التصريف الصناعية لمعمل الاشيدية الذي يعد واحدا من صناعات مناجم الفوسفات في الأردن، ويستخدم نحو ٤٥٠٠٠٠ متر مكعب من مياه التصريف الصناعية شهريا والناجمة عن عمليات التعويمية التي بحاجة الى معالجة محكمة لأغراض إعادة التدوير. ان مياه التصريف الصناعية، موضوع الدراسة، تحتوي بشكل رئيسي على مخلفات الفوسفات وأيونات الكلوريد. وتعد عملية الترسيب بواسطة اضافة المبلمرات المزدوجة لإزالة ونزع المياه من المخلفات الفوسفاتية، تتبعها عملية التبادل الأيوني المزدوج المستمر لإزالة الملح الذائب والمتبقي في الماء الطافي.

وقد تم دراسة تأثير جرع مختلفة من الخلائط الثنائية الكاتيونية و الانيونية للمبلمرات على التلبد عن طريق قياس امكانية التعكر والزيتا . تم الحصول على جرعة أمثل للمبلمرات الثنائية المرتبطة بمقدار الزيتا 5.6-mv كهدف. يساعد التلبد على زيادة كل من معدل الترسيب ومعدل نزع المياه من المخلفات الفوسفاتية من أجل زيادة إعادة تدوير المياه .المعايير السابقة ازدادت ٢٠ مرة من قبل المبلمرات الكاتيونية (Zetag 7557) والايونية (Magnafloc 633) بالمقارنة مع المعدل الطبيعي لترسيب المخلفات نفسها، فضلا عن انخفاض ٧٠٪ في حجم المخلفات.

دراسة عمود التبادل الأيوني استنتجت باستخدام Purolite® A400 و Purolite® MB400 باعتباره عامل امتصاص لإزالة CL^- ، SO_4^{2-} والصوديوم من المياه . الدراسة المكثفة تستعرض بحث في الآثار المترتبة على المعلمات التجريبية المختلفة، مثل الجرعة الممتصة والتركيز الأولي لإزالة الأيونات وتم الحصول على النجاعة او الكفاءة القصوى البالغة ٥٨.٩٥ % باستعمال ٥ غم من عامل الامتصاص و ٢٠٠ مغم/لتر تركيز اولى للكلورايد .وربطت بيانات توازن الامتصاص مع نماذج الايزوثرم الانكماير و فروندليخ.

وأجريت تجارب العمود لدراسة تأثير المعالم الهامة مثل ارتفاع العمود الراسب ، ومعدل التدفق، وتركيز التطعيم الاولي ووجود الأيونات المشتركة في منحنى الاختراق، وكفاءة إزالة وأداء عملية التبادل الايوني المزدوج .ان اختراق منحنيات للأيونات الثلاثة، المخلوط في نسبة من المخلفات السائلة الى تركيز مؤثر مقابل وقت التشغيل المقاس بالدقائق تعطي نتائج مفصلة حول الآثار المترتبة على الظروف المحيطة. وقد تم تطوير النموذج الرياضي الذي اقترح آلية نفاذية مزدوجة لمحاكاة أداء التبادل الايوني المزدوج. تم حل هذا النموذج باستخدام برنامج ماتلاب وتمت مقارنة النتائج النظرية مع المختبرية.

شكر و تقدير

أتقدم بخالص الشكر و الأمتنان لأستاذي الدكتور أبرائيل سركيس يارو , المشرف على الرسالة , لما أبداه لي من جهد في التوجيه و الإرشاد و المتابعة.

أود ايضاً أن أشكر الدكتور باسم عبيد حسن , رئيس قسم الهندسة الكيمياوية , و الكادر التدريسي في القسم لمساعدتهم في أنجاز هذا البحث.

كما يشرفني أن اتقدم بجزيل الشكر الى الأستاذ الدكتور محسن جبر جويج , عميد كلية الهندسة , والدكتور محمد باقر محمد صادق الشديدي , معاون العميد للشؤون العلمية و الطلبة , على معاملتهم و تعاونهم الرائع مع الطلبة.

ساندرا سولاقا بولص

معالجة المياه الصناعية باستخدام التبادل الايوني

رسالة

مقدمة إلى كلية الهندسة

في جامعة النهريين وهي جزء من متطلبات

نيل درجة دكتوراه فلسفة

في

الهندسة الكيمياءوية

من قبل

ساندرا سولاقا بولص

(ماجستير في الهندسة الكيمياءوية ٢٠٠١)

١٤٣٤

٢٠١٢

محرم

كانون الأول